

***In silico* and *in vitro* inhibition of α -
glucosidase and α -amylase by
compounds from culinary herbs and
spices, for possible treatment of type 2
diabetes**

by

Morné Tolmie

Submitted in partial fulfilment of the requirements for the degree

Master of Science

in

Biochemistry

in the

Faculty of Natural and Agricultural Sciences

University of Pretoria

Pretoria

November 2020

Prof. Z. Apostolides

Prof. M. J. Bester



UNIVERSITEIT VAN PRETORIA
UNIVERSITY OF PRETORIA
YUNIBESITHI YA PRETORIA

DECLARATION OF ORIGINALITY

University of Pretoria

Faculty of Natural and Agricultural Sciences

Subject of the work: *In silico* and *in vitro* inhibition of α -glucosidase and α -amylase by compounds from culinary herbs and spices, for possible treatment of type 2 diabetes.

I, **Morné Tolmie**

Student number: 15018131

Declare that the dissertation, which I hereby submit for the degree Master of Science in Biochemistry at the University of Pretoria, is my own work and has not previously been submitted by me for a degree at this or any other tertiary institution.

Signature



.....

Date

November 2020

.....

RESEARCH OUTPUTS

To be published:

M. Tolmie, M. J Bester, Z. Apostolides. 2020. Inhibition of α -glucosidase and α -amylase by herbal compounds, for the treatment of type 2 diabetes: a validation of *in silico* reverse docking with *in vitro* enzyme assays. Journal of Diabetes, (waiting for page numbers).

National conferences:

M. Tolmie, Z. Apostolides. Inhibition of α -glucosidase and α -amylase by herbal compounds, for the treatment of type 2 diabetes: a validation of *in silico* reverse docking with *in vitro* enzyme assays. BGM Monday Seminar series (University of Pretoria), Pretoria, South Africa, 13 July 2020 (Oral presentation).

ACKNOWLEDGEMENTS

I would like to express my immense gratitude to:

My supervisors

Professors Apostolides and Bester, thank you for your invaluable contribution, guidance, assistance and advise. Thank you for the opportunity to do my MSc under your supervision.

The University of Pretoria

I appreciate the assistance of the University of Pretoria and the Department of Biochemistry, Genetics and Microbiology for allowing me to undertake this study, and the staff for their support throughout the duration of this study. I would like to thank Ms. Nell from the Pharmacology department for helping with the maintenance of the cells.

My Friends

My laboratory partners and friends. Marissa thank you for your constant encouragement and prayers. Kadima and Jamie thank you for your support and joining me in the laboratory.

My Parents and my Brothers

Thank you for your love support and prayers. You all are my greatest fans and genuinely believe in me.

My Husband

Janré, thank you for all your help, constant encouragement and advice. Thank you for always believing in me and wanting the best for me.

Father God

Without whom, this would not have been possible. Thank you for every blessing and Your provision.

ABSTRACT

Diabetes is one of the largest health challenges of the 21st century and is amongst the top 10 causes of death globally. There is no cure for type 2 diabetes (T2DM) and the search for new and improved treatments is ongoing. Various pharmaceuticals are available to treat T2DM, but with varied success. Many traditional herbal medicines are also used to treat T2DM, but mostly without scientific validation. Alternative treatment strategies, like herbal medicines and associated active compounds, can prove to be more cost-effective and may lack undesirable side-effects. This study aimed to assess the *in vitro* hypoglycaemic, toxicity and insulin mimicking effects of seven compounds found in commercially available herbs and spices, using *in silico* and *in vitro* relationship studies. These herbal compounds were acetyleugenol, apigenin, cinnamic acid, eriodictyol, myrcene, piperine and rosmarinic acid, they were chosen based on scientific reports on pleiotropic effects related to the inhibition of starch hydrolysing enzymes and insulin mimicking effects.

Various *in silico* physiochemical properties of each compound was evaluated and compared with the antidiabetic drug, acarbose. All the herbal compounds had better drug-like features than acarbose. Candidate compounds were further analysed using the Search Tool for Interactions of Chemicals (STITCH) database to explore drug-target interactions, for possible harmful cross-reactions. The drug-target networks generated on STITCH showed no undesirable cross-reactions and highlighted the anti-carcinogenic and anti-inflammatory properties of the herbal compounds. The enzyme inhibitory nature was evaluated using *in silico* docking analysis with the Glide algorithm in the Maestro software and was further confirmed by *in vitro* α -amylase and α -glucosidase colorimetric assays.

Alpha-amylase and α -glucosidase have been identified as important therapeutic targets for the management of T2DM. The inhibition of these enzymes would lead to a decrease in postprandial hyperglycaemia, however most clinically used drugs have undesirable side effects. Herbs and spices such as parsley, cinnamon, pepper, oregano, mint and cloves alleviate flatulence, diarrhoea and abdominal pain, counteracting the side effects commonly caused by α -amylase and α -glucosidase inhibitors. The *in silico* results identified which herbal compounds had better docking scores (more negative delta G values) than acarbose namely, apigenin, eriodictyol, piperine and rosmarinic acid. The *in vitro* studies revealed that all compounds, except myrcene, inhibited α -amylase and α -glucosidase in a dose-dependent manner. The K_i value of acarbose ($170 \pm 80 \mu\text{M}$), a widely prescribed α -glucosidase inhibitor, and eriodictyol ($130 \pm 70 \mu\text{M}$), apigenin ($160 \pm 50 \mu\text{M}$) and piperine ($280 \pm 120 \mu\text{M}$) were similar ($p > 0.05$). For α -amylase inhibition, the K_i value of acarbose ($3.8 \pm 1.9 \mu\text{M}$) and those of rosmarinic acid ($4.5 \pm 2.9 \mu\text{M}$), apigenin ($7.8 \pm 2.7 \mu\text{M}$) and cinnamic acid ($8.0 \pm 4.5 \mu\text{M}$) were similar ($p > 0.05$). The relationship between the *in silico* and *in vitro* results correlated well, where a more negative docking score translated to a higher *in vitro* inhibitory activity.

The effect of the herbal compounds on cell viability in C2C12 myotubes and HepG2 hepatocarcinoma cells, using the sulforhodamine B assay, was then determined. Eriodictyol and apigenin displayed noticeable toxicity against HepG2 and C2C12 cells. Acetyeugenol, cinnamic acid, myrcene, piperine and rosmarinic acid had similar ($p > 0.05$) IC_{50} values to acarbose in both cell lines.

Fluorescence detection was used to investigate the effects of each herbal compound on glucose uptake in HepG2 and C2C12 cells. All of the compounds significantly increased glucose uptake in these cell lines, compared to the control ($p < 0.05$), with efficacy in the same order as the positive control, insulin ($p > 0.05$).

This study provides evidence for the antidiabetic potential of herbal compounds in terms of their ability to prevent post-prandial hyperglycaemia, through the inhibition of starch hydrolysing enzymes, and alleviate hyperglycaemia by mimicking the action of insulin. The most promising compounds were cinnamic acid, piperine and rosmarinic acid. Using herbs and spices would have several advantages, including their widespread availability, easily cultivatable nature, affordability and health benefits. These compounds can easily be consumed through teas or using herbs and spices to flavour food.

Keywords:

Type 2 diabetes; α -amylase; α -glucosidase; herbal compounds; reverse molecular docking, *in vitro* cytotoxicity, insulin mimicking activity

TABLE OF CONTENTS

DECLARATION OF ORIGINALITY.....	
RESEARCH OUTPUTS.....	I
ACKNOWLEDGEMENTS.....	II
ABSTRACT.....	III
TABLE OF CONTENTS.....	VI
LIST OF FIGURES.....	IX
LIST OF TABLES.....	XI
LIST OF EQUATIONS.....	XII
LIST OF SYMBOLS AND NOTATIONS.....	XII
LIST OF ABBREVIATIONS.....	XIII
1. INTRODUCTION.....	1
1.1 DIABETES MELLITUS.....	1
1.2 THE GLOBAL PREVALENCE OF DIABETES MELLITUS.....	2
1.3 CLASSIFICATION OF DIABETES MELLITUS.....	4
1.3.1 <i>Type 2 diabetes mellitus</i>	4
1.3.2 <i>Gestational diabetes mellitus</i>	5
1.3.3 <i>Other causes of diabetes mellitus</i>	6
1.4 COMPLICATIONS CAUSED BY DIABETES MELLITUS.....	7
1.4.1 <i>Diabetic nephropathy</i>	7
1.4.2 <i>Diabetic neuropathy</i>	8
1.4.3 <i>Diabetic retinopathy</i>	8
1.4.4 <i>Cardiovascular diseases</i>	9
1.5 GLUCOSE METABOLISM AND REGULATION OF T2DM.....	9
1.5.1 <i>Glucose metabolism</i>	9
1.5.2 <i>Insulin and the regulation of glucose levels</i>	10
1.5.3 <i>Alpha-amylase and alpha-glucosidase</i>	12
1.6 TREATMENT OF TYPE 2 DIABETES.....	15
1.6.1 <i>Oral drugs</i>	15

1.6.2	<i>Injectable agents</i>	19
1.6.3	<i>Lifestyle changes</i>	19
1.7	HERBAL COMPOUNDS	20
1.8	<i>IN SILICO</i> METHODS USED TO IDENTIFY POSSIBLE ANTI-DIABETIC COMPOUNDS	24
1.8.1.	<i>Enzyme docking</i>	25
i.	<i>To obtain docking scores</i>	26
ii.	<i>To explore insulin regulatory properties</i>	27
1.9.	<i>IN VITRO</i> MODELS USED TO ASSESS ANTI-DIABETIC COMPOUNDS.....	29
1.9.1.	<i>Inhibition of carbohydrate hydrolysing enzymes</i>	29
1.9.2.	<i>Glucose uptake in liver and muscle cells</i>	30
1.9.3.	<i>Cell toxicity</i>	31
2.	AIM AND HYPOTHESES	32
3.	RESEARCH OBJECTIVES	34
4.	EXPERIMENTAL DESIGN AND METHODOLOGY	35
4.1	<i>IN SILICO</i> STUDY	35
i.	<i>Docking studies on Maestro</i>	35
ii.	<i>Docking to insulin-regulating targets</i>	37
iii.	<i>Calculation of physiochemical properties</i>	37
iv.	<i>Determination of chemical – protein cross reactions on STITCH</i>	38
4.2	<i>IN VITRO</i> STUDY	38
4.2.1	<i>Chemicals</i>	38
4.2.2	<i>Kinetics of α-amylase inhibition</i>	39
4.2.3	<i>Kinetics of α-glucosidase inhibition</i>	42
4.2.4	<i>Cell toxicity</i>	45
4.2.5	<i>Glucose uptake assay</i>	48
4.3	DATA ANALYSIS	50
5.	RESULTS	51
5.1	MOLECULAR DOCKING	51
5.2	DOCKING TO INSULIN-REGULATING TARGETS.....	55
5.3	<i>IN SILICO</i> PHYSIOCHEMICAL PROPERTIES	56
5.4	CHEMICAL – PROTEIN CROSS REACTIONS	57

5.5	INHIBITION OF A-AMYLASE AND A-GLUCOSIDASE	64
5.6	CYTOTOXICITY IN C2C12 AND HEPG2 CELL LINES	68
5.7	GLUCOSE UPTAKE IN C2C12 AND HEPG2 CELL LINES	69
5.8	DAILY HERBAL DOSE EQUIVALENT TO ACARBOSE DOSE	70
6.	DISCUSSION	72
6.1	<i>IN SILICO</i> DOCKING TO CARBOHYDRATE HYDROLYSING ENZYMES	73
6.2	<i>IN SILICO</i> DOCKING TO INSULIN-REGULATING TARGETS.....	74
6.3	<i>IN SILICO</i> PHYSIOCHEMICAL PROPERTIES	75
6.4	DRUG-TARGET NETWORKS THROUGH STITCH.....	77
6.5	INHIBITION OF A-AMYLASE AND A-GLUCOSIDASE	81
6.6	CYTOTOXICITY IN C2C12 AND HEPG2 CELL LINES	85
6.7	INSULIN MIMICKING EFFECTS <i>IN VITRO</i>	87
6.8	POSSIBLE MECHANISM(S) OF ACTION OF THE HERBAL COMPOUNDS.....	89
6.9	DOSAGE.....	98
7.	STUDY OVERVIEW	99
8.	CONCLUSION.....	103
9.	FUTURE WORK	105
10.	REFERENCES	107
11.	APPENDIX I: ADDITIONAL RESULTS	133
11.1	<i>IN SILICO</i> RESULTS	133
11.2	<i>IN VITRO</i> RESULTS.....	137
12.	APPENDIX II: ETHICAL APPROVAL	145

LIST OF FIGURES

Figure 1: Global estimate of diabetes (T1DM and T2DM).....	3
Figure 2: The structure of Insulin.	11
Figure 3: Insulin mediated glucose uptake and metabolism, via the translocation of GLUT-4 in muscle (C2C12) cells.	12
Figure 4: The structures of the enzymes (a) α -amylase (PDB code: 4GQR) and (b) α -glucosidase (3L4Y).....	13
Figure 5: An example of the reaction catalysed by α -amylase.....	14
Figure 6: An example of a reaction catalysed by α -glucosidase.....	14
Figure 7: The structure of metformin.....	15
Figure 8: (a) The general structure of sulfonylureas.	17
Figure 9: (a) The general structure of thiazolidinediones	17
Figure 10: The structures of the anti-diabetic drugs; (a) acarbose, (b) miglitol and (c) voglibose..	18
Figure 11: Schematic illustration of docking a small molecule ligand (green) to a protein target (black) producing a stable complex.....	25
Figure 12: Maestro's Glide docking 'funnel', showing the glide docking hierarchy.	27
Figure 13: The reduction of DNSA (yellow) to ANSA (orange red) in the presence of a reducing sugar.....	39
Figure 14: α -glucosidase catalyses the reaction of the substrate pNPG to produce glucose and p-nitrophenolate, with the addition of sodium hydroxide.....	42
Figure 15: The structure of (a) glucose and (b) the fluorescent glucose analog 2-NBDG.	48
Figure 16: Drug-target interaction network of acarbose.	58
Figure 17: Drug-target interaction network of eriodictyol.....	59
Figure 18: Drug-target interaction network of apigenin.	60
Figure 19: Drug-target interaction network of cinnamic acid.	61
Figure 20: Drug-target interaction network of piperine.....	62
Figure 21: Drug-target interaction network of rosmarinic acid.	63
Figure 22: The correlation between negative delta G versus the K_i value of herbal compounds for α -amylase.....	67
Figure 23: The correlation between negative delta G versus the K_i value of herbal compounds for α -glucosidase.	67

Figure 24: The effect of herbal compounds on glucose uptake in C2C12 cells.....	69
Figure 25: The effect of herbal compounds on glucose uptake in HepG2 cells.	70
Figure 26: Insulin mediated glucose uptake and metabolism, via the translocation of GLUT-4 in muscle (C2C12) cells.....	89
Figure 27: GLUT-4 translocation, mediated by the MAPK and AMPK pathways through the binding of adiponectin in C2C12.....	92
Figure 28: GLUT-1 biosynthesis in HepG2 cells.	93
Figure 29: Inhibition of PTP1B to prevent dephosphorylation of the insulin receptor substrate, which activates the PI3K/AKT insulin signalling cascade.....	95
Figure 30: The proposed mechanisms of the anti-diabetic and hypoglycaemic effects of the herbal compounds.....	102
Figure S1: Ligand interaction diagrams showing the amino acids interacting acarbose and the herbal compounds in the active site of the enzyme, α -amylase (4GQR)	134
Figure S2: Ligand interaction diagrams showing the amino acids interacting with acarbose and the herbal compounds in the active site of the enzyme, α -glucosidase (3L4Y)	136
Figure S3: The linear increase in absorbance with increasing concentrations of maltose (0 – 0.46 mM).	137
Figure S4: The linear increase in absorbance with increasing concentrations of p-nitrophenol (0 – 200 μ M). From this standard curve the slope is used to calculate the molar extinction coefficient of p-nitrophenol.	138
Figure S5: Michaelis-Menten graphs of the inhibition of α -amylase by acarbose (control) and herbal compounds.....	139
Figure S6: Michaelis-Menten graphs of the inhibition of α -glucosidase by acarbose (control) and herbal compounds.....	140
Figure S7: Lineweaver-Burk graphs of the inhibition of α -amylase by acarbose (control) and herbal compounds.....	141
Figure S8: Lineweaver-Burk graphs of the inhibition of α -glucosidase by acarbose (control) and herbal compounds.....	142
Figure S9: Viability of C2C12 cells after 72 h exposure to acarbose (control) and herbal compounds.....	143
Figure S10: Viability of HepG2 cells after 72 h exposure to acarbose (control) and herbal compounds.....	144

LIST OF TABLES

Table 1: WHO diabetes diagnostic criteria	1
Table 2: The metabolic processes that influence blood glucose levels.....	10
Table 3: Properties of investigated herbal compounds, and their sources.....	23
Table 4: DIA-DB protein targets affecting insulin secretion and/or sensitivity	28
Table 5: The final number of nano moles of each reagent in every reaction (well) of the maltose standard curve.....	40
Table 6: The final amount of each reagent in every reaction (well) of the α -amylase inhibition assay	42
Table 7: The final number of nano moles of each reagent in every reaction (well) of the p-nitrophenolate standard curve.....	43
Table 8: The final amount of each reagent in every reaction (well) of the α -glucosidase inhibition assay.....	44
Table 9: Ascending Glide HTVS docking scores of the herbal compounds docked to α -amylase	52
Table 10: Ascending Glide HTVS docking scores of the herbal compounds docked to α -glucosidase	52
Table 11: The structures of the herbal compounds	53
Table 12: Amino acids interacting with starch and the herbal compounds in the active site of the enzyme, α -amylase (4GQR).....	54
Table 13: Amino acids interacting with starch and the herbal compounds in the active site of the enzyme, α -glucosidase (3L4Y)	54
Table 14: Docking scores (kcal/mol) of the herbal compounds to protein targets (PDB code) regulating insulin secretion and/or sensitivity	55
Table 15: In silico physiochemical properties of herbal compounds	56
Table 16: Action between targets represented by line colour	57
Table 17: Drug-target interactions of acarbose, arranged from high to low scores	58
Table 18: The drug-protein interactions of eriodictyol arranged from high to low scores	59
Table 19: The drug-protein interactions of apigenin arranged from high to low scores	60
Table 20: The drug-protein interactions of cinnamic acid arranged from high to low scores	61
Table 21: The drug-protein interactions of piperine arranged from high to low scores.....	62

Table 22: The drug-protein interactions of rosmarinic acid, arranged from high to low scores	63
Table 23: Michaelis-Menten parameters for the inhibition of α -amylase by herbal compounds	65
Table 24: Michaelis-Menten parameters for the inhibition of α -glucosidase by herbal compounds.....	65
Table 25: Inhibitory activity of herbal compounds against porcine pancreatic α -amylase.....	66
Table 26: Inhibitory activity of herbal compounds against yeast α -glucosidase.....	66
Table 27: IC_{50} values of herbal compounds on C2C12 and HepG2 cells.....	68
Table 28: The herbal dosage equivalent to a daily dose of acarbose with the potential to inhibit α -amylase and α -glucosidase	71
Table 29: Overview of the most significant in vitro and in silico results of the study.....	99

LIST OF EQUATIONS

Equation 1: The Beer Lambert law. A is the absorbance, ϵ is the molar absorption coefficient ($M^{-1}.cm^{-1}$), λ is the light path (cm) and c is the concentration (M).	40
Equation 2: The equation used to calculate cell viability as a percentage of the control.....	47
Equation 3: The equation used to calculate the relative fluorescent units.	49

LIST OF SYMBOLS AND NOTATIONS

α	Alpha
$^{\circ}C$	Degrees Celsius
μM	Micromolar
μL	Microliter
%	Percentage
λ	Wavelength
λ_{em}	Emission wavelength
λ_{ex}	Excitation wavelength

LIST OF ABBREVIATIONS

2-NBDG 2-deoxy-2-[(7-nitro-2,1,3-benzoxadiazol-4-yl) amino]-D-glucose

A

AdipoR1 Adiponectin receptor 1
ADMET Absorption, distribution, metabolism, excretion and toxicity
AMP Adenosine monophosphate
AMPK Adenosine monophosphate activated protein kinase
ANSA 3-amino-5-nitrosalicylic acid
APPL1 Adaptor protein
ATP Adenosine triphosphate
AUC Area under curve

C

C2C12 Immortalized mouse myoblast cell line
cAMP Cyclic adenosine monophosphate
CCR₃ Chemokine receptor 3
CYP Cytochrome
CYP_{1B1} Cytochrome p450

D

DM Diabetes Mellitus
DME Diabetic macular oedema
DMEM Dulbecco's modified Eagle's medium
DN Diabetic neuropathy
DNSA 3,5-dinitrosalicylic acid
DR Diabetic retinopathy

F

FCS	Foetal calf serum
FFAR1	Free fatty acid receptor 1

G

<i>g</i>	Gravitational force
G6P	Glucose-6-phosphate
GDM	Gestational diabetes mellitus
GIT	Gastrointestinal
GLP-1	Glucagon-like peptide-1
GLUT	Glucose transporters
GST	Glutathione S-transferase

H

h	Hour
HBSS	Hank's balanced salt solution
HepG2	Human liver cancer cell line
HG	Hyperglycaemia
HMOX ₁	Heme oxygenase

I

IDF	International Diabetes Federation
IKBKB	Inhibitor of kappa light polypeptide gene enhancer
IL ₂	Interleukin 2
IL ₆	Interleukin 6

K

K _i	Inhibition constant
K _m	Michaelis constant

M

MAPK	Mitogen-activated protein kinase
MET	Mitochondrial electron transport
mTOR	Mammalian target of rapamycin

N

NADH	Nicotinamide adenine dinucleotide
NOAEL	No observed adverse effect level

P

p53	Tumour protein p53
p70S6K	Small ribosomal subunit protein 6 kinase
PBS	Phosphate buffered saline
PDB	Protein data bank
PK1	PIP ₃ – dependent kinase 1
PEPCK	Phosphoenolpyruvate carboxykinase
PI3K	Phosphatidylinositol-3-kinase
PIP ₃	Phosphatidylinositol-3,4,5-triphosphate
PKA	Protein kinase A
PKB	Protein kinase B
PKC	Protein kinase C
pNPG	p-nitrophenol glucopyranoside
PPAR-λ	Peroxisome proliferator-activated receptor-gamma
PPARs	Peroxisome proliferator-activated receptors
PTP1B	Protein tyrosine phosphatase 1B

R

ROS	Reactive oxygen species
-----	-------------------------

rpm Revolutions per minute

RXR Retinoid x receptor

S

SA South Africa

SD Standard deviation

SMILES Simplified molecular input line entry system

SRB Sulforhodamine B

SUR Sulfonylurea receptors

T

TBK₁ TANK-binding kinase 1

TCA Trichloroacetic acid

T1DM Type 1 Diabetes mellitus

T2DM Type 2 Diabetes mellitus

TNF Tumour necrosis factor

TYR Tyrosine kinase

TZD Thiazolidinediones

V

vdW van der Waals

V_{max} Maximum velocity

VSW Virtual Screening Workflow

W

WHO World Health Organization

w/v Weight per volume

U

UGT_{1A1} UDP glucuronosyl-transferase 1

1. INTRODUCTION

1.1 Diabetes mellitus

Diabetes mellitus (DM), commonly called diabetes, is a chronic endocrinological and metabolic disorder characterised by abnormal high blood glucose levels (hyperglycaemia) (Goldenberg & Punthakee, 2013). Hyperglycaemia (HG) occurs either when the pancreas does not produce enough insulin or when the body cannot effectively use the produced insulin (Ighodaro, 2018). As a result, defective carbohydrate, lipid and protein metabolism becomes apparent (Silverthorn & Johnson, 2010). Consequently, high blood glucose levels affect many organs including; the heart, eyes, kidneys, and nerves, these effects further contribute to complications that develop later on (Cho *et al.*, 2018). Diabetes is diagnosed based on the criteria in Table 1 (IDF, 2019).

Table 1: WHO diabetes diagnostic criteria

	Normal	Impaired Glucose Tolerance	Diabetes
Fasting Plasma Glucose (mmol/L)	< 5.6	≥ 5.6 and < 7	≥ 7.0
2 h Plasma Glucose (mmol/L)	< 7.8	≥ 7.8 and < 11.1	≥ 11.1
HbA1c (mmol/mol)	< 42	≥ 42 and < 46	≥ 48
Random Plasma Glucose (mmol/mol)			> 11.1

(IDF, 2019)

1.2 The global prevalence of diabetes mellitus

DM is one of the greatest health challenges of the 21st century and is amongst the top 10 causes of mortality globally. Initially, the global adult DM prevalence in 1995 was estimated to be 4% and was expected to rise to 5.4% by the year 2025 (King *et al.*, 1998), with the number of cases expected to rise from 135 million in 1995 to 300 million in 2025 (King *et al.*, 1998). However, this estimate was surpassed less than a decade and a half later; by 2010, 366 million people were already living with DM. Currently, there are about 463 million (8.8%) people across the world with DM, with 4.2 million deaths in 2019 alone (IDF, 2019).

The top 10 countries, from the highest to lowest number of DM cases are China, India, USA, Pakistan, Brazil, Mexico, Indonesia, Germany, Egypt and Bangladesh, (IDF, 2019). The top 10 countries, from highest to lowest prevalence of DM are Marshall Islands, Mauritius, Tuvalu, Kiribati, Sudan, New Caledonia, Pakistan, Solomon Islands, Guam and French Polynesia, (IDF, 2019). This identifies the Middle East, Northern Africa, Northern America and Caribbean, Western Pacific and South East Asia as the regions with the highest incidence of DM, accounting for approximately 62% of the global DM cases (IDF, 2019).

On the African continent, there are about 20 million people with DM and this number is expected to double by 2045 (IDF, 2019). South Africa is one of the countries with the highest number of DM in Africa. The International Diabetes Federation (2019) reported that 12.7% (Figure 1) of the South African population suffers from DM, which is around 7 million people. A major challenge is that one in two people that develops DM are undiagnosed, with Africa having the second-highest incidence of undiagnosed DM in the world. Therefore, a more accurate prediction of the percentage of DM in South Africa is about 20% (Williams *et al.*, 2019).

DM is the second highest cause of death in South Africa, second only to tuberculosis (Stats SA, 2017). Worldwide, DM kills around 4 million people per year (IDF, 2019). Six hundred and ninety thousand people died of HIV/AIDS-related illnesses in 2019 (UNAIDS, 2019), while malaria and tuberculosis (TB) killed about 400 000 (WHO, 2020a) and 1.5 million (WHO, 2020b) people worldwide respectively. Thus, DM kills more people per year than HIV/AIDS, TB and malaria combined.

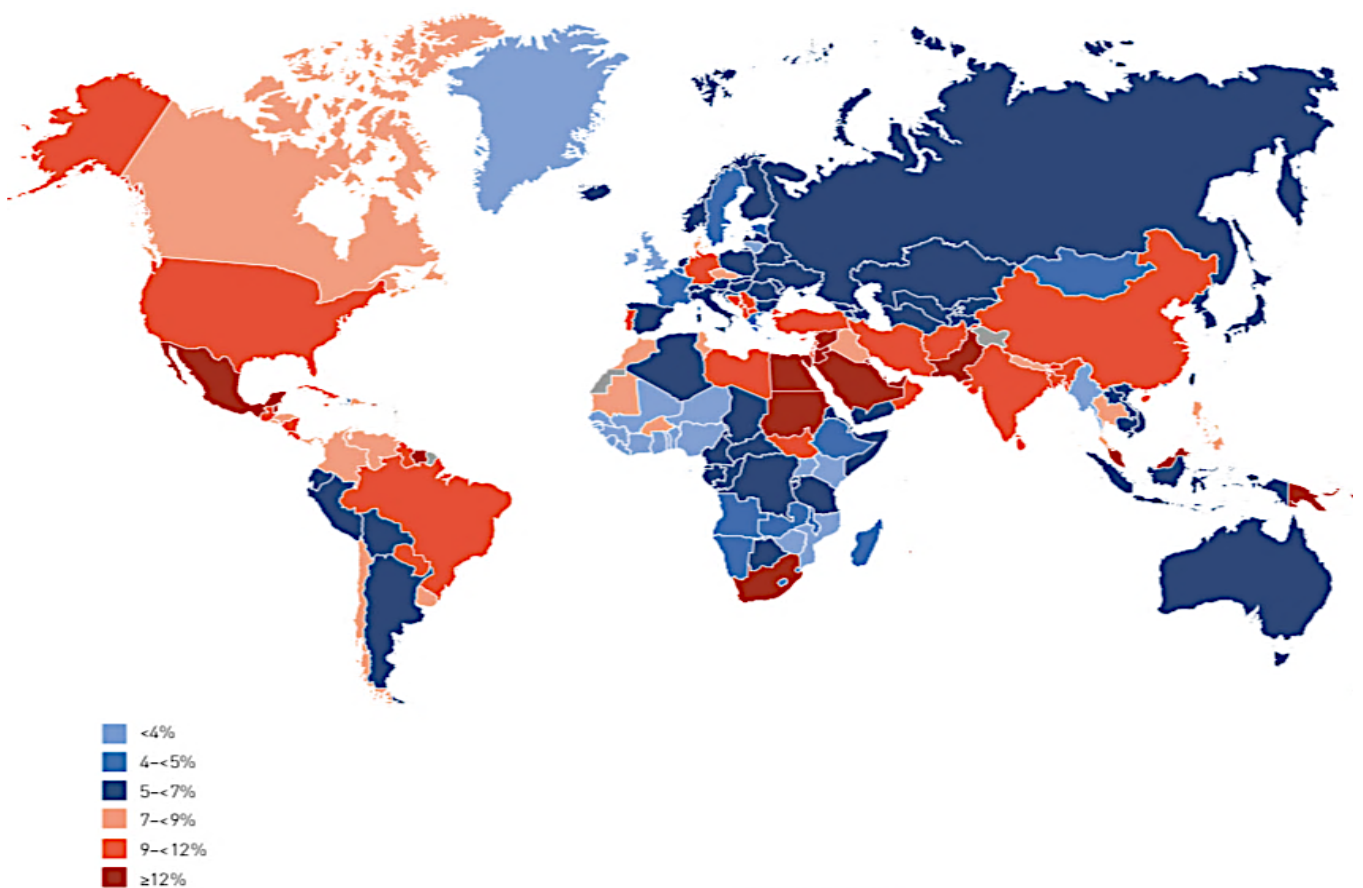


Figure 1: Global estimate of diabetes (T1DM and T2DM). The percentage of people diagnosed with diabetes mellitus per country, in 2019, amongst 20 to 79-year-old individuals (Williams *et al.*, 2019)

1.3 Classification of diabetes mellitus

The correct classification of DM is an essential requirement for clinical management, epidemiological and clinical research (Alberti *et al.*, 1998). DM was classified based on the age of onset or type of therapy, however the pathogenic process that leads to hyperglycaemia has become the primary basis on which DM is classified today (Powers, 2013).

We can distinguish between three major types of diabetes:

- Type 1 diabetes mellitus (T1DM)
- Type 2 diabetes mellitus (T2DM)
- Gestational diabetes mellitus (GDM)

1.3.1 Type 2 diabetes mellitus

T2DM is the most prevalent type of diabetes, despite it being largely preventable. It accounts for almost 90% of all diabetic cases (Williams *et al.*, 2019). T2DM is also frequently called adult-onset diabetes or non-insulin-dependent DM (Alberti *et al.*, 1998). In T2DM, hyperglycaemia occurs because of insulin resistance and relative (not absolute) insulin deficiency. The exact cause of T2DM is unknown, however autoimmune destruction of pancreatic β -cells does not occur. Various factors can contribute to the pathophysiological disorders responsible for impaired glucose homeostasis in T2DM, including environmental influences (unhealthy diet, obesity, inactivity) and genetic factors (Alberti *et al.*, 1998). An unhealthy diet refers to a diet high in fat, salt, sugar and cholesterol, and low in fibre (National Institute of Diabetes and Digestive and Kidney Diseases, 2016). Inactivity refers to less than 30 minutes of physical activity for 5 days per week (National Institute of Diabetes and Digestive and Kidney Diseases, 2016).

Some of the risk factors for T2DM (Alberti *et al.*, 1998) include:

- Overweight or obese
- Family history of DM
- Aged over 45
- High blood pressure ($\geq 140/90$ mmHg)
- History of gestational DM
- History of heart disease or stroke
- Ethnicity (African or African American)

Although T2DM is mostly seen in adults, there is a surge in the number of children and adolescents with T2DM and this is due to an increase in poor diets, physical inactivity, and obesity. T2DM can be managed by losing excess weight and choosing a healthy lifestyle combined with medical treatment.

1.3.2 Gestational diabetes mellitus

GDM can be defined as glucose intolerance first detected during pregnancy (Alberti *et al.*, 1998), it occurs in about 13% of all births (Alberti *et al.*, 1998). GDM only last for the duration of the pregnancy however, 50% of women may develop T2DM later in life (Kampmann *et al.*, 2015). GDM occurs as the placenta produces various hormones during pregnancy, which may diminish the effect of insulin (Kampmann *et al.*, 2015). Most symptoms of T2DM are also seen in GDM, but GDM is usually diagnosed through prenatal screening (a fasted glucose test) rather than reported symptoms (Alberti *et al.*, 1998). Gestational DM can be managed by a healthy diet, physical exercise, blood-glucose monitoring and oral medication (Williams *et al.*, 2019).

1.3.3 Other causes of diabetes mellitus

Despite their low prevalence, this category was created to accommodate diabetic states that occur due to clearly established, non-classical causes of DM that can either be acquired or be caused by genetics (Jones & Hattersley, 2010). These causes include the following subtypes, monogenic causes of DM, drug-induced DM, endocrine disorders, and pancreatic disorders (Jones & Hattersley, 2010).

Monogenic causes of diabetes result from a single gene mutation that causes β -cell dysfunction or, less commonly, insulin resistance (Jones & Hattersley, 2010). Drug-induced DM can be caused by many frequently used drugs that interfere with glucose homeostasis and can provoke hyperglycaemia or worsen glycaemic control in patients who already have DM (Gittoes *et al.*, 2010). Some of these drugs include; glucocorticoids, diuretics, β -blockers, phenytoin, cyclosporine, diazoxide, and nicotinic acid derivatives (Gittoes *et al.*, 2010). Phenytoin, an anti-seizure medication, can induce hyperglycaemia through the inhibition of insulin release (al-Rubeaan & Ryan, 1991). Immunosuppressant treatment with cyclosporine can result in the impairment of insulin synthesis and secretion (Dresner *et al.*, 1989). Diazoxide is prescribed to treat hypoglycaemia, however excess use can cause increased glucose production, decreased insulin production and inhibition of glucose uptake (Altzuler *et al.*, 1977). Glucocorticoids are anti-inflammatory drugs that can cause increased insulin resistance, increased glucose intolerance and suppression of glucose production (Suh & Park, 2017). β -blockers are prescribed to reduce blood pressure but can impair the release of insulin from pancreatic β -cells (Rehman *et al.*, 2011), while diuretics can cause insulin resistance, inhibition of glucose uptake and a decrease in insulin release (Rehman *et al.*, 2011).

Many endocrine disorders such as acromegaly, Cushing syndrome, pheochromocytoma, glucagonoma, and thyrotoxicosis can lead to DM due to excess hormones, which counter regulate insulin and act by inhibiting insulin secretion and/or action (Hanley, 2010). Pancreatic disorders are a rare cause of DM however, chronic pancreatitis can lead to DM due to endo- and exocrine damage to the pancreas (Unnikrishnan & Mohan, 2010).

1.4 Complications caused by diabetes mellitus

People suffering from T1DM or T2DM can develop serious complications (Nickerson & Dutta, 2012) that are responsible for significant morbidity and mortality. The magnitude and duration of hyperglycaemia caused by DM will determine the severity of these complications. The complications can be broadly divided into microvascular and macrovascular, with the former having a much higher prevalence than the latter (Papatheodorou *et al.*, 2018). Some of the most common microvascular complications include nephropathy, neuropathy, and retinopathy (Papatheodorou *et al.*, 2018). Macrovascular complications mostly consist of peripheral artery disease, coronary heart disease, and stroke.

1.4.1 Diabetic nephropathy

Diabetic nephropathy is seen in one-third of all diabetic patients and refers to the deterioration of kidney function due to hyperglycaemia (Sulaiman, 2019). Various studies indicate that DM is the leading cause of end-stage renal failure (Rychilik *et al.*, 1998). Diabetic nephropathy is a degenerative disease in which the glomeruli are damaged, affecting the filtration capacity of the kidneys. The disease can be diagnosed by identifying an increased amount of protein excreted in the urine (albuminuria). The development and progression of nephropathy are prevented by drugs that reduce the activity of the renin-angiotensin-aldosterone system (Williams *et al.*, 2019).

1.4.2 Diabetic neuropathy

Diabetic neuropathy (DN) affects over 90% of all diabetic patients (Williams *et al.*, 2019). It can be defined as signs and symptoms of peripheral nerve dysfunction in a patient with DM (Bansal, 2006). High blood glucose causes damage to the nerves (Williams *et al.*, 2019). Peripheral neuropathy is the most common form of DN and is characterised by pain, numbness, and tingling of the extremities (Williams *et al.*, 2019). It affects the distal nerves of the limbs, predominantly those of the feet, causing diabetic foot. Damage to the foot muscles leads to immobility which produces foot deformities that create pressure points (Pendsey, 2010), where subsequent skin breakdown and ulceration can occur (Pendsey, 2010). Bacterial infections can occur and eventually, if not treated effectively, can lead to the development of gangrene. Treatment and prevention include glycaemic control, frequent foot assessments, suitable footwear and patient education (Pendsey, 2010).

1.4.3 Diabetic retinopathy

Diabetic retinopathy (DR) is one of the most common microvascular complications of DM (Duh *et al.*, 2017) and affects millions of people worldwide (Duh *et al.*, 2017). It occurs because of chronic hyperglycaemia, which leads to damage of the retinal capillaries. DR can cause cataracts, glaucoma and diabetic macular oedema (DME), all of which may lead to loss of vision and eventually blindness (Williams *et al.*, 2019). Regular retinal screening is necessary as DR is largely asymptomatic in the early stages. DM management is the primary prevention intervention for DR (Duh *et al.*, 2017).

1.4.4 Cardiovascular diseases

According to the IDF, people with DM are 2 to 3 times more likely to have cardiovascular diseases (CVD). Although the mechanism of action in which DM causes CVD is poorly understood, it is theorised that hyperglycaemia over activates the blood coagulation system causing clot formation. DM is also associated with high cholesterol and blood pressure, thus diseases such as coronary artery disease (CAD), strokes and peripheral artery disease (PAD) develops (Williams *et al.*, 2019). Blood glucose management is essential to prevent CVD. A healthy lifestyle with increased physical activity, smoking cessation and avoidance of excessive alcohol consumption is also necessary (Williams *et al.*, 2019).

1.5 Glucose metabolism and regulation of T2DM

1.5.1 Glucose metabolism

Glucose is a monosaccharide best known for its role as a primary metabolite for energy production in the body. Complex carbohydrates are broken down into simple sugars such as glucose, fructose or galactose (Williams *et al.*, 2019). The liver, pancreas and small intestine regulate the absorption, storage, and production of glucose (Aronoff *et al.*, 2005). Blood glucose concentration is a function of the rate of glucose entering against the rate of glucose removal from the circulation. Hormones such as insulin, cortisol, and glucagon regulate blood glucose levels (Aronoff *et al.*, 2005). These hormones regulate glucose entry into cells and affect metabolic processes (Table 2) such as glycolysis, gluconeogenesis, and glycogenolysis. Glycolysis is the main catabolic pathway that occurs in the body. It uses glucose as its substrate to provide energy in the form of ATP (Adenosine triphosphate) (Patolia & Mahmood, 2018).

Table 2: The metabolic processes that influence blood glucose levels

Process	Description	Glucose	Organ
Glycolysis	Glucose molecules are split and converted to two three-carbon units (pyruvate)	↓ glucose	Liver
Gluconeogenesis	New glucose molecules from non-carbohydrate and carbohydrate precursors	↑ glucose	Liver Kidney
Glycogenolysis	Glycogen is broken down to glucose	↑ glucose	Liver Muscle
Glycogenesis	Glucose molecules are added to chains of glycogen (glycogen synthesis)	↓ glucose	Liver

1.5.2 Insulin and the regulation of glucose levels

Insulin (Figure 2) is a peptide hormone secreted by the β -cells of the pancreatic islets of Langerhans (Wilcox, 2005). This hormone facilitates cellular glucose uptake and regulates carbohydrate, protein and lipid metabolism to maintain normal blood glucose levels (Wilcox, 2005). The synthesis and secretion of insulin is primarily regulated by glucose. Other hormones like oestrogen, melatonin, leptin and the growth hormone might also affect insulin secretion (Fu *et al.*, 2013). Glucose intake disrupts the balance between glucose production and glucose uptake by tissues. As soon as the plasma blood glucose concentration is increased the pancreatic β -cells are stimulated to release insulin. Once insulin is secreted, it stimulates glucose uptake and suppresses endogenous glucose production (Cersosimo *et al.*, 2018). Insulin binds to specialised receptors found on the surface of target cells in the adipose tissue, liver and skeletal muscle. As seen in Figure 3, as soon as insulin binds to these receptors a series of phosphorylation reactions occur. These reactions lead to the translocation of glucose transporters (GLUT) to cellular membranes (Nolte, 2009). The increased number of glucose transporters will allow more cellular glucose uptake, decreasing the blood glucose levels (Patolia & Mahmood, 2018).

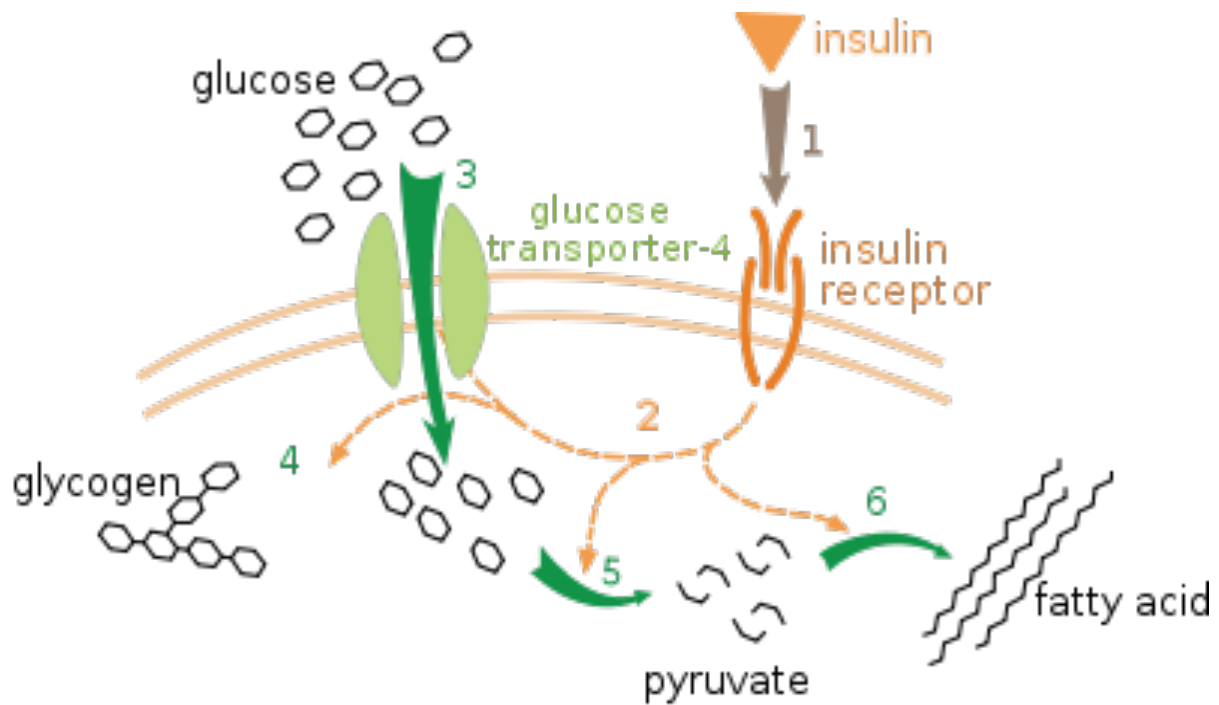
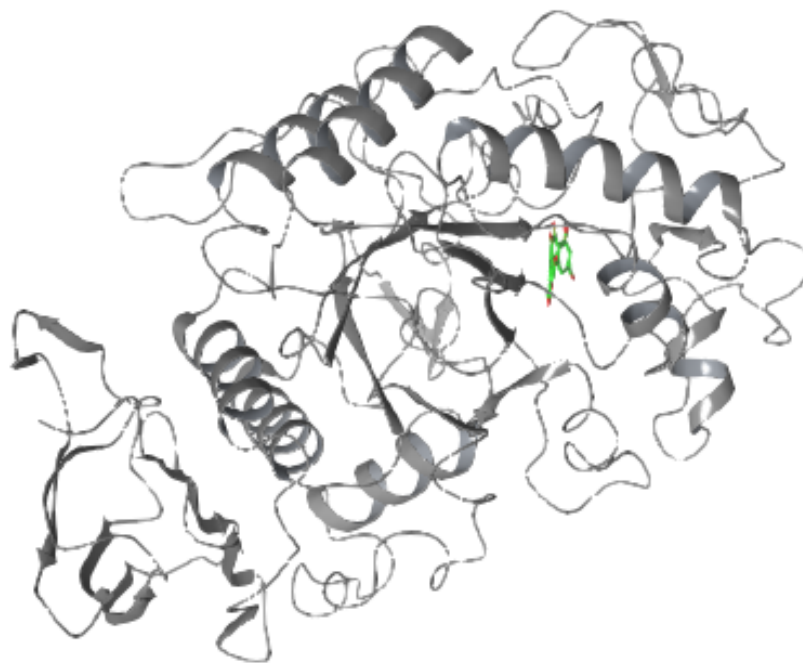


Figure 3. Insulin mediated glucose uptake and metabolism, via the translocation of GLUT-4 in muscle (C2C12) cells. (1) Insulin bind to the INSR receptor, (2) activation of protein cascades involving PI3K and AKT, (3) translocation of GLUT-4 transporters to the plasma membrane, (4) influx of glucose, (5) glycogen synthesis, (6) glycolysis and (7) fatty acid synthesis. This image was obtained from an open source public domain, information was validated to be in accordance with Meyer *et al.* (2008)

1.5.3 Alpha-amylase and alpha-glucosidase

Alpha-amylase (Figure 4a) and alpha-glucosidase (Figure 4b) are enzymes found in the GIT and play an important role in the metabolism of carbohydrates. As soon as carbohydrates enter the intestinal lumen, the pancreas secretes α -amylase (Meyer *et al.*, 2008) that cleaves the $\alpha(1,4)$ -glycosidic bonds in starch. Amylase mediates the hydrolysis (Figure 5) of polysaccharides containing more than three glucose units, into smaller molecules (di- and trisaccharides) (Proença *et al.*, 2019), which can be digested further by α -glucosidase (Proença *et al.*, 2017; Proença *et al.*, 2019; Rivera-Chavez *et al.*, 2013).

a.



b.

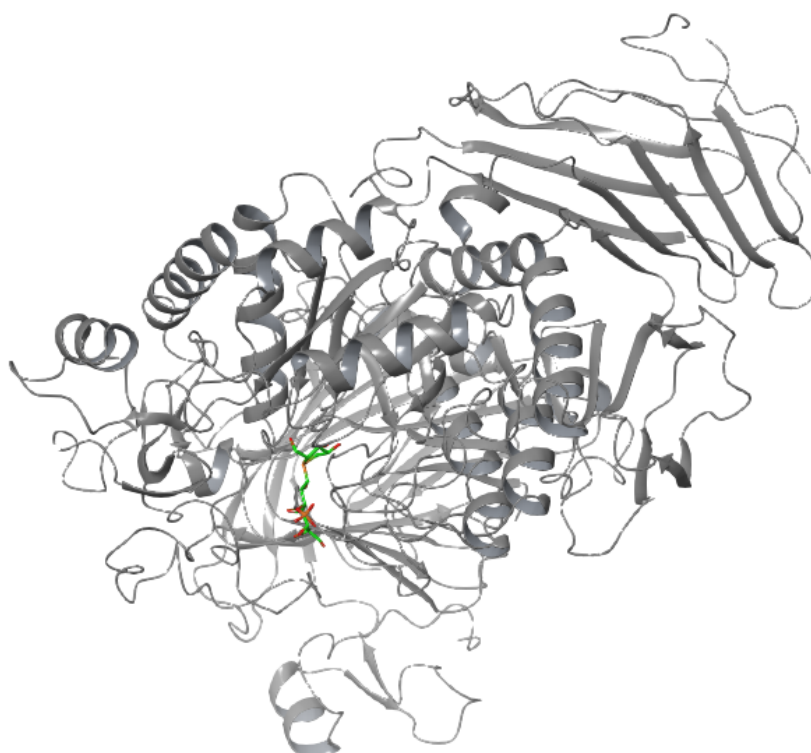


Figure 4: The structures of the enzymes (a) α -amylase (PDB code: 4GQR) (Williams *et al.*, 2012) and (b) α -glucosidase (3L4Y) (Sim *et al.*, 2010). The chains are shown in grey and the ligand in green. The structures were generated on Maestro (Maestro, 2020).

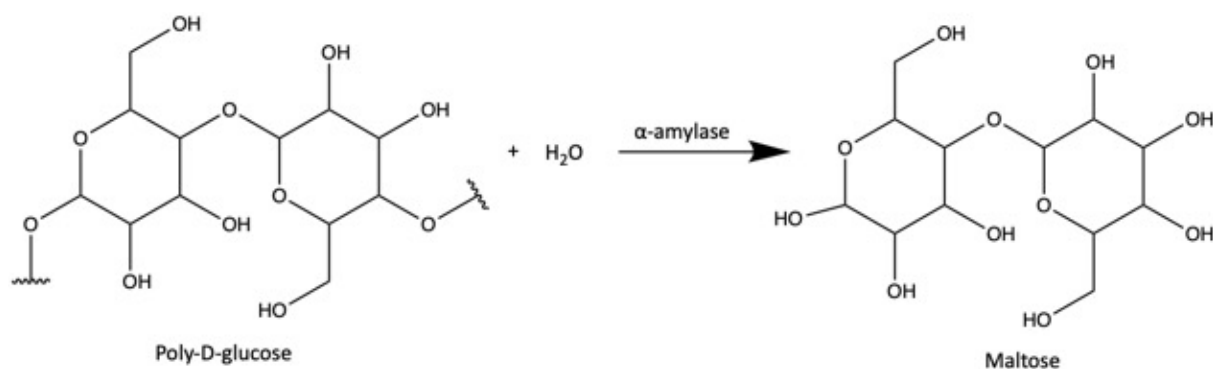


Figure 5: An example of the reaction catalysed by α -amylase. Starch is hydrolysed to form simpler sugars such as maltotriose, maltose and glucose. Created using ChemDraw version 19.1 (ChemDraw, 2020).

Alpha-glucosidase is found in the brush border of the intestine and is responsible for the hydrolysis of $\alpha(1,4)$ -glycosidic bonds at the nonreducing end of oligosaccharides (Feher, 2017). This hydrolysis reaction (Figure 6) will release a terminal glucose molecule. Once the glucose molecule is released it can be absorbed into the bloodstream, increasing the blood glucose levels (Brayer *et al.*, 2000; Powers *et al.*, 2003; Proenca *et al.*, 2017).

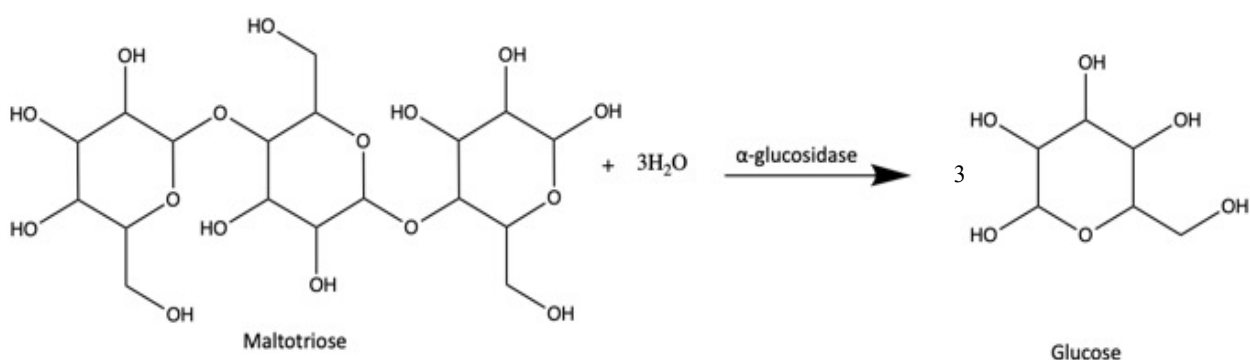


Figure 6: An example of a reaction catalysed by α -glucosidase. Maltotriose will be further hydrolysed to release a terminal glucose molecule. Created using ChemDraw version 19.1 (ChemDraw, 2020).

1.6 Treatment of type 2 diabetes

The treatment of T2DM includes oral drugs and injectable agents (Marin-Penalver *et al.*, 2016) and lifestyle changes, the aim of which to treat hyperglycaemia and relieve diabetic symptoms (Bastaki, 2005). The secondary aim is to prevent long-lasting complications and eliminate risk factors to increase longevity (Bastaki, 2005). Patients with T1DM rely on insulin therapy, while lifestyle and diet modifications form the cornerstone for T2DM management and treatment.

1.6.1 Oral drugs

Oral drugs are prescribed to treat underlying metabolic disorders, such as insulin resistance or inadequate insulin secretion and should be combined with a healthy diet and physical activity (Bastaki, 2005).

1.6.1.1 Metformin

Metformin (Figure 7) is a first-line treatment for T2DM since it is more effective than other oral drugs. The mechanism of action of metformin involves changing the composition of the gut microbiota and activating mucosal adenosine monophosphate (AMP)-activated protein kinase (AMPK), which is responsible for the maintenance of the intestinal barrier integrity (Marin-Penalver *et al.*, 2016).

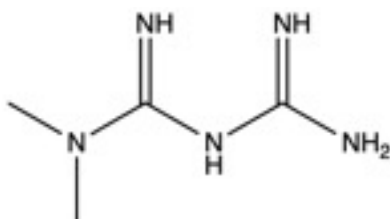


Figure 7: The structure of metformin. Created using ChemDraw version 19.1 (ChemDraw, 2020).

Studies have shown that metformin can inhibit gluconeogenesis through four possible mechanisms (Marin-Penalver *et al.*, 2016), activating hepatic AMPK through liver-kinase B1, inhibition of glucagon cyclic adenosine monophosphate (cAMP) production by blocking adenylyl cyclase, inhibiting nicotinamide adenine dinucleotide (NADH) coenzyme Q oxidoreductase in the mitochondrial electron transport chain (MET) to ATP and increase AMP/ATP ratio which activates AMPK and lastly through the inhibition of mitochondrial glycerol phosphate dehydrogenase.

Metformin is generally well tolerated. However, it can cause gastrointestinal (GIT) side effects such as nausea, abdominal discomfort, and diarrhoea.

1.6.1.2 Sulfonylureas

Patients with T2DM often use sulfonylureas (Figure 8) as a second-line treatment. The mechanism of action of sulfonylureas involves the stimulation of pancreatic β -cells to release insulin by binding to the sulfonylurea receptors (SUR) on their plasma membrane. This causes a closure of ATP-sensitive potassium channels leading to a depolarisation of the cell membrane. The depolarisation causes the voltage-gated channels to open, allowing an influx of calcium ions and ultimately insulin release (Bastaki, 2005). Studies have also shown that long-term administration of sulfonylureas may increase insulin levels by reducing the hepatic clearance of the hormone (Bastaki, 2005). Some of the most common side effects of sulfonylureas include hypoglycaemia and weight gain (Marin-Penalver *et al.*, 2016). The drug is known to lose efficacy when used over a long period (Marin-Penalver *et al.*, 2016).

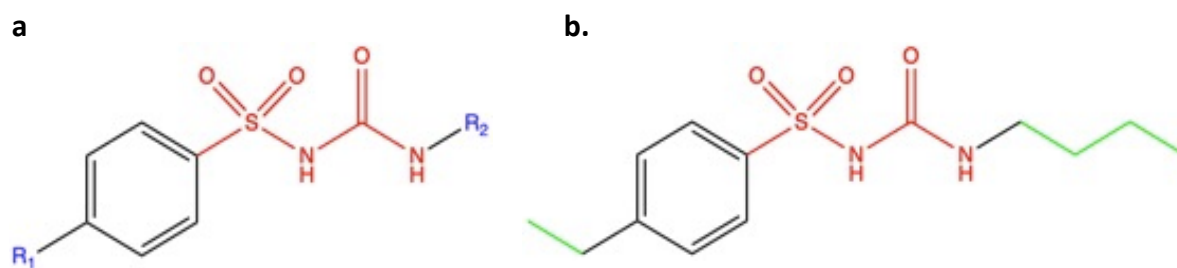


Figure 8: (a) The general structure of sulfonylureas. The sulfonylurea backbone is shown in red and the side chains that distinguish different sulfonylureas compounds in blue. (b) An example of a sulfonylureas drug, tolbutamide, with a methyl (R₁) and a butane (R₂) side chain shown in green. Created using ChemDraw version 19.1 (ChemDraw, 2020).

1.6.1.3 Thiazolidinediones

Thiazolidinediones (TZD) (Figure 9) cause insulin sensitivity. They act as agonists for nuclear peroxisome proliferator-activated receptor-gamma (PPAR- λ). Peroxisome proliferator-activated receptors (PPARs) are found in muscle, adipose tissue, and liver (Marin-Penalver *et al.*, 2016) and play an important role in regulating genes involved adipocyte differentiation, insulin signal transduction, and glucose and lipid metabolism. Therefore, TZDs bind to PPARs to increase glucose utilisation, decrease glucose production and regulate carbohydrate and lipid metabolism (Marin-Penalver *et al.*, 2016). Their main adverse effects are weight gain and fluid retention (Bastaki, 2005).

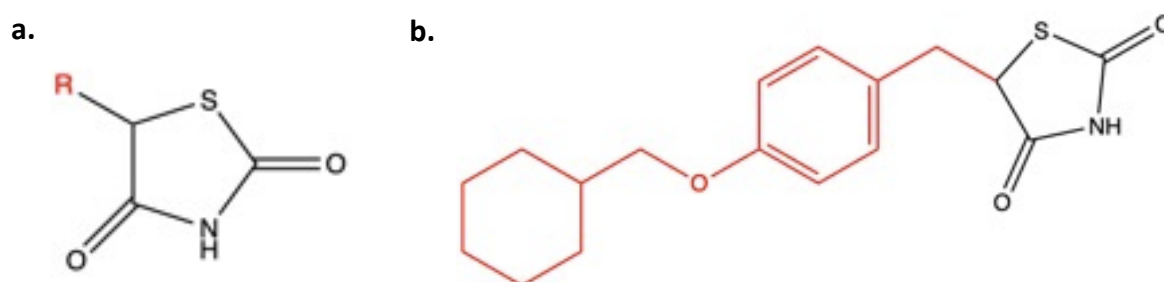


Figure 9: (a) The general structure of thiazolidinediones, with the side chain is show in red and the backbone in black. (b) An example of a thiazolidinedione drug, ciglitazone. Created using ChemDraw version 19.1 (ChemDraw, 2020).

1.6.1.4 Alpha-glucosidase inhibitors

Alpha-glucosidase (Figure 10) inhibitors replicate the effect of a low glycaemic index by delaying the digestion of complex carbohydrates to decrease the rise in postprandial plasma blood glucose (Bastaki, 2005). The drugs are structurally similar to oligosaccharides and thus bind with a higher affinity (competitively) to the active site of the enzyme, where the saccharide is supposed to bind. There are three α -glucosidase drugs on the market; acarbose, miglitol and voglibose (Marin-Penalver *et al.*, 2016). The side effects of α -glucosidase inhibitors are predominantly gastrointestinal and cause flatulence, diarrhoea, bloating and abdominal pain. The symptoms are usually mild but are one of the main reasons for the discontinuation of treatment (Bastaki, 2005).

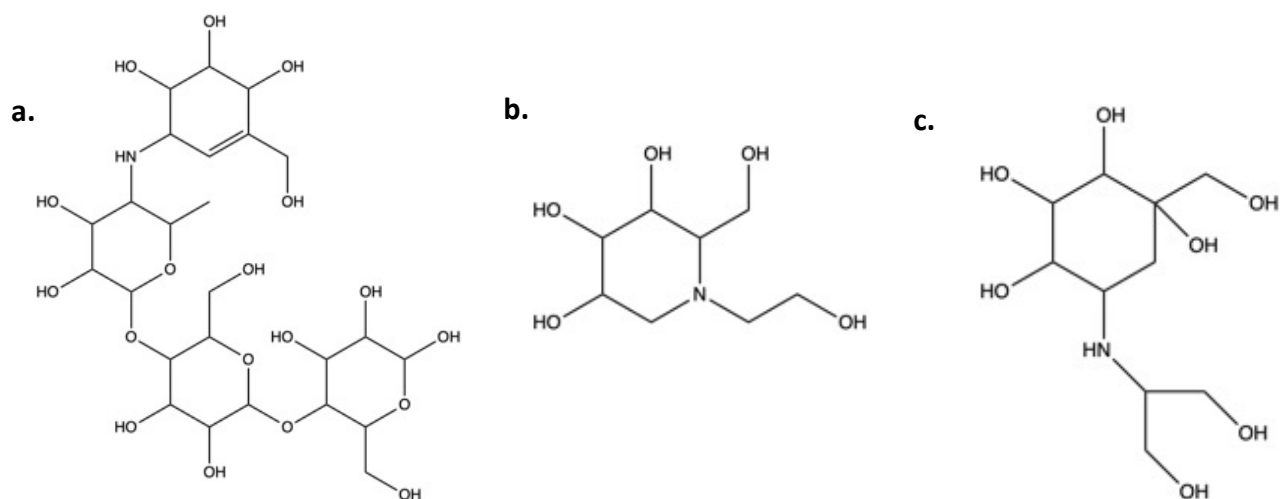


Figure 10: The structures of the anti-diabetic drugs; (a) acarbose, (b) miglitol and (c) voglibose. Created using ChemDraw version 19.1 (ChemDraw, 2020).

1.6.2 Injectable agents

Insulin is the main injectable agent used to treat DM and is usually prescribed when blood glucose levels cannot be managed by oral drugs or lifestyle changes. It is well known that insulin is the most potent blood glucose-lowering agent however, hypoglycaemia is a major dose-limiting factor (Bastaki, 2005). Insulin therapy should aim to mimic the effect of natural insulin. Although effective in limiting postprandial hyperglycaemia and preventing hypoglycaemia between meals, an exact replication of a normal glycaemic profile is not possible (Bastaki, 2005).

The different insulin preparations are rapid-acting with a fast onset and short duration of action, short-acting, long-acting and lastly ultra-long acting with a longer duration of action (Bastaki, 2005). The most frequent side effects of insulin therapy include hypoglycaemia, nausea, vomiting, and headache (Bastaki, 2005).

1.6.3 Lifestyle changes

Although pharmacological treatment offers therapeutic possibilities, lifestyle changes are important for the treatment of DM. An improved diet and physical exercise will ensure that the patient reaches optimal results while using therapeutic agents. Diet plays a vital role in the achievement of the desired blood glucose, blood pressure and weight (Marin-Penalver *et al.*, 2016). There are various benefits of physical exercise including; increased insulin sensitivity in tissues, improved glycaemic control, positive effect on lipid profile and blood pressure, weight loss and cardiovascular benefits (Marin-Penalver *et al.*, 2016).

1.7 Herbal compounds

Herbs and spices are primarily used to flavour, colour or preserve food and include dried seeds, fruits, roots, barks or vegetable substances (Asowata-Ayodele *et al.*, 2016). According to the European Spice Association (ESA): “culinary herbs and spices are the edible parts of plants traditionally added to foodstuff for their natural flavourings, aroma, visual appearance and preservative purposes”. Besides their use in culinary arts, herbs and spices are also used to prevent and treat chronic diseases.

The Merriam Webster dictionary defined herbal medicine as “the art or practice of using herbs and herbal preparations to maintain health and to prevent, alleviate, or cure disease” (Merriam-Webster, 2020). Various studies have shown that herbs and spices such as cardamom, cayenne pepper, cinnamon, garlic, ginger, ginseng, and turmeric are of particular interest due to their desired effects on ageing, atherosclerosis, arthritis, cancer, DM, free radicals, immune deficiency, inflammation, microbes, mental health, and obesity (Asowata-Ayodele *et al.*, 2016). There has been an exponential increase in the use of plant-based drugs over the past few years (Asowata-Ayodele *et al.*, 2016). The WHO organisation reported that 80% of the world’s population relies on herbal medicine daily (WHO, 2013). Traditional medicine is often the only readily available and affordable source of treatment for most people living in developing countries.

DM has been treated with herbs long before the westernisation of modern medicine. One such example is metformin. Metformin (see structure in section 1.6.1.1) is an ancient herbal remedy derived from the French lilac (*Galega officinalis*) in 1922 (Thomas & Gregg, 2017). The plant was found to be rich in the compound guanidine, which possessed hypoglycaemic effects (Bailey, 2017). Today, metformin is the widest prescribed oral anti-diabetic drug (Bailey, 2017). Metformin has an insulin sensitising effect and is used to lower blood glucose levels in patients with non-insulin-dependent DM (Bailey & Turner, 1996).

Worldwide, over 400 herb and plant preparations have been documented to possess beneficial effects to treat DM. However, only a few have been medically and scientifically evaluated to assess their efficacy (Bailey & Day, 1989). More studies are required to establish the mechanism of action, safety and efficacy of the herbal remedies (Dham *et al.*, 2006).

Previous research in our group has documented the anti-diabetic effect of herbs, including rosemary, oregano, black pepper, cinnamon, clove and parsley (Pereira *et al.*, 2019). They also identified the most bioactive compounds found in each of these herbs, for example a bioactive compound in black pepper is piperine. In this study, the anti-diabetic effect of some of these bioactive herbal compounds was evaluated for the regulation of two key diabetic targets, inhibition of the enzymes α -amylase and α -glucosidase, and insulin mimetic properties. The antidiabetic effect of some of these herbal compounds have been shown *in vivo* however, the mechanism of action in which most of these herbal compounds give rise to hypoglycaemia is not known. Each herbal compound tested in the study is found in commercially available herbs and spices, consequently it can be assumed, these compounds are safe at culinary relevant levels.

The chosen herbal compounds and their properties as well as the sources thereof are listed in Table 3. Acetyeugenol is a phenol ester found most abundantly in *Syzygium aromaticum* (cloves) (Shan *et al.*, 2005). The flavone apigenin is found in *Petroselinum crispum* (parsley) (Haytowitz *et al.*, 2018). Cinnamic acid a phenylpropanoid acid is found in *Cinnamomum loureiroi* (cinnamon) (Lee *et al.*, 2015a). The flavone eriodictyol is found in *Lippia graveolens* (Mexican oregano) (Haytowitz *et al.*, 2018). Myrcene is a monoterpene found in *Mentha spicata* (Spearmint) (Duke, 1992). Piperine is an alkaloid found abundantly in *Piper nigrum* (black pepper) (Duke, 1992) and rosmarinic acid is a polyphenol found abundantly in *Origanum vulgare* (Oregano) (Duke, 1992). Previous studies have shown that herbs and spices such as cinnamon, cloves, mint, nutmeg, oregano, parsley and pepper alleviate abdominal pain, diarrhea and flatulence (Peter, 2012), counteracting the side effects commonly caused by α -amylase and α -glucosidase inhibitors.

Table 3: Properties of investigated herbal compounds, and their sources.

Compound	Properties	Richest sources
Acetyeugenol	Antimicrobial	<ul style="list-style-type: none"> • <i>Syzygium aromaticum</i> (Cloves) • <i>Cinnamomum cassia</i> (Cinnamon)
Apigenin	Antioxidant Anti-inflammatory Antidepressant Antimutagenic Anticancer Antiviral Antibacterial Cardioprotective Hepatoprotective (Kashyap <i>et al.</i> , 2018) Antidiabetic (<i>In vivo</i>) (Panda & Kar, 2007)	<ul style="list-style-type: none"> • <i>Petroselinum crispum</i> (Parsley) • <i>Thymus vulgaris</i> (Common thyme) • <i>Origanum onite</i> (Common oregano) • <i>Mentha spicata</i> (Spearmint) (Kashyap <i>et al.</i>, 2018)
Cinnamic acid	Antimicrobial (Kuchi <i>et al.</i> , 2018) Antidiabetic (<i>In vivo</i>) (Hafizur <i>et al.</i> , 2015)	<ul style="list-style-type: none"> • <i>Cinnamomum cassia</i> (Cinnamon)
Eriodictyol	Anti-inflammatory Antimicrobial (Singh & Sharma, 2015) Antidiabetic (<i>In vitro</i>) (Zhang <i>et al.</i> , 2012a)	<ul style="list-style-type: none"> • <i>Origanum onite</i> (Common oregano) • <i>Thymus vulgaris</i> (Common thyme) • <i>Ocimum basilicum</i> (Sweet basil) • <i>Petroselinum crispum</i> (Parsley) (Singh & Sharma, 2015)
Myrcene	Antibacterial Antimicrobial (Sela <i>et al.</i> , 2015)	<ul style="list-style-type: none"> • <i>Cymbopogon</i> (Lemon grass) • <i>E. cardamomum</i> (Cardamom) • <i>Thymus vulgaris</i> (Common thyme) (Sela <i>et al.</i>, 2015)
Piperine	Diuretic Anti-asthmatic (Shityakov <i>et al.</i> , 2019) Antidiabetic (<i>In vivo</i>) (Essop <i>et al.</i> , 2014)	<ul style="list-style-type: none"> • <i>Origanum onite</i> (Common oregano) • <i>Petroselinum crispum</i> (Parsley) • <i>Mentha spicata</i> (Spearmint) (Shityakov <i>et al.</i>, 2019)
Rosmarinic acid	Antiviral Antibacterial Anti-inflammatory Antioxidant (Petersen & Simmonds, 2003) Antidiabetic (<i>In vivo</i>) (Runtuwene <i>et al.</i> , 2016)	<ul style="list-style-type: none"> • <i>Origanum onite</i> (Common oregano) • <i>Salvia officinalis</i> (Common sage) • <i>Thymus vulgaris</i> (Common thyme) • <i>Ocimum basilicum</i> (Sweet basil) • <i>Mentha spicata</i> (Spearmint) • <i>Rosmarinus officinalis</i> (Rosemary) • <i>Mentha × piperita</i> (Peppermint) (Petersen <i>et al.</i>, 2009)

1.8 *In silico* methods used to identify possible anti-diabetic compounds

In silico refer to methods or predictions using computational approaches (Saeidnia *et al.*, 2013). Computational, *in silico* methods play an integral part in the development and testing of hypotheses (Ekins *et al.*, 2007). These methods have frequently been used for the discovery and optimisation of novel molecules, physicochemical characterisation and clarification of absorption, distribution, metabolism, excretion and toxicity (ADMET) properties (Ekins *et al.*, 2007). Computational methods can assist in the identification of novel antagonists or agonists for a specific target, it can also aid in understanding the fundamental biology using networks/pathways based on signalling cascades (Ekins *et al.*, 2007). The prime benefit of using *in silico* methods is it being faster than *in vivo* and *in vitro* work, allowing results to be observed in minutes rather than months (Amberg, 2013). Some other advantages include fast predictions for a large set of compounds, reduced animal and reagent use and reduce the need for expensive laboratory work and clinical trials (Amberg, 2013). However, all results must be confirmed in laboratory-based studies.

1.8.1. Enzyme docking

Enzyme docking (Figure 11) is a technique used in drug discovery. Computational enzyme docking can be defined as a procedure that mimics the process in human bodies, through binding potential ligands to protein targets in a three-dimensional space and ranking the results in a specific order (Amaro *et al.*, 2018).

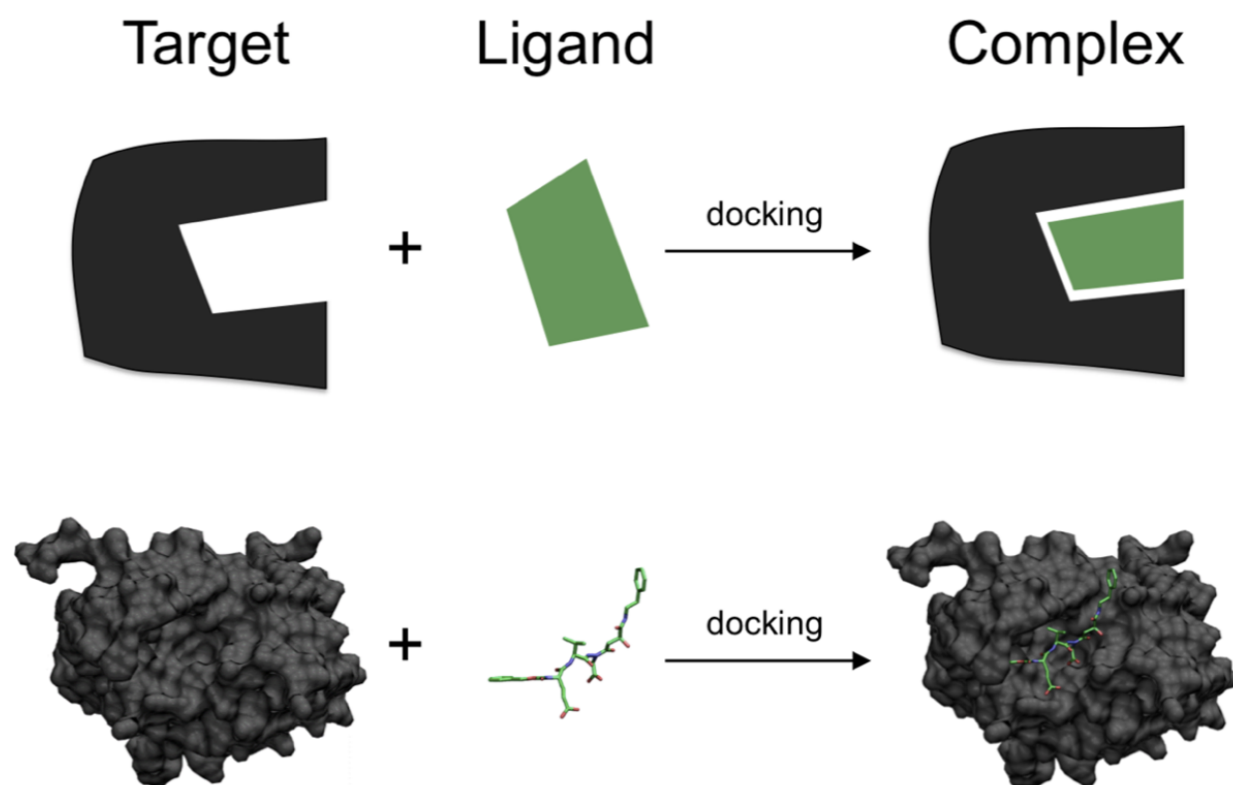


Figure 11: Schematic illustration of docking a small molecule ligand (green) to a protein target (black) producing a stable complex (Kumar, 2016).

i. To obtain docking scores

There are various computational programs available to perform docking, Schrodinger's Maestro (Maestro, 2020) program is one of them. There are different scoring functions available to predict docking scores, Maestro (Maestro, 2020) uses Schrödinger's GlideScore scoring function (Figure 12). This algorithm recognises favourable hydrophobic, hydrogen-bonding, and metal-ligation interactions, and penalises steric clashes between the ligand and the protein (Singh & Sharma, 2015). Glide makes use of three docking methodologies; Glide HTVS, Glide SP and Glide XP. Glide HTVS and SP use hierarchical filters to search for possible locations of the ligand in the binding-site region of a receptor (Friesner *et al.*, 2004). This hierarchical search function gives it exceptional high accuracy (Singh & Sharma, 2015). The shape and properties of the receptor are represented on a grid by different fields that provide progressively more accurate scoring of the ligand pose. Glide XP is a stricter function which severely penalise poses that violate physical chemistry principles (Friesner *et al.*, 2004). The GlideScore function is used to rank compounds, from those that bind tightly to those who don't. It accounts for lipophilic-lipophilic bonds, hydrogen bonds, rotatable bond penalties, and contributions from protein-ligand coulomb-vdW energies (Schrodinger, 2017).

The program generates a table in which the ligands are ranked according to their docking score to enzyme targets. The docking score mimics the Gibbs free energy change when the inhibitor and enzyme come together. Thus, a high negative score corresponds to spontaneous binding while a low negative score corresponds to a less spontaneous binding. Maestro (Maestro, 2020) can also generate a figure which indicates all the interactions between the protein and a specific ligand.

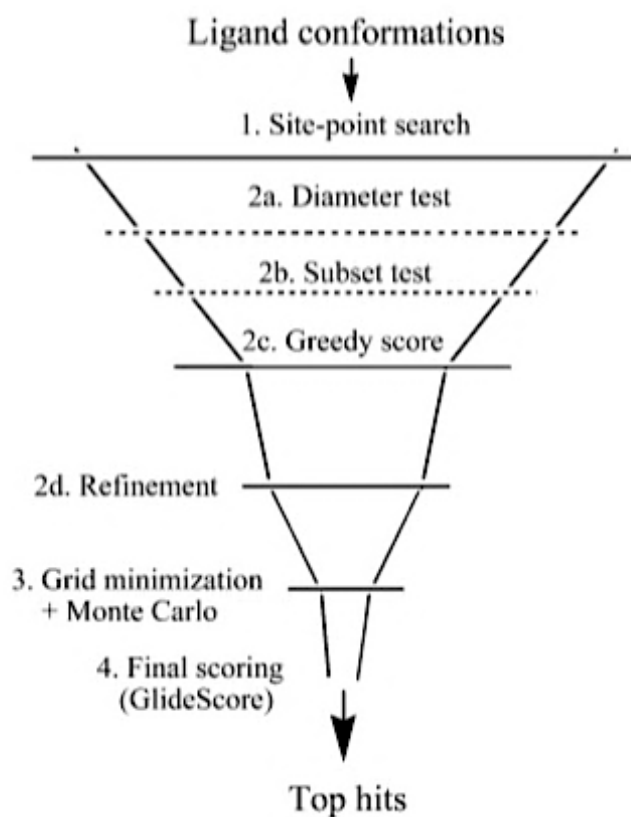


Figure 12: Maestro's Glide docking 'funnel', showing the glide docking hierarchy (Barua *et al.*, 2016).

ii. To explore insulin regulatory properties

DIA-DB (Sánchez-Pérez *et al.*, 2015) is another well-known web-based database used for the prediction of anti-diabetic drugs. The server is open to all users and is accessible at <http://bio-hpc.eu/dia-db>. DIA-DB employs inverse virtual screening of certain input molecules against key diabetic protein targets. In Autodock Vina the ligand is docked to a set of grids describing the target protein (Trott & Olson, 2009). The docking algorithm does not require choosing atom types or the pre-calculation of grid maps. Instead, it calculates the grids internally for the atom types needed (Trott & Olson, 2009). The results are clustered in a manner transparent to the user.

Inverse virtual screening of compounds with Autodock Vina is employed against a set of 18 protein targets associated with DM. These targets are aldose reductase (AKR1B1), corticosteroid 11- β -dehydrogenase isozyme 1 (CSD11B1), dipeptidyl peptidase 4 (DPP4), free fatty acid receptor 1 (FFAR1), fructose-1,6-bisphosphatase (FBP1), glucokinase (GCK), glycogen phosphorylase (PYGL), insulin receptor (INSR), maltase glucoamylase (MGAM), nuclear receptor subfamily 5 group A member 2 (NR5A2), pancreatic alpha-amylase precursor (AM2A), peroxisome proliferator activated receptor α (PPARA), peroxisome proliferator-activated receptor δ (PPARD), peroxisome proliferator-activated receptor γ (PPARG), pyruvate dehydrogenase [(acetyl transferring)] kinase isozyme 2 (PDK2), retinol-binding protein 4 (RBP4), retinoid X receptor α (RXRA) and tyrosine-protein phosphatase (PTP1B). The protein targets can be divided into groups according to their mode of action. There are six target proteins (Table 4) capable of regulating insulin secretion and/or sensitivity. The docking scores of the herbal compounds to these targets can determine whether the compounds might affect insulin secretion and/or sensitivity.

Table 4: DIA-DB protein targets affecting insulin secretion and/or sensitivity

Protein target	PDB code	Function
DPP4	4A5S	Decreases insulin secretion from the pancreas through degradation and inactivation of glucagon-like peptide-1
FFAR1	4PHU	Increases glucose - stimulate insulin secretion through fatty acid binding
CSD11B1	4K1L	Counteracts the effect of insulin through the activation of glucocorticoids
INSR	3EKN	Regulates glucose uptake
PTP1B	4GE6	Decreases insulin sensitivity by dephosphorylating the insulin receptor
RBP4	2WR6	Secreted as an adipokine that reduces insulin signalling and promotes gluconeogenesis

1.9. *In vitro* models used to assess anti-diabetic compounds

Following *in silico* evaluation it is essential, in the pathway to drug discovery, to use *in vitro* models. The usefulness during early drug development is that these models simulate events at cellular, sub-cellular and molecular levels. These models are especially useful in the initial stages of drug screening when many compounds are tested for certain pharmacological activities (Rotshteyn & Zito, 2004). Furthermore, *in vitro* models are more cost-effective, faster and require less testing material compared to *in vivo* testing (Van Tonder, 2011). Part of the aim of the study was to evaluate the anti-diabetic activity of herbal compounds using *in vitro* models, evaluating two key targets, inhibition of starch-hydrolysing enzymes and glucose uptake in liver and muscle cells.

1.9.1. Inhibition of carbohydrate hydrolysing enzymes

Several authors have described *in vitro* assays for the inhibition of two starch hydrolysing enzymes, α -amylase and α -glucosidase. Inhibition of both enzymes decreases the rate of starch hydrolysis and prevent a sudden surge in glucose, resulting in lower postprandial hyperglycemia (Israili, 2011; Powers *et al.*, 2003; Rivera-Chavez *et al.*, 2013). One of the therapeutic approaches for discovering novel anti-diabetic agents involves the search for compounds that possess mild α -amylase and strong α -glucosidase inhibitory properties (Kwon *et al.*, 2006).

1.9.2. Glucose uptake in liver and muscle cells

DM is characterised by insulin resistance and/or an insulin deficiency (American Diabetes Association, 2008). DM causes reduced glucose uptake in peripheral tissues in response to insulin, leading to chronically elevated levels of glucose in circulation (Zou *et al.*, 2005). Insulin has three main target tissues, adipose tissue, skeletal muscle and the liver. Current anti-diabetic research focusses on the development and screening of compounds with potential insulin mimicking effects, to stimulate glucose uptake into cells (Zou *et al.*, 2005). Cell lines commonly used to assess glucose uptake include HepG2 human hepatoma cells, Chang liver cells (human), C2C12 mouse myoblasts, 3T3-L1 mouse fibroblasts and L6 rat myoblast cells. Glucose uptake assays assess the ability of compounds to increase glucose uptake in the major tissue target of insulin, represented by the cell lines. If a compound enhances glucose uptake in these cell lines, it suggests that the compound has insulin mimicking effects and could be a potential anti-diabetic drug, which could alleviate hyperglycaemia by enhancing glucose uptake (Mousinho *et al.*, 2013).

Previously, most studies on glucose uptake were carried out using radiotracers (Zou *et al.*, 2005). However, using radioactive compounds have several disadvantages, including its harmful nature and radioactive clean-up (Karam, 2017). Other methods to measure glucose uptake based on fluorescence and flow cytometry have been developed and optimised and are in use (Zou *et al.*, 2005).

1.9.3. Cell toxicity

The risks that chemicals and drugs might have on humans have to be assessed prior to evaluation as therapeutic agents. Effects on cell health and metabolism can occur via destruction of cell membranes, prevention of protein synthesis and inhibition of enzyme reactions (Aslantürk, 2018). High proliferation rates and cell viability are indicators of healthy cells (Aslantürk, 2018). In order to determine the toxic effect of compounds on cells there is a need for inexpensive, reliable and fast assays (Aslantürk, 2018; Zink *et al.*, 2020). This initial evaluation is important considering the use of animals to assess toxicity due to the drawbacks in terms of ethical, economic and scientific limitations (Yoon *et al.*, 2012). Human cell-based *in vitro* methods are increasingly being combined with bioinformatics and *in silico* modelling to improve the assessment of risks associated with drugs (Zink *et al.*, 2020).

Cell-based *in vitro* assays have several advantages, the most important being that these assays are inexpensive and rapid in comparison with animal experiments (Aslantürk, 2018; Zink *et al.*, 2020). The use of established cell lines eliminates inter-species variability and has high reproducibility (Yoon & Robyt, 2003; Zink *et al.*, 2020). The aim of cytotoxic experiments is to determine how many viable cells remained and/or how many cells are dead at the end of the experiment. Various different types of cytotoxic assays can be used, the assays can be classified based on the measurement of their endpoints (Aslantürk, 2018). We can distinguish between dye exclusion (trypan blue, eosin and erythrosine B), colorimetric (diphenyltetrazolium bromide, sulforhodamine B, crystal violet etc.), fluorometric (AlamarBlue and CFDA-AM) and luminometric (ATP and real-time viability) assays (Aslantürk, 2018). These cellular models do not account for ADMET effects of an organism but are still essential in drug discovery, since assessment in animal models is only acceptable if extensive preliminary evaluation has been undertaken in an *in vitro* environment.

2. AIM AND HYPOTHESES

The aim of this study was to find monotherapeutic agents, with pleiotropic effects from commercially available herbs and spices, to inhibit α -amylase and α -glucosidase and stimulate glucose uptake in cells, using *in silico* and *in vitro* relationship studies.

H1₀: There will be no statistically significant difference between the Michaelis-Menten parameters when no inhibitor is present as opposed to when an inhibitor (acarbose or new drugs) is present at the 95% level of confidence.

H1_a: There will be a statistically significant difference between the Michaelis-Menten parameters when no inhibitor is present as opposed to when an inhibitor is present (acarbose or new drugs) at the 95% level of confidence.

H2₀: The K_i values of the new drugs will not be lower than the K_i value of acarbose at a 95% level of confidence.

H2_a: The K_i values of the new drugs will be lower than the K_i value of acarbose at a 95% level of confidence.

H3₀: There will be no statistically significant difference between the IC_{50} of acarbose and the new drugs at the 95% level of confidence.

H3_a: There will be a statistically significant difference between the IC_{50} of acarbose and the new drugs at the 95% level of confidence.

H4₀: There will be no statistically significant difference in the glucose uptake of the untreated (control) cells and the treated (new drugs) cells at the 95% level of confidence.

H4_a: There will be a statistically significant difference in the glucose uptake of the untreated (control) cells and the treated (new drugs) cells at the 95% level of confidence.

H5₀: There will be no statistically significant difference in the glucose uptake of insulin stimulated cells, and the cells stimulated by the new drugs at the 95% level of confidence.

H5_a: There will be a statistically significant difference in the glucose uptake of insulin stimulated cells, and the cells stimulated by the new drugs at the 95% level of confidence.

3. RESEARCH OBJECTIVES

The objectives of the study were to:

- Computationally evaluate the inhibitory effect of a list of compounds found in herbs and spices on α -glucosidase and α -amylase.
- Identify the compounds with the best docking scores to α -glucosidase and α -amylase, respectively.
- Assess the *in silico* toxicity, bioavailability and druggability of the top-ranked compounds.
- Assess the ability of the compounds to affect insulin secretion and/or sensitivity *in silico*.
- Determine the α -amylase inhibitory activity of the selected herbal compounds using a colorimetric enzymatic assay.
- Determine the α -glucosidase inhibitory activity of the selected herbal compounds using a colorimetric enzymatic assay.
- Evaluate the cytotoxicity of the compounds on C2C12 myotubes and HepG2 hepatoma cells using the Sulforhodamine B assay.
- Determine the effect of the compounds on glucose uptake in C2C12 myotubes and HepG2 hepatoma cells using the fluorescent 2-NBDG assay.
- Determine the dosage of each herb required to be equivalent to the daily dose of acarbose.

4. EXPERIMENTAL DESIGN AND METHODOLOGY

4.1 *In silico* study

i. Docking studies on Maestro

The docking studies were performed on Schrodinger's Maestro (Maestro, 2020) (Maestro v 11.5, Schrodinger LLC, New York) program. The virtual screening workflow (VSW) of Maestro involves four consecutive steps: (a) ligand preparation; (b) protein preparation; (c) receptor grid generation and (d) Glide ligand docking. The Glide function uses a grid-based method to search for favourable interactions between a receptor molecule and one or more ligand molecules.

Ligand preparation

In this study, the isomeric SMILES of roughly a thousand compounds, identified from 30 commercially available herbs and spices (Pereira *et al.*, 2019), were uploaded onto Maestro (Maestro, 2020). Acarbose was selected as a standard drug reference molecule. The 3D structure of the ligands were prepared using the LigPrep function, which generates several poses from each input structure (Subramaniyan *et al.*, 2017). The default parameters, including "Retain specified chiralities" were kept.

Protein preparation

The crystal structure of the two enzymes (PDB entries: 3L4Y and 4GQR for α -glucosidase and α -amylase respectively) were downloaded from the protein data bank (PDB) (Berman *et al.*, 2000) and uploaded to Maestro (Maestro, 2020). The protein preparation wizard was used to prepare the proteins for *in silico* experimentation. The imported 3D protein structure should be made fit to study the docking (Balachandran *et al.*, 2016). Therefore, all the cofactors and water molecules were removed from the proteins, and the hydrogen bonding was optimised, followed by an energy minimisation step.

Receptor grid generation and docking

A grid representing the active site of each protein was created using the receptor grid generation tool (Dizdaroglu *et al.*, 2019). The default parameters, a van der Waals scaling factor of 1.00 and charge cut-off of 0.25 subjected to an OPLS 2001 force field, was kept (Banerjee *et al.*, 2011). Protein docking was carried out using the Glide HTVS (high-throughput virtual screening) peptide docking module of the virtual screening workflow (VSW) function of Maestro (Maestro, 2020). HTVS is intended to be used for the rapid screening of a large number of ligands. The default settings of VSW were used. The interactions between the ligands and protein were quantified with the glide score (Balachandran *et al.*, 2016). The best-docked pose with the most negative Glide score value was recorded for each ligand, and docking interaction diagrams were generated for each compound to evaluate which amino acids form interactions with the enzymes.

Previous work done by our group using DIA-DB, identified herbs and spices with known α -amylase and α -glucosidase inhibition, and insulin mimicking effects (Pereira *et al.*, 2019). We validated their findings using Schrodinger's Maestro (Maestro, 2020) program and identified seven bioactive compounds found in these herbs and spices to be tested for their inhibitory activity *in vitro*. Acarbose was a positive control. We chose four compounds with stronger docking than acarbose and three compounds with weaker docking than acarbose as negative controls.

ii. Docking to insulin-regulating targets

The seven chosen herbal compounds were later docked to six insulin-regulating protein targets to determine whether they affect insulin regulation. The six insulin-regulating targets were dipeptidyl peptidase 4 (PDB: 4A5S) (Sutton *et al.*, 2012), free fatty acid receptor 1 (PDB: 4PHU) (Srivastava *et al.*, 2014), corticosteroid 11- β -dehydrogenase isozyme 1 (PDB: 4K1L) (Bohme *et al.*, 2013), insulin receptor precursor (PDB: 3EKN) (Chamberlain *et al.*, 2009), tyrosine-protein phosphatase non-receptor type 9 (PDB: 4GE6) (Zhang *et al.*, 2012b) and retinol-binding protein 4 precursor (PDB: 2WR6) (Motani *et al.*, 2009). Before the docking was performed, on Maestro (Maestro, 2020), the proteins were prepared (see section 4.1.i), and receptor grids were created for each target. The best-docked pose with the most negative Glide score value was recorded for each ligand. Each insulin-regulating target had a different positive control, a drug currently on the market or in development for that specific protein target.

iii. Calculation of physiochemical properties

Schrodinger's Canvas (Canvas v 3.5.011, Schrodinger LLC, New York) program was used to determine the bioavailability and toxicity of the eight compounds. The SMILES of each compound was imported into Canvas, after which the physiochemical properties were calculated. Each compound-structure was minimised to obtain three-dimensional (3D) structures before the Qikprop descriptors were computed. Once the calculations were completed the percentage human oral absorption, QPLogHERG and #stars for each compound were recorded.

iv. Determination of chemical – protein cross reactions on STITCH

The herbal compounds were evaluated on the Search Tool for Interactions of Chemicals (STITCH) (Szklarczyk *et al.*, 2016) to determine the known and predicted interactions between the herbal compounds and proteins in the human body. The server is open to all users and is accessible at <http://stitch.embl.de>. Before searching, the name of each herbal compound was typed in the “Item name” box, and the organism was set to “Homo sapiens”. The interaction score was set to “high confidence (0.700)”, and network edges were set to “molecular action”. The active interaction sources were set to include text mining, experiments, databases and predictions. Once the outcomes were generated the image was downloaded and the results table were exported for each herbal compound.

4.2 *In vitro* study

4.2.1 Chemicals

The following analytical grade reagents were purchased from Sigma-Aldrich Co (St Louis, MO, USA): α -glucosidase (EC 3.2.1.20) from *Saccharomyces cerevisiae*, porcine pancreatic α -amylase (EC 3.2.1.1), *p*-nitrophenyl- α -D-glucopyranoside (*p*NPG), 3,5-dinitrosalicylic acid (DNSA), *p*-nitrophenol, maltose monohydrate, starch from potato, trichloroacetic acid, sulforhodamine B (SRB), acetic acid, tris, Dulbecco’s Modified Eagle Media (DMEM), glucose-free DMEM, foetal calf serum (FCS), acarbose, rosmarinic acid, cinnamic acid, apigenin, eriodictyol, piperine, myrcene and acetyeugenol. 2-deoxy-2-[(7-nitro-2,1,3-benzoxadiazol-4-yl) amino]-D-glucose (2-NBDG) was obtained from Thermofisher Scientific (Waltham, MA, USA).

4.2.2 Kinetics of α -amylase inhibition

i. Background

The porcine pancreatic α -amylase activity was determined by the method described by *Bernfeld (1955)*. Alpha-amylase hydrolyses starch molecules to release reducing sugars, such as maltose. These reducing sugars can be revealed by adding DNSA, that is reduced (Figure 13) to 3-amino-5-nitrosalicylic acid (ANSA) in the presence of maltose (*McKee, 2017*). ANSA is a bright orange-red compound, which can be detected spectrophotometrically at 540 nm (*Valentina et al., 2017*). Inhibition of α -amylase activity will cause a decrease of ANSA formed.

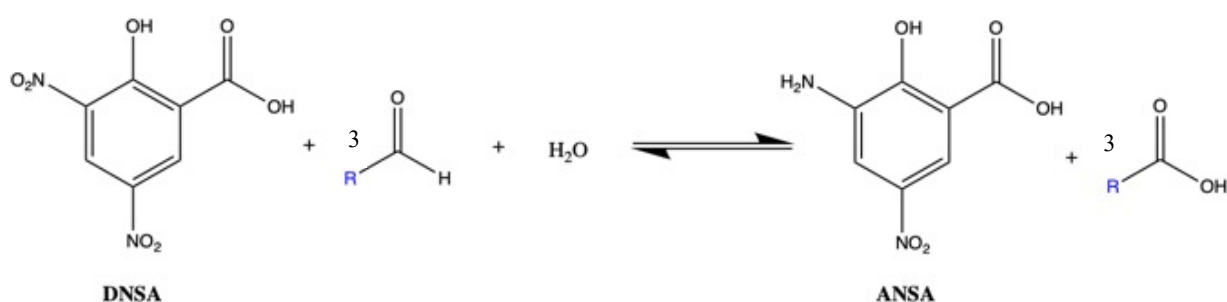


Figure 13: The reduction of DNSA (yellow) to ANSA (orange red) in the presence of a reducing sugar (*Thongprajukaew et al., 2014*).

ii. Method

Maltose standard curve

Before the inhibition assay could be performed a standard curve with maltose was obtained, to get a molar absorption coefficient accurately specific for the experimental conditions used in this study. The determined molar absorption coefficient was then used to calculate the concentration maltose released in the enzymatic reaction using the Beer-Lambert law (equation 1). Once the concentration maltose released was known, the velocity of the reaction was calculated. The velocity of the reaction was used to construct the Michaelis-Menten graphs and Lineweaver-Burk plots.

$$A = \epsilon \lambda c$$

Equation 1: The Beer Lambert law. A is the absorbance, ϵ is the molar absorption coefficient ($M^{-1}.cm^{-1}$), λ is the light path (cm) and c is the concentration (M).

A 0.2 % (w/v) maltose solution was prepared by dissolving 0.02 g maltose monohydrate in 10 mL double distilled water (ddH₂O). The DNSA colour solution was prepared by mixing potassium tartrate (12 g) in sodium hydroxide (8 mL, 2 M) with DNSA (0.437 g) dissolved in ddH₂O (20 mL). The experiment was performed in Eppendorf tubes. Each tube contained: 100 μ L DNSA, varying volumes of maltose (0 - 0.46 mM) and ddH₂O to a total volume of 300 μ L. The tubes were placed in a dry bath at 85°C for 15 min to stop the reaction. Once the reactions reached room temperature, 900 μ L ddH₂O was added and 200 μ L of the reaction mixture was pipetted into a 96-well plate (Greiner, clear F-bottom). The absorbance was measured at 540 nm (Molecular Devices, Spectramax paradigm).

Table 5: The final number of nano moles of each reagent in every reaction (well) of the maltose standard curve

Compound	nMoles
Maltose - 0.09 mM	27
- 0.18 mM	54
- 0.27 mM	81
- 0.37 mM	111
- 0.46 mM	138
DNSA	1.14 x 10 ⁶

Inhibition assay

The substrate, potato starch (1%, w/v), was prepared by mixing 0.25 g starch with 25 mL of sodium phosphate buffer (20 mM) containing 6.7 mM sodium chloride (pH 6.9). The α -amylase solution was prepared at 2 U/mL in the same phosphate buffer. The DNSA (96 mM) colour solution was prepared at 85°C by mixing potassium tartrate (12 g) in 8 mL sodium hydroxide (2 M) with 0.437 g DNSA dissolved in 20 mL ddH₂O. The herbal compounds were prepared in phosphate buffer.

The experiment was performed in Eppendorf tubes. Into each tube was pipetted: 100 μ L inhibitor (10 μ M), 100 μ L enzyme and sodium phosphate buffer (20 mM). After incubating the mixture for 10 min at room temperature, 100 μ L starch (0 - 6.6 mg/mL) was added. The reaction mixtures were further incubated for 10 min before 100 μ L DNSA was added. The reactions were stopped, by placing the tubes in a dry bath at 85°C for 10 min. The final mixture was diluted with 1.1 mL ddH₂O, and 200 μ L was pipetted into a 96-well plate (Greiner, clear F-bottom). The absorbance was measured at 540 nm (Molecular Devices, Spectramax paradigm).

A concentration range of 2.5 – 10 μ M acarbose was used as positive control. Blanks were tubes containing 100 μ L buffer, 100 μ L inhibitor, starch (0 - 6.6 mg/mL) and 100 μ L DNSA and served to account for any chemical interference. The experiment was repeated with 5 μ M and 2.5 μ M concentrations of the inhibitors.

Table 6: The final amount of each reagent in every reaction (well) of the α -amylase inhibition assay

Reagent	Final amount in well
α - Amylase	0.5 U/mL
Inhibitor - 2.5 μ M	1 nmole
- 5 μ M	2 nmoles
- 10 μ M	4 nmoles
DNSA	1.14×10^6 nmoles
Maltose (no inhibitor, highest substrate concentration)	971.8 nmoles

4.2.3 Kinetics of α -glucosidase inhibition

i. Background

The enzymatic activity of α -glucosidase was also established through a colorimetric assay. The method used was first described by Collins *et al.* (1997). In this assay, the substrate *p*NPG is hydrolysed (Figure 14) to produce two products, glucose and *p*-nitrophenolate. The yellow *p*-nitrophenolate can be measured spectrophotometrically at 405 nm (Priscilla *et al.*, 2014). Inhibition of α -glucosidase activity will cause a decrease in the amount of *p*-nitrophenolate.

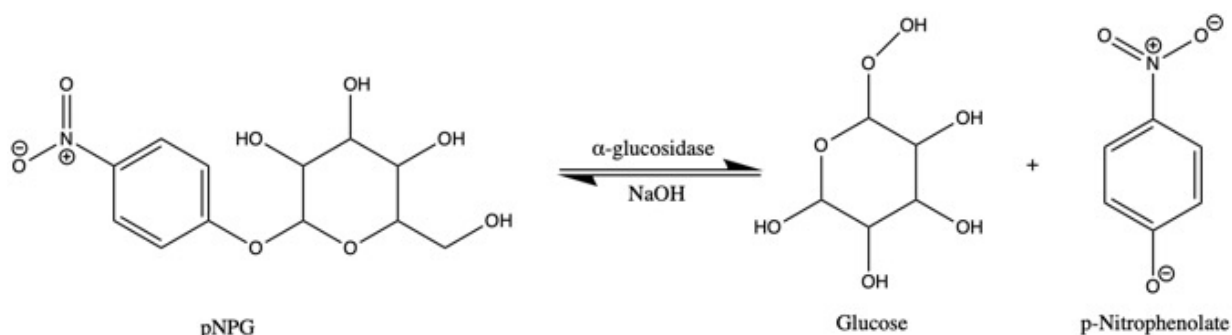


Figure 14: α -glucosidase catalyses the reaction of the substrate *p*NPG to produce glucose and *p*-nitrophenolate, with the addition of sodium hydroxide. *p*-Nitrophenolate is detected spectrophotometrically at 405nm. Created using ChemDraw version 19.1 (ChemDraw, 2020).

i. Method

p-nitrophenolate standard curve

A standard curve of *p*-nitrophenolate was generated from which the molar absorption coefficient specific to our experimental conditions was calculated, using the Beer-Lambert equation (equation 1).

A 200 μM *p*-nitrophenolate solution was prepared by dissolving 0.014 g *p*-nitrophenol in 50 mL sodium phosphate buffer (100 mM, pH 6.9) and a 0.9 M sodium hydroxide solution (NaOH) was prepared in ddH₂O. The experiment was performed in a 96-well plate (Greiner, clear F-bottom). Each well contained: 25 μL NaOH (0.1 M), varying concentrations *p*-nitrophenol (0-200 μM) and buffer to a final volume of 225 μL . The absorbance of the reactions was read at 405 nm (Molecular Devices, Spectramax paradigm).

Table 7: The final number of nano moles of each reagent in every reaction (well) of the *p*-nitrophenolate standard curve

Reagent	nMoles
<i>p</i> -nitrophenol - 40 μM	9
- 80 μM	18
- 120 μM	27
- 160 μM	36
- 200 μM	45
Sodium hydroxide	22 500

Inhibition assay

α -Glucosidase (0.2 U/mL) sourced from *Saccharomyces cerevisiae*, was prepared in sodium phosphate buffer (100 mM, pH 6.9). The substrate *p*NPG (5 mM) was prepared by dissolving 0.075 g in 50 mL sodium phosphate buffer (100 mM, pH 6.9).

The experiment was performed in 96-well plates (Greiner, clear F-bottom). To each well 25 μ L enzyme and 100 μ L inhibitor (250 μ M) was added. The reaction mixtures were incubated for 10 min at 37°C. Thereafter 25 μ L *p*NPG (0-1.4 mM) and 25 μ L buffer were added to obtain a reaction volume of 175 μ L. The reaction mixtures were further incubated for 30 min at 37°C before 50 μ L NaOH (0.1 M) was added to stop the reactions. The final pH of the reactions was 9.91. The absorbance was measured at 405nm (Molecular Devices, Spectramax paradigm).

Acarbose was used as a positive control. Blanks were used to eliminate chemical interference, containing 50 μ L buffer, 100 μ L inhibitor, 25 μ L *p*NPG (0.08 - 5 mM) and 25 μ L NaOH. The experiment was repeated with 500 μ M and 1000 μ M of the inhibitors.

Table 8: The final amount of each reagent in every reaction (well) of the α -glucosidase inhibition assay

Reagent	Final amount in well
α - Glucosidase	0.029 U/mL
Inhibitor - 250 μ M	44 nmoles
- 500 μ M	88 nmoles
- 1000 μ M	175 nmoles
Sodium hydroxide	22 500 nmoles
Sodium phosphate buffer	997- 5000
<i>p</i> NPG	0 – 250 nmoles

4.2.4 Cell toxicity

i. Background

In vitro cytotoxicity of compounds is an important parameter that needs to be evaluated before further therapeutic effects can be investigated. The purpose of testing *in vitro* cytotoxicity is to evaluate the ability of a compound to kill cells *in vitro*. Various factors affect the toxicity of a compound, however the most important include; the dosage, duration of exposure and the mechanism of toxicity (Riss & Moravec, 2004).

In this experiment, an SRB assay was used to evaluate the cytotoxicity of the herbal compounds *in vitro*. SRB is a pink dye that binds stoichiometrically to the cellular proteins (Vichai & Kirtikara, 2006). The SRB assay is popular due to its ease, sensitivity and practicality. SRB assays have been used extensively in previous cytotoxicity studies involving herbs and natural compounds (Hajirahimkhan *et al.*, 2013). The experiment will be performed in two relevant cell lines, HepG2 human hepatocarcinoma cells that represent metabolism and C2C12 mouse myotubes that are an insulin target.

ii. Method

Cell maintenance and harvesting

The cells were maintained and harvested by Ms Margot Nell (University of Pretoria, Department of Pharmacology). In short, the method she used involved the cultivation of cells in in flasks containing DMEM, penicillin/streptomycin (1%), 10% FCS and L-glutamine. The media was replaced every 2-3 days, and the cells were harvested once 80% confluency was reached. This was done by removing the cell culture media and washing the monolayer with phosphate buffered saline (PBS) to remove all traces of serum. One millilitre trypsin/versene solution was added, and the flask was incubated at 37°C to allow cells to detach. The detached cell solution was collected, and fresh culture medium was added. The cell lines were not differentiated.

Cell counting

The cell suspension was transferred to a sterile 15 mL tube and were washed by adding cell culture media. The cells were collected by centrifugation at 200 *g* for 5 min. The supernatant was decanted, and the pellet was resuspended in 1 mL fresh DMEM supplemented with 10% FCS. To a volume of 20 µL cell suspension 180 µL trypan blue (0.2 %, w/v), prepared in PBS was added. The mixture was loaded in a haemocytometer, and the viable, unstained cells were counted with a microscope.

SRB assay

The SRB assay was performed in sterile 96 well plates. The HepG2 and C2C12 cells were seeded (100 μ L) at 1×10^5 per well and were left overnight at 37°C. A volume of 100 μ L herbal compounds (0.005-500 μ M) was added, and the plates were further incubated for 72 h at 37°C. Wells containing media only served as blanks, while wells containing cells and media served as the negative control. Saponin was used as a positive control. The cells were fixed by adding 50 μ L 50% (w/v) trichloroacetic acid (TCA) and incubating the plates at 4°C for 24 h. The plates were washed four times with tap water and dried in the oven overnight before 100 μ L SRB dye (0.057% w/v) were added to each well. After a 30 min incubation period, the unbound dye was removed by washing the plates at least four times with 1% acetic acid. The plates were dried overnight in the oven before 200 μ L tris (10 mM, pH 10.5) was added to dissociate bound dye. The plate was shaken gently (550 rpm) for 1 h, and the absorbance was read at 540 nm. The cell viability, as a percentage of the negative control, was calculated with the following equation:

$$\text{Cell viability (\%)} = \frac{\text{Avg sample abs} - \text{Avg blank abs}}{\text{Avg negative control abs} - \text{Avg blank abs}} \times 100$$

Equation 2: The equation used to calculate cell viability as a percentage of the control.

4.2.5 Glucose uptake assay

i. Background

2-NBDG (Figure 15) is a fluorescent deoxyglucose analogue (Zou *et al.*, 2005) that can be used to monitor glucose uptake in cells. The analogue is actively transported across cell membranes through GLUT transporters (Lloyd *et al.*, 1999). Once the 2-NBDG molecule is inside the cell, it gets trapped within and can be detected fluorometrically. If a compound possesses insulin-mimetic effects the rate of glucose uptake increased, this is associated with an increase in fluorescence at an excitation and emission wavelength of 445 nm and 565 nm respectively.

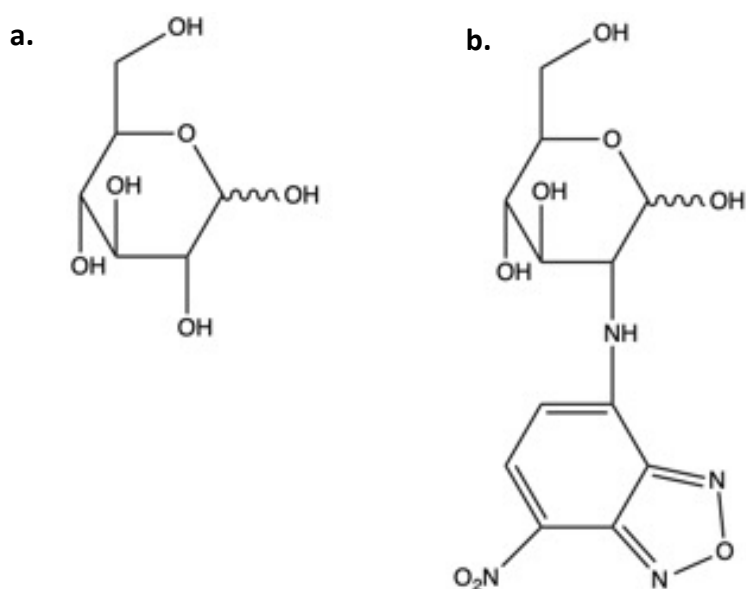


Figure 15: The structure of (a) glucose and (b) the fluorescent glucose analog 2-NBDG. Created using ChemDraw version 19.1 (ChemDraw, 2020).

ii. Method

2-NBDG assay

The hypoglycaemic activity of the herbal compounds was determined by a method described by Zou *et al.* (2005). The cells were maintained and counted as explained in Section 4.2.4. The 2-NBDG assay was performed in sterile black, clear-bottom 96-well plates. The HepG2 and C2C12 cells (80 μ L) were seeded at a density of 1.5×10^4 cells/well and left overnight at 37°C to attach. The media were aspirated and replaced with glucose-free DMEM supplemented with 2.5% FCS. After overnight incubation, the media was aspirated once more, and the cells were treated for 24 h with three sub-toxic concentrations (0.1, 1 and 10 μ M) of the herbal compounds (80 μ L) made up in glucose-free media. Fifty microliters of the fluorescent dye, 2-NBDG (80 μ M) were added to the cells, and the plates were incubated for 60 min in darkness. All of the liquid was aspirated, and the cells were washed with PBS before the fluorescence was read at $\lambda_{ex}= 445$ nm and $\lambda_{em}= 555$ nm. Insulin (25 nM) served as the positive control. Wells containing 100 μ L PBS and no cells served as blank and pre-seeded wells treated with 2-NBDG and glucose-free DMEM served as control. The results were expressed as relative fluorescent units, and the activity was evaluated by comparing the fluorescent intensities of the experimental wells with the controls.

Relative fluorescent units (RFU)

$$= \text{Avg sample fluorescence} - \text{Avg blank fluorescence}$$

Equation 3: The equation used to calculate the relative fluorescent units.

4.3 Data analysis

The experiments were carried out in triplicate, and the results represent at least three independent experiments. The results are expressed as mean \pm standard deviation (SD). It was assumed that all sample variances were different (heteroscedastic). The kinetic parameters of the compounds and the type of inhibition exerted was evaluated on GraphPad Prism (version 8.3.0) using Michaelis-Menten kinetics and the corresponding Lineweaver-Burk double reciprocal plots. The K_i values were obtained with secondary plots. The reciprocal of the slope of the Lineweaver-Burk graphs were plotted against the inhibitor concentration to obtain a straight line equation (Castonguay *et al.*, 2002). The K_i was calculated from the equation of the straight line when $y = 0$. The K_i values were analysed using a one-sided unpaired Student's t-test. A one-sided t-test was used, since we were more interested in K_i values smaller than that of acarbose, indicating stronger binding affinity. The IC_{50} of the compounds were calculated by plotting the percentage cell viability against the log drug concentration on GraphPad Prism (version 8.3.0). The kinetic parameters, IC_{50} values and glucose uptake results were subjected to a two-sided, unpaired Student's t-test. Differences were considered significant at $p < 0.05$.

5. RESULTS

5.1 Molecular docking

We investigated roughly a thousand herbal compounds *in silico* for α -amylase and α -glucosidase inhibition through docking analysis. To reduce the number of compounds for *in vitro* analysis, we used a literature review, previously published by our group (Pereira *et al.*, 2019), to identify compounds in our own docking study with confirmed inhibitory activity of both α -amylase and α -glucosidase activity. Identifying compounds with both α -amylase and α -glucosidase inhibitory activity increased our chances of finding monotherapeutic targets.

The results in Table 9 and 10 shows the docking scores of these herbal compounds docked to α -amylase and α -glucosidase, respectively. The compounds that had better docking scores than acarbose were rosmarinic acid, eriodictyol, apigenin and piperine. While acetyeugenol, cinnamic acid and myrcene had weaker docking scores than acarbose. The structures of the herbal compounds can be seen in Table 11.

Ligand interaction diagrams (Figures S1 and S2) were generated in order to identify the amino acids, within the active site of each enzyme, interacting with the herbal compounds. The results were generated on Maestro and the interactions between starch (the control) and the enzymes were compared to literature. All the amino acids that show interactions between the substrate (starch) or the herbal compounds, within 3Å from the centre of the grid, based on the ligand docked to α -amylase (4GQR) (Williams *et al.*, 2012) are listed in Table 12. While the amino acids that show interactions between the substrate (starch) or the herbal compounds docked to α -glucosidase (3L4Y) (Sim *et al.*, 2010) are listed in Table 13.

Table 9: Ascending Glide HTVS docking scores of the herbal compounds docked to α -amylase

Compound	Glide score (kcal/mol)
Rosmarinic acid	-7.9
Eriodictyol	-7.4
Apigenin	-6.6
Piperine	-5.8
Acarbose (positive control)	-5.2
Acetyeugenol	-4.3
Cinnamic acid	-4.2
Myrcene	-1.6

Table 10: Ascending Glide HTVS docking scores of the herbal compounds docked to α -glucosidase

Compound	Glide score (kcal/mol)
Eriodictyol	-5.5
Rosmarinic acid	-5.4
Apigenin	-5.3
Piperine	-4.2
Acarbose (positive control)	-4.1
Cinnamic acid	-3.4
Acetyeugenol	-3.4
Myrcene	-1.4

Table 11: The structures of the herbal compounds

Positive control	Acarbose	
Compounds with better docking scores than acarbose	Apigenin	Eriodictyol
	Piperine	Rosmarinic acid
Compounds with weaker docking scores than acarbose (Negative controls)	Acetylleugenol	Cinnamic acid
	Myrcene	

Created using ChemDraw version 19.1 (ChemDraw, 2020).

Table 12: Amino acids interacting with starch and the herbal compounds in the active site of the enzyme, α -amylase (4GQR)

Amino acids	Starch (Literature*)	Starch (Maestro)	Acarbose	Acetyeugenol	Apigenin	Cinnamic acid	Eriodictyol	Myrcene	Piperine	Rosmarinic acid
ASP 197	✓	✓	✓	✓	✓		✓		✓	
GLN 63	✓	✓			✓	✓				✓
HIE 101		✓	✓	✓	✓				✓	
LEU 162	✓	✓	✓	✓		✓				
LEU 165	✓	✓	✓		✓	✓		✓	✓	✓
TRP 58	✓	✓	✓	✓			✓	✓	✓	✓
TRP 59	✓	✓	✓	✓	✓	✓	✓	✓	✓	✓
TYR 62		✓	✓	✓	✓	✓	✓	✓	✓	✓
THR 163		✓	✓							✓

*(Machius *et al.*, 1996)**Table 13:** Amino acids interacting with starch and the herbal compounds in the active site of the enzyme, α -glucosidase (3L4Y)

Amino acids	Starch (Literature*)	Starch (Maestro)	Acarbose	Acetyeugenol	Apigenin	Cinnamic acid	Eriodictyol	Myrcene	Piperine	Rosmarinic acid
ASP 203	✓	✓	✓	✓	✓		✓	✓		✓
ASP 327	✓	✓	✓		✓	✓	✓	✓		✓
ASP 542	✓	✓	✓		✓	✓	✓	✓	✓	✓
ASP 443	✓	✓	✓	✓		✓		✓	✓	
ARG 526	✓	✓	✓	✓	✓	✓		✓	✓	
ILE 328	✓	✓	✓				✓	✓		✓
ILE 364	✓	✓	✓		✓	✓	✓	✓	✓	✓
HIE 600	✓	✓	✓		✓		✓	✓	✓	✓
MET 444	✓	✓	✓	✓			✓	✓		
PHE 450		✓		✓					✓	
PHE 575		✓	✓	✓	✓	✓	✓	✓		✓
SER 448		✓								
TRP 406		✓	✓	✓	✓	✓	✓	✓	✓	✓
TRP 441	✓	✓	✓		✓	✓	✓		✓	✓
TRP 539		✓	✓						✓	
TYR 299	✓	✓			✓	✓	✓		✓	✓

*(Sim *et al.*, 2008)

5.2 Docking to insulin-regulating targets

The docking scores of the herbal compounds to six insulin-regulating targets were evaluated on Maestro (Maestro, 2020). The docking scores of the herbal compounds were compared to the docking scores of drugs (currently on the market or in clinical trials) for each different insulin-regulating target.

Table 14: Docking scores (kcal/mol) of the herbal compounds to protein targets (PDB code) regulating insulin secretion and/or sensitivity

		Protein targets					
		2WR6	3EKN	4A5S	4GE6	4K1L	4PHU
Test compounds	Acetyeugenol	-5.6	-4.2	-3.4	-2.9	-5.5	-6.8
	Apigenin	-9.2	-7.4	-4.8	-5	-7.2	-7.7
	Cinnamic acid	-6.3	-3.9	-3.5	-5.3	-4.4	-5.7
	Eriodictyol	-8.6	-7.2	-5.1	-5.7	-8.9	-5.8
	Myrcene	-2.2	-2.9	-1.7	-0.2	-2.7	-3.7
	Piperine	-7.5	-6.6	-6.3	-3.6	-5.4	-8.5
	Rosmarinic acid	-8.7	-6.1	-5.3	-6.4	-5.8	-7.7
Positive controls	Linolenic acid	-4.9					
	Insulin		-8.6				
	Anagliptin			-4.2			
	75A				-6.7		
	SFF					-7.8	
	Fasiglifam						-9.9

5.3 *In silico* physiochemical properties

Canvas was used to evaluate the toxicity, bioavailability and druggability of the chosen herbal compounds *in silico*. These parameters were tested independently from the enzymes. The results are purely based on the structure of the compound itself. The oral bioavailability of each herbal compound was calculated and is shown in Table 15. Acetyeugenol, myrcene and piperine had the highest percentage human oral absorption, while acarbose had the lowest at 0%. The QP LogHERG value of each compound was calculated as a measure of the toxicity of the compound. Cinnamic acid and rosmarinic acid had the lowest HERG toxicity, while acarbose had the highest. The #stars of each compound were calculated to determine how drug-like each herbal compound is. Acarbose had the lowest druggability score at 13 stars. All the herbal compounds had fewer than five stars, substantially less than acarbose.

Table 15: *In silico* physiochemical properties of herbal compounds

Compound	Human oral absorption ^a (%)	QPLogHERG ^b	#Stars ^c
Acarbose (positive control)	0	-5.6	13
Eriodictyol	63	-4.9	0
Piperine	90	-4.8	1
Acetyeugenol	100	-4.6	0
Myrcene	100	-3.8	5
Apigenin	71	-3.8	3
Rosmarinic acid	35	-3.7	2
Cinnamic acid	45	-3.7	4

^a Predicted human oral absorption on a scale from 0 to 100%. A value of >80% is considered high and < 25% is considered poor (Schrodinger-Press, 2012).

^b Predicted IC₅₀ value for blockage of HERG K⁺ channels. A value below -5 is a concern (Schrodinger-Press, 2012).

^c Number of property or descriptor values that fall outside the 95% range of similar values for known drugs. The recommended range is 0 – 5; where 0 indicates no violation or best candidate (Schrodinger-Press, 2012).

5.4 Chemical – protein cross reactions

STITCH was used to determine whether the herbal compounds have any cross reactions with proteins found in the human body. The drug-target interaction network for each herbal compound is shown in Figures 16-21. The drug (herbal compound) is represented by a red oblong in the centre, and the target proteins are represented by spheres at the periphery. Associated nodes are joined by lines, where the colour represents the type of action (see Table 16). STITCH generated no cross reactions for myrcene and acetylugenol.

Each protein interaction generated in STITCH is annotated with a score. The scores are an indication of the likelihood of the interactions taking place. All scores are ranked between 0 and 1, with 1 being the highest possible confidence. A score of 0.5 would indicate that roughly every second interaction might be a false positive.

Table 16: Action between targets represented by line colour

Line colour	Action type
Green	Activation
Dark blue	Binding
Light blue	Phenotype
Black	Reaction
Red	Inhibition
Purple	Catalysis
Pink	Posttranslational modification
Yellow	Transcriptional regulation

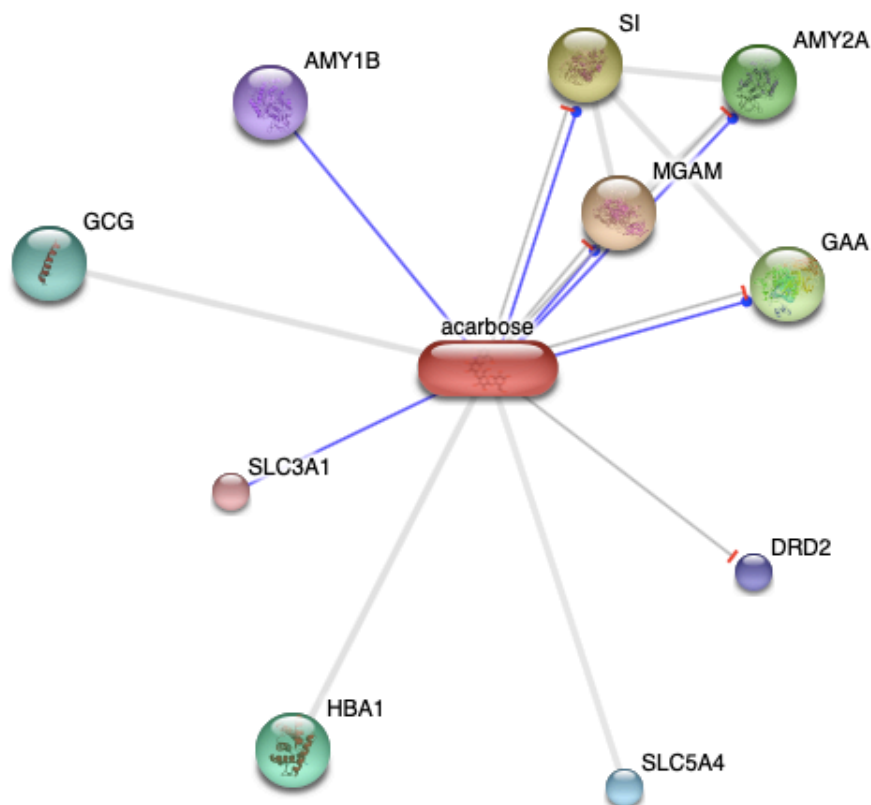


Figure 16: Drug-target interaction network of acarbose. The function of each target protein is summarised in Table 17.

Table 17: Drug-target interactions of acarbose, arranged from high to low scores

Abbreviation	Name	Function	Score
MGAM	Maltase-glucoamylase (alpha-glucosidase)	Role in digestion of oligosaccharides	0.997
SI	Sucrase-isomaltase	Important role in final stage of carbohydrate digestion.	0.997
GAA	Alpha-glucosidase	Essential for degradation of glycogen to glucose in lysosomes	0.956
AMY _{2A}	Pancreatic alpha-amylase	-	0.939
HBA ₁	Hemoglobin A1	Involved in oxygen transport from the lung to the various peripheral tissues	0.907
GCG	Glucagon	Modulate gastric acid secretion and the gastro-pyloro-duodenal activity	0.893
SLC _{5A4}	Solute carrier family 5	Dopamine receptor whose activity is mediated by G proteins which inhibit adenylyl cyclase	0.836
DRD ₂	Dopamine receptor D2	Activity mediated by G proteins which inhibit adenylyl cyclase	0.800
AMY _{1B}	Salivary alpha-amylase	-	0.783
SLC _{3A1}	Solute carrier family 3	Amino acid transporters and activator of cystine	0.768

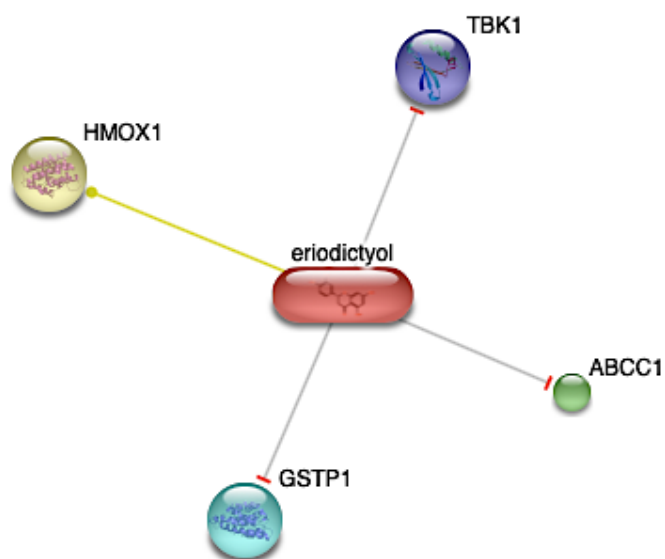


Figure 17: Drug-target interaction network of eriodictyol. The function of each target protein is summarised in Table 18.

Table 18: The drug-protein interactions of eriodictyol arranged from high to low scores

Abbreviation	Name	Function	Score
HMOX ₁	Heme oxygenase 1	Form biliverdin through cleavage of the heme ring	0.824
ABCC ₁	ATP-binding cassette, sub-family C member 1	-	0.725
GSTP ₁	Glutathione S-transferase pi 1	Form electrophiles through the conjugation of glutathione	0.700
TBK ₁	TANK-binding kinase 1	Plays an essential role in regulating inflammatory responses to foreign agents.	0.700

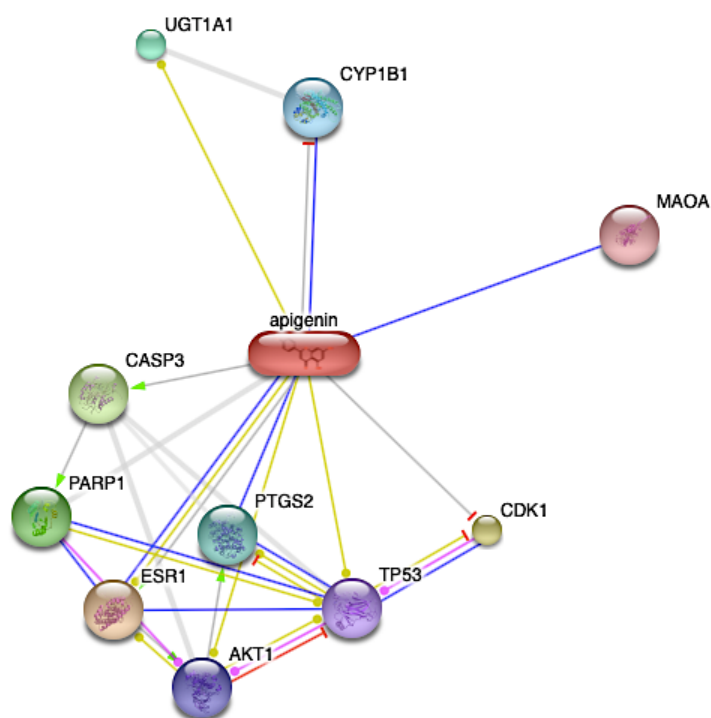


Figure 18: Drug-target interaction network of apigenin. The function of each target protein is summarised in Table 19.

Table 19: The drug-protein interactions of apigenin arranged from high to low scores

Abbreviation	Name	Function	Score
ESR ₁	Estrogen receptor 1	Regulate eukaryotic gene expression and has an effect on cellular differentiation of proliferation	0.961
CDK ₁	Cyclin-dependent kinase 1	Modulate the centrosome cycle and mitotic onset to control cell cycle	0.949
CASP ₃	Caspase 3	Role in apoptosis through the activation cascade of caspases	0.947
PARP ₁	Polymerase 1	Involved in the base excision repair pathway	0.944
UGT _{1A1}	UDP glucuronosyl-transferase 1	Role in elimination of toxic compounds	0.938
PTGS ₂	Prostaglandin-endoperoxide synthase 2	Mediates the formation of prostaglandins from arachidonate. Role as mediator of inflammation.	0.877
CYP _{1B1}	Cytochrome p450	Role in the electron transport chain	0.876
AKT ₁	v-akt murine thymoma viral oncogene homolog 1	Regulate many processes including metabolism, proliferation, cell survival, growth and angiogenesis.	0.876
TP ₅₃	Tumour protein p53	Acts as tumour suppressor. Induce growth arrests or apoptosis. Involved in cell cycle regulation.	0.868
MAOA	Monoamine oxidase A	Catalyse the oxidative deamination of biogenic and xenobiotic amines.	0.848

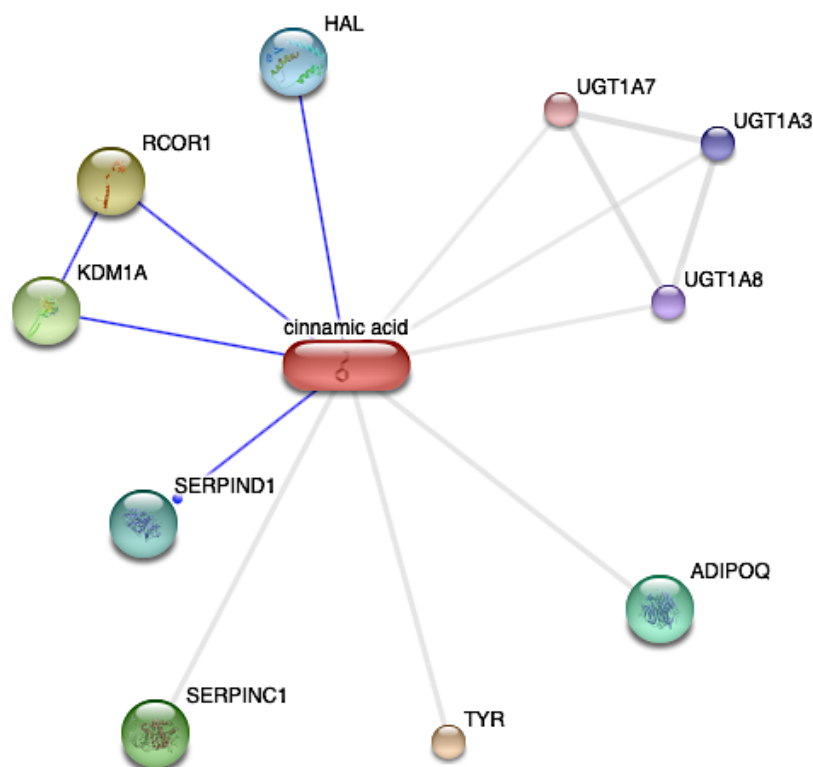


Figure 19: Drug-target interaction network of cinnamic acid. The function of each target protein is summarised in Table 20.

Table 20: The drug-protein interactions of cinnamic acid arranged from high to low scores

Abbreviation	Name	Function	Score
TYR	Tyrosinase	Role in pigment formation	0.801
RCOR ₁	REST corepressor 1	Prevent neuron-specific gene transcription	0.800
KDM ₁ A	Lysine (K)-specific demethylase 1A	-	0.800
SERPINC ₁	Serpin peptidase inhibitor	-	0.800
ADIPOQ	Adiponectin	Role in fat metabolism and insulin sensitivity regulation	0.800
SERPIND ₁	Serpin peptidase inhibitor	-	0.800
HAL	Histidine ammonia-lyase	-	0.787
UGT ₁ A ₃	UDP glucuronosyltransferase 1 family, polypeptide 3	Role in elimination of toxic compounds	0.700
UGT ₁ A ₈	UDP glucuronosyltransferase 1 family, polypeptide A8	Role in elimination of toxic compounds	0.700
UGT ₁ A ₇	UDP glucuronosyltransferase 1 family, polypeptide A7	Role in elimination of toxic compounds	0.700

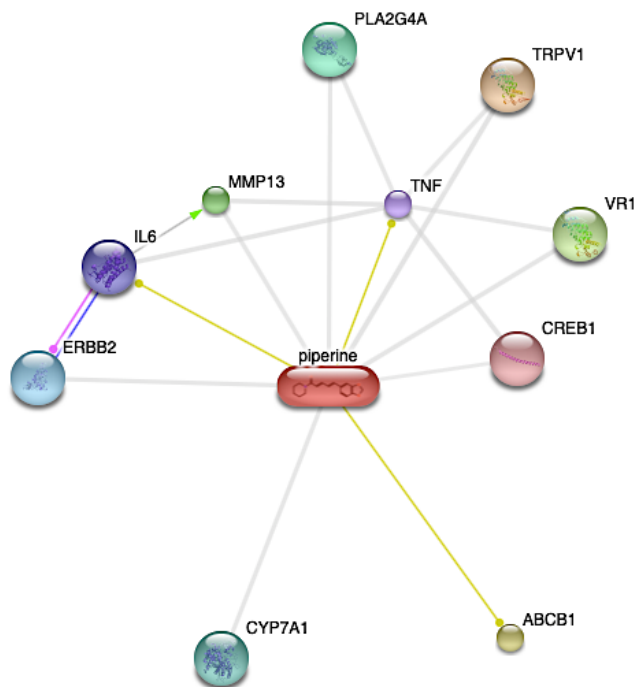


Figure 20: Drug-target interaction network of piperine. The function of each target protein is summarised in Table 21.

Table 21: The drug-protein interactions of piperine arranged from high to low scores

Abbreviation	Name	Function	Score
TRPV ₁	Transient receptor potential cation channel	Detect thermal and chemical stimuli	0.918
ABCB ₁	ATP-Binding cassette	Efflux pump that plays a role in the prevention of drug accumulation.	0.859
VR ₁	Transient receptor potential cation channel	Detect thermal and chemical stimuli	0.848
MMP ₁₃	Matrix metalloproteinase 13	Degrades collagen type I.	0.815
PLA ₂ G ₄ A	Phospholipase A2	Hydrolyse phospholipids to release arachidonic acid	0.800
CYP ₇ A ₁	Cytochrome P450, family 7 subfamily A polypeptide 1	Role in bile acid synthesis and cholesterol catabolism	0.800
ERBB ₂	v-erb-b2 erythroblastic leukaemia viral oncogene	Regulates outgrowth and stabilization of peripheral microtubules.	0.800
IL ₆	Interleukin 6	Cytokine with a wide variety of biological functions.	0.725
TNF	Tumour necrosis factor		0.725
CREB ₁	cAMP responsive element binding protein 1	Phosphorylation-dependent transcription factor that stimulates transcription.	0.700

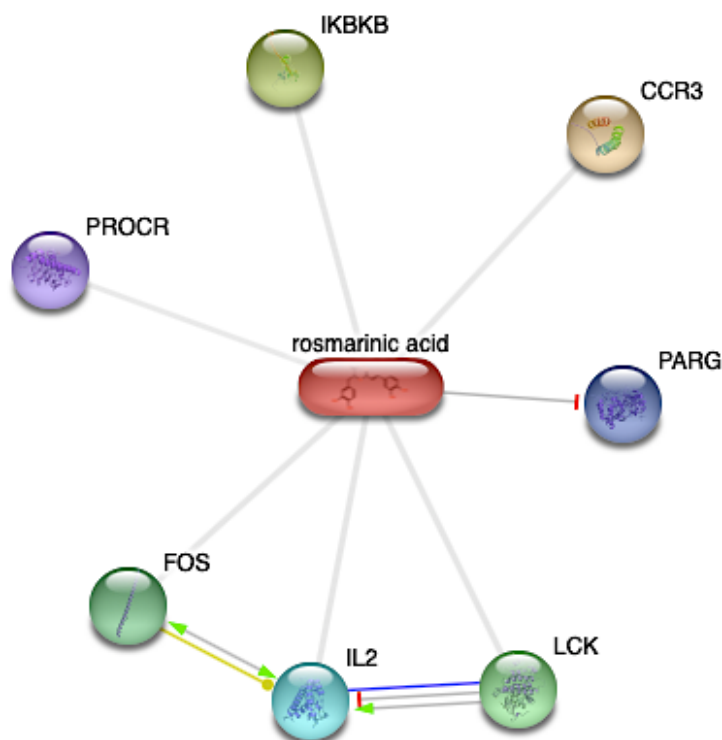


Figure 21: Drug-target interaction network of rosmarinic acid. The function of each target protein is summarised in Table 22.

Table 22: The drug-protein interactions of rosmarinic acid, arranged from high to low scores

Abbreviation	Name	Function	Score
CCR ₃	Chemokine receptor 3	Increase intracellular calcium ion levels to transduce a signal	0.800
IKKBK	Inhibitor of kappa light polypeptide gene enhancer	Role in NF kappa B signalling pathway.	0.800
LCK	Lymphocyte-specific protein tyrosine kinase	-	0.800
FOS	FBJ murine osteosarcoma viral oncogene homolog	Regulates the development of cells destined to form and maintain the skeleton.	0.800
IL ₂	Interleukin 2	Important role in immune response and required for T-cell proliferation	0.800
PARG	Poly (ADP-ribose) glycohydrolase	Role in the elimination of toxic compounds	0.700
PROCR	Protein C receptor	Function in blood coagulation	0.700

5.5 Inhibition of α -amylase and α -glucosidase

The ability of the herbal compounds to inhibit α -amylase and α -glucosidase were investigated *in vitro*. The inhibitory characteristics of the herbal compounds were explored by performing kinetic assays, with double reciprocal Lineweaver-Burk plots used to calculate the kinetic parameters. The Lineweaver-Burk plots generate a straight line for the uninhibited and each inhibited reaction. As seen in Figures S7 and S8, the straight lines of the inhibited reactions intersect with the straight line of the uninhibited reaction. The point of intersection can be used to determine the type of inhibition that has occurred. A statistical analysis (two-sided Student's t-test, $p < 0.05$) was done between the kinetic parameters of the uninhibited reaction and the kinetic parameters (Tables 23 and 24) of the inhibited reactions to validate the type of inhibition observed in the Lineweaver-Burk plots.

Regarding the inhibition of α -amylase, it can be concluded that acarbose and piperine were competitive inhibitors whereas eriodictyol, cinnamic acid, and rosmarinic acid were non-competitive inhibitors. Acetyeugenol and apigenin showed mixed inhibition. Acetyeugenol and cinnamic acid inhibited α -glucosidase non-competitively, while acarbose, apigenin, eriodictyol, and piperine and showed mixed inhibition. Rosmarinic acid showed uncompetitive inhibition. Myrcene showed no statistically significant inhibition of α -amylase or α -glucosidase.

Table 23: Michaelis-Menten parameters for the inhibition of α -amylase by herbal compounds

Compound	K_m and K_m (app) (mg/mL)			V_{max} (μ Moles.min ⁻¹)		
	2.5 μ M	5 μ M	10 μ M	2.5 μ M	5 μ M	10 μ M
α -Amylase with no inhibitor		3.28 \pm 0.4		0.15 \pm 0.03		
Acarbose (positive control)	7.66 \pm 1.7*	7.08 \pm 0.7*	23.6 \pm 3.2*	0.19 \pm 0.02	0.14 \pm 0.03	0.16 \pm 0.01
Eriodictyol	5.39 \pm 0.9	3.56 \pm 0.6	7.57 \pm 4.2	0.09 \pm 0.01*	0.10 \pm 0.01*	0.09 \pm 0.02*
Piperine	4.98 \pm 1.1*	5.82 \pm 2.1*	7.08 \pm 2.1*	0.15 \pm 0.06	0.12 \pm 0.04	0.16 \pm 0.08
Apigenin	3.25 \pm 0.2	3.53 \pm 1.1	5.06 \pm 1.1*	0.13 \pm 0.05	0.10 \pm 0.01*	0.09 \pm 0.02*
Rosmarinic acid	3.37 \pm 0.4	4.11 \pm 1.8	7.54 \pm 4.2	0.09 \pm 0.01*	0.09 \pm 0.02*	0.06 \pm 0.01*
Cinnamic acid	3.50 \pm 1.9	4.72 \pm 2.9	5.99 \pm 2.3	0.06 \pm 0.02*	0.06 \pm 0.02*	0.07 \pm 0.03*
Acetylugenol	5.44 \pm 0.7*	5.34 \pm 2.5*	6.36 \pm 1.9*	0.10 \pm 0.01*	0.11 \pm 0.01*	0.11 \pm 0.01*
Myrcene	14.0 \pm 8.3	3.17 \pm 0.9	3.98 \pm 1.6	0.43 \pm 0.09	0.16 \pm 0.03	0.13 \pm 0.01

Data are represented as mean \pm SD (n = 3). The asterisks (*) denote values significantly different ($p < 0.05$) from the uninhibited reaction, as determined by a two-sided Student's t test.

Table 24: Michaelis-Menten parameters for the inhibition of α -glucosidase by herbal compounds

Compound	K_m and K_m (app) (mM)			V_{max} (mM.min ⁻¹)		
	250 μ M	500 μ M	1000 μ M	250 μ M	500 μ M	1000 μ M
α -Glucosidase with no inhibitor		0.35 \pm 0.07		0.008 \pm 0.001		
Acarbose (positive control)	0.75 \pm 0.28*	0.59 \pm 0.01*	1.14 \pm 0.18*	0.008 \pm 0.001*	0.005 \pm 0.003*	0.004 \pm 0.002*
Eriodictyol	0.28 \pm 0.01	0.34 \pm 0.07	2.66 \pm 2.08	0.005 \pm 0.001*	0.005 \pm 0.001*	0.006 \pm 0.001*
Piperine	0.39 \pm 0.01	0.47 \pm 0.20	1.24 \pm 1.05	0.006 \pm 0.000*	0.004 \pm 0.002*	0.007 \pm 0.006
Apigenin	0.74 \pm 0.42	0.55 \pm 0.21	0.31 \pm 0.04	0.004 \pm 0.001*	0.005 \pm 0.001*	0.005 \pm 0.001*
Rosmarinic acid	1.30 \pm 0.35*	0.79 \pm 0.09*	0.01 \pm 0.01*	0.001 \pm 0.001*	0.001 \pm 0.000*	0.003 \pm 0.000*
Cinnamic acid	0.37 \pm 0.08	0.84 \pm 0.51	1.02 \pm 0.80	0.005 \pm 0.001*	0.004 \pm 0.002*	0.003 \pm 0.002*
Acetylugenol	0.36 \pm 0.10	0.32 \pm 0.09	0.31 \pm 0.04	0.007 \pm 0.003	0.004 \pm 0.002*	0.005 \pm 0.002*
Myrcene	0.50 \pm 0.01	0.46 \pm 0.08	0.60 \pm 0.51	0.008 \pm 0.001	0.008 \pm 0.001	0.007 \pm 0.003

Data are represented as mean \pm SD (n = 3). The asterisks (*) denote values significantly different ($p < 0.05$) from no inhibition, determined with a two-sided Student's t test

The inhibition potential of each compound was evaluated and compared based on their K_i values (Tables 25 and 26). The K_i was calculated with the help of secondary graphs by plotting the reciprocal of the Lineweaver-Burk plot slope against the inhibitor concentration. A one-sided Student's t-test was used to compare the K_i of the herbal compounds to the K_i of acarbose. There was no significant ($p > 0.05$) difference between the K_i value of acarbose and those of apigenin, cinnamic acid and rosmarinic acid when inhibiting α -amylase. Acetyლეugenol, eriodictyol, piperine, and myrcene had significantly higher K_i values than acarbose. For α -glucosidase inhibition, there was no significant ($p > 0.05$) difference between the K_i value of acarbose and those of apigenin, eriodictyol and piperine while acetyლეugenol, cinnamic acid, myrcene and rosmarinic acid had a significantly higher K_i than acarbose.

Table 25: Inhibitory activity of herbal compounds against porcine pancreatic α -amylase

Compound	Type of inhibition	K_i (μM)
Acarbose (positive control)	Competitive	3.8 ± 1.9
Rosmarinic acid	Non-competitive	4.5 ± 2.9
Apigenin	Mixed	7.8 ± 2.7
Cinnamic acid	Non-competitive	8.0 ± 4.5
Eriodictyol	Non-competitive	$10.5 \pm 3.6^*$
Piperine	Competitive	$10.9 \pm 5.5^*$
Acetyლეugenol	Mixed	$12.1 \pm 5.8^*$
Myrcene	None	$49.0 \pm 33.7^*$

Data are represented as mean \pm SD ($n = 3$). The asterisks (*) denote values significantly different ($p < 0.05$) from acarbose, determined with a one-sided Student's t test.

Table 26: Inhibitory activity of herbal compounds against yeast α -glucosidase

Compound	Type of inhibition	K_i (μM)
Eriodictyol	Mixed	130 ± 70
Apigenin	Mixed	160 ± 50
Acarbose (positive control)	Mixed	170 ± 80
Piperine	Mixed	280 ± 120
Cinnamic acid	Non-competitive	$620 \pm 380^*$
Acetyლეugenol	Non-competitive	$950 \pm 240^*$
Myrcene	None	$1580 \pm 650^*$
Rosmarinic acid	Uncompetitive	$2580 \pm 550^*$

Data are represented as mean \pm SD ($n = 3$). The asterisks (*) denote values significantly different ($p < 0.05$) from acarbose, determined with a one-sided Student's t test.

The negative delta G was plotted against the K_i of each compound in Figures 22 and 23 to determine the relationship between the parameters. There is a positive relationship between the negative delta G score and the K_i values of the herbal compounds when inhibiting α -glucosidase and α -amylase. The K_i of rosmarinic acid, inhibiting α -glucosidase, was identified as an outlier with undue influence on the slope and was not included in any calculations.

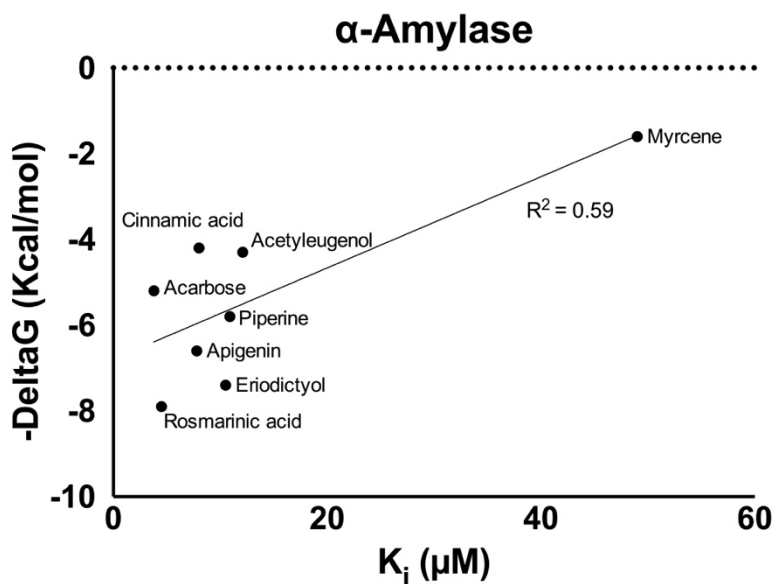


Figure 22: The correlation between negative delta G versus the K_i value of herbal compounds for α -amylase.

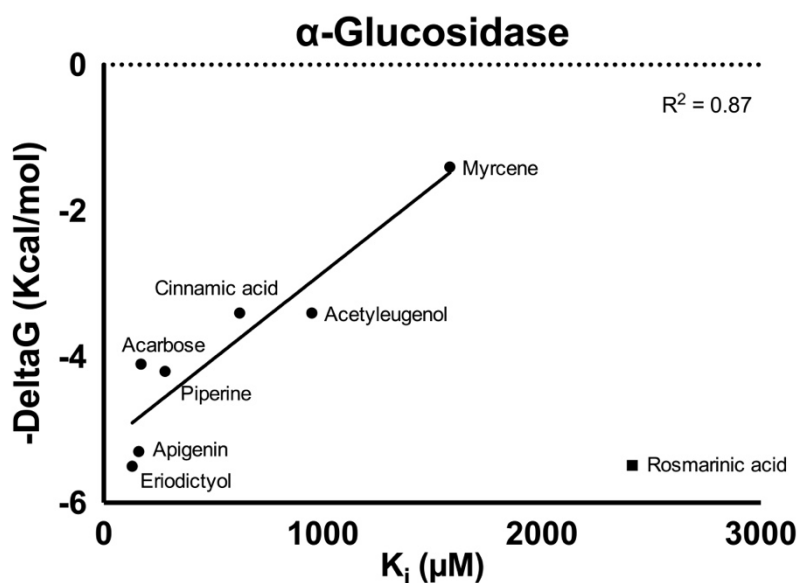


Figure 23: The correlation between negative delta G versus the K_i value of herbal compounds for α -glucosidase. Rosmarinic acid (shown with square symbol) was identified as an outlier with undue influence on the slope.

5.6 Cytotoxicity in C2C12 and HepG2 cell lines

The cytotoxic effects of the herbal compounds on the viability of C2C12 and HepG2 cells was evaluated by measuring the IC₅₀ values (Table 27). All herbal compounds, except for apigenin and eriodictyol displayed limited cytotoxicity in the HepG2 cell line, where concentrations up to 500 µM did not induce 50% cell death (Figure S9) therefore, accurate IC₅₀ values could not be calculated. Eriodictyol displayed substantial toxicity (IC₅₀ = 41 ± 2 µM) while apigenin displayed milder toxicity (IC₅₀ = 210 ± 41 µM) against this cell line.

The C2C12 cells were generally more sensitive to the herbal compounds than the HepG2 cells. Acetylugenol, cinnamic acid, myrcene, piperine, and rosmarinic acid displayed toxicity at the highest concentration (500 µM), although not statistically more significant ($p > 0.05$) when compared with acarbose at the same concentration (500 µM). Eriodictyol (IC₅₀ = 11 ± 2 µM) and apigenin (IC₅₀ = 31 ± 4 µM) were significantly ($p < 0.05$) more toxic than acarbose (IC₅₀ = 60 ± 15 µM).

Table 27: IC₅₀ values of herbal compounds on C2C12 and HepG2 cells

Compound	C2C12 IC ₅₀ (µM)	HepG2 IC ₅₀ (µM)
Eriodictyol	11 ± 2*	41 ± 2
Apigenin	31 ± 4*	210 ± 41
Acarbose (positive control)	60 ± 15	> 500
Piperine	79 ± 8	> 500
Rosmarinic acid	83 ± 2	> 500
Myrcene	84 ± 3	> 500
Cinnamic acid	87 ± 2	> 500
Acetylugenol	96 ± 24	> 500

Data are represented as mean ± SD (n = 3). The asterisks (*) denote values significantly different ($p < 0.05$) from acarbose, determined with a two-sided Student's t test.

5.7 Glucose uptake in C2C12 and HepG2 cell lines

C2C12 and HepG2 cells were treated with a range of non-cytotoxic herbal concentrations (0.1, 1 and 10 μM), to investigate whether the herbal compounds directly affected glucose metabolism in C2C12 and HepG2 cells. The herbal compounds significantly ($p < 0.05$) enhanced 2-NBDG uptake in C2C12 and HepG2 cells compared to the control. The stimulatory effect of the herbal compounds was similar to that of insulin ($p > 0.05$). In C2C12 cells (Figure 24) acetylugenol, apigenin, eriodictyol, and myrcene enhanced glucose uptake. In HepG2 cells (Figure 25) acetylugenol, apigenin, cinnamic acid, eriodictyol, piperine and rosmarinic acid enhanced glucose uptake.

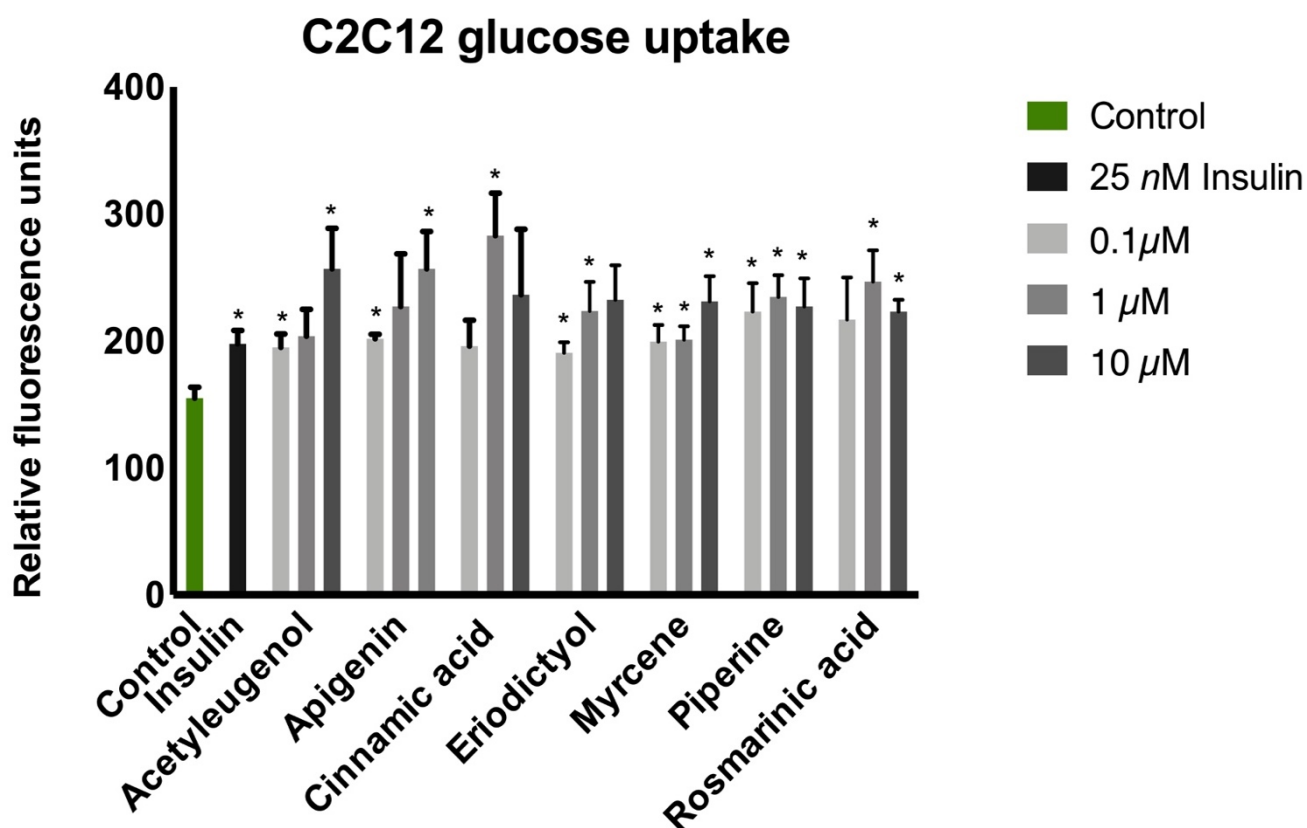


Figure 24: The effect of herbal compounds on glucose uptake in C2C12 cells. The asterisks (*) denote fluorescence intensities significantly ($p < 0.05$) increased relative to the control, determined with a two-sided Student's t test. There is no significant ($p > 0.05$) difference in the fluorescence intensity of the herbal compounds relative to insulin (positive control), determined with a two-sided Student's t test.

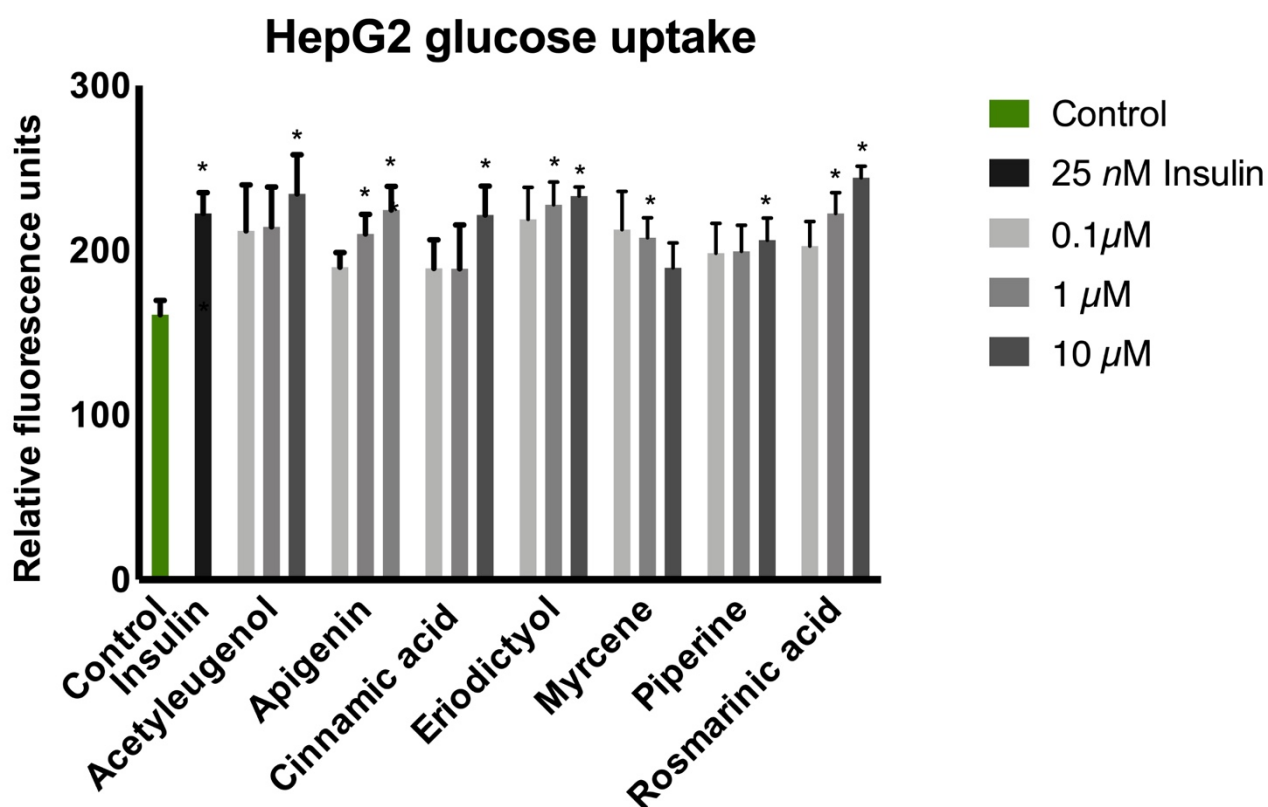


Figure 25: The effect of herbal compounds on glucose uptake in HepG2 cells. The asterisks (*) denote fluorescence intensities significantly ($p < 0.05$) increased relative to the control, determined with a two-sided Student's t test. There is no significant ($p > 0.05$) difference in the fluorescence intensity of the herbal compounds relative to insulin (positive control), determined with a two-sided Student's t test.

5.8 Daily herbal dose equivalent to acarbose dose

The USDA (Haytowitz *et al.*, 2018) and DUKE (Duke, 1992) databases were used to search for natural sources containing each herbal compound. The databases give the amount (mg/100 g) of each compound found in different herb or spice sources. This was used to calculate the amount (g) of each herbal compound required to relate to the average daily dose (150 mg) of acarbose (Table 28).

Table 28: The herbal dosage equivalent to a daily dose of acarbose with the potential to inhibit α -amylase and α -glucosidase

Compound	Main source	Amount in herb/spice (mg/100 g)	Amount (g) needed to relate to daily dose of acarbose	NOAEL (g)*
Piperine	<i>Piper nigrum</i> (Black pepper)	7750	1.9	2.9
Rosmarinic acid	<i>Origanum vulgare</i> (Oregano)	6800	2.2	18
Cinnamic acid	<i>Cinnamomum loureiroi</i> (Cinnamon)	4760	3.2	16.5
Apigenin	<i>Petroselinum crispum</i> (Parsley)	4504	3.3	3.8
Acetyeugenol	<i>Syzygium aromaticum</i> (Cloves)	2075	7.2	15
Eriodictyol	<i>Lippia graveolens</i> (Mexican oregano)	93	161	1.2
Myrcene	<i>Mentha spicata</i> (Spearmint)	122	123	2.6

Sourced from USDA (Haytowitz *et al.*, 2018) and DUKE (Duke, 1992) database.

Based on a 150 mg acarbose dose per day.

*NOAEL values based on a 60 kg individual

6. DISCUSSION

The control of postprandial hyperglycaemia is of great significance in the treatment of T2DM and the prevention of short- and long-term complications (Ademiluyi & Oboh, 2013; Dowshen, 2018). An important therapeutic approach for reducing postprandial hyperglycaemia involves the inhibition of enzymes involved in carbohydrate metabolism, α -amylase and α -glucosidase (Ademiluyi & Oboh, 2013). Recently, the application of herbal plants have been of significant interest due to their low cost, natural origin and easily cultivatable nature (Luyen *et al.*, 2019). Also compounds with multiple targets for the same disease might have a beneficial effect due to synergistic effects. For example, in T2DM such a beneficial effect would be the inhibition of the amylase and glucosidase activity, with if bioavailable, the stimulation of glucose uptake.

This study highlights the hypoglycaemic effect of seven herbal compounds through glucose uptake stimulation and inhibition of yeast α -glucosidase and porcine pancreatic amylase. The herbal compounds assessed were acetyleugenol, apigenin, cinnamic acid, eriodictyol, myrcene, piperine, and rosmarinic acid.

6.1 *In silico* docking to carbohydrate hydrolysing enzymes

The predicted binding of the herbal compounds to α -amylase and α -glucosidase were studied *in silico* before any studies were performed in the laboratory. Docking scores of the herbal compounds docked to α -amylase and α -glucosidase were generated through Maestro (Maestro, 2020). The herbal compounds were docked to both enzymes where it associated with amino acids through a negative binding energy, indicating a spontaneous binding and potential inhibition. Ligand interaction diagrams (Figures S1 and S2) were generated to identify the enzymatic amino acids interacting with the ligands, and to ensure that the docking occurred in the active sites of the enzymes. The interactions were either through hydrogen bonds, water bridges, or pi-pi stackings. The amino acids (Tables 12 and 13), of α -amylase and α -glucosidase, interacting with starch (the control) corresponds well with literature, indicating that the docking occurred in the active sites of the enzymes.

With α -amylase, the decreasing order of the positive binding and potential inhibition was rosmarinic acid > eriodictyol > apigenin > piperine > acarbose > acetyeugenol > cinnamic acid > myrcene (Table 9). In the case of α -glucosidase it was eriodictyol > rosmarinic acid > apigenin > piperine > acarbose > cinnamic acid > acetyeugenol > myrcene (Table 10). The docking scores of these herbal compounds were compared to the interactions of acarbose with α -amylase and α -glucosidase, whose binding energies were -5.2 kcal/mol and -4.1 kcal/mol, respectively. Evidently apigenin, eriodictyol, piperine, and rosmarinic acid had better docking scores to α -amylase and α -glucosidase than acarbose. Acetyeugenol, cinnamic acid and myrcene showed weaker docking scores than acarbose. The results of the docking analysis encouraged us to investigate the enzyme inhibitory activity further using enzyme assays.

6.2 *In silico* docking to insulin-regulating targets

The ability of the herbal compounds to mimic the effect of insulin through glucose regulation was studied *in silico* through inverse docking. From our results (Table 14) it can be seen that apigenin, eriodictyol, piperine, and rosmarinic acid has higher negative docking scores than anagliptin (positive control) to DPP4 (PDB: 4A5S) (Sutton *et al.*, 2012) and thus stronger binding, possibly translating to better inhibition. DPP4 decrease insulin secretion from the pancreas through degradation and inactivation of glucagon-like peptide-1 (GLP-1), therefore inhibition of DPP4 is required to treat T2DM (Abbas *et al.*, 2019). The tight binding of apigenin, eriodictyol, piperine, and rosmarinic acid to DPP4 will theoretically lead to the inhibition of DPP4, which will increase insulin secretion from the pancreas, giving rise to hypoglycaemia.

Eriodictyol has a better docking score than SFF (positive control) to HSD11B1 (PDB: 4K1L) (Bohme *et al.*, 2013). Inhibition of HSD11B1 leads to the inhibition of glucose production by the liver and improves glucose-dependent insulin sensitivity (Zhu *et al.*, 2018). Thus, according to the *in silico* results, eriodictyol might decrease hyperglycaemia and increase insulin sensitivity through the inhibition of HSD11B1.

All the herbal compounds, except myrcene, had higher negative docking scores to RBP4 (PDB: 2WR6) (Motani *et al.*, 2009) than linolenic acid (positive control) indicating a stronger binding. RBP4 is secreted as an adipokine that disrupts insulin signalling, reduce glucose uptake by muscles and promotes glucose production by the liver (Berry & Noy, 2012; Pereira *et al.*, 2019). The high negative docking scores of the herbal compounds suggest theoretical inhibition of RBP4, which will lead to increased glucose uptake by muscles and decreased glucose production by the liver.

The positive controls 75A, fasiglifam and insulin, have the highest negative docking scores to PTPN9 (PDB: 4GE6) (Zhang *et al.*, 2012b), FFAR1 (PDB: 4PHU) (Srivastava *et al.*, 2014) and INSR (PDB: 3EKN) (Chamberlain *et al.*, 2009) respectively. Inhibition of PTPN9 leads to insulin sensitisation and improved glucose homeostasis (Yoon *et al.*, 2018). Agonists of FFAR1 will stimulate insulin secretion from pancreatic β -cells (Eleazu *et al.*, 2018). Insulin sensitivity and glucose uptake can be improved, through agonists activating INSR to stimulate the insulin signalling pathway (Qiung *et al.*, 2014).

6.3 *In silico* physiochemical properties

Selected physiochemical parameters of the herbal compounds were evaluated *in silico*. The cardiotoxicity of each herbal compound was assessed using the QPlogHERG function, which is the projected log IC₅₀ value for the blockage of HERG potassium (K⁺) channels. The Canvas software calculates the distances and angles between the carbon atoms of each herbal compound and predicts the pIC₅₀. A value between 0 and -5 is desired. Once a more negative value is observed, it can lead to a disorder called long Q-T syndrome. All the herbal compounds had more positive QPlogHERG values than acarbose (Table 15), indicating that these compounds have a lower probability of causing the long Q-T syndrome than acarbose.

The percentage human oral absorption is calculated by studying the number of metabolites, rotatable bonds, logP, solubility and cell permeability of each compound. Oral absorption is defined as the amount of an administered drug that reaches systemic circulation (Turner & Agatonovic-Kustrin, 2007). Acarbose had a human oral absorption of 0%. Since acarbose is an orally administered drug, a low oral absorption is expected and acarbose must work locally

within the gastrointestinal tract therefore, no oral absorption is therapeutically desired. Rosmarinic acid had a human oral absorption of 35%, which is the lowest of all the herbal compounds, while cinnamic acid, eriodictyol, apigenin and piperine had an oral absorption of 45%, 63%, 71% and 90%, respectively. These values are substantially higher than the oral absorption of acarbose. However, for the compounds to exert insulin mimicking activity some bioavailability is required to reach the systemic circulation. It would be ideal if some of the drug can stay in the GIT to inhibit α -amylase and α -glucosidase, while some of the drug reach the skeletal muscle and liver to increase glucose uptake. A bioavailability of 35% indicates that 35% of the administered dose will reach systemic circulation and the peripheral tissues to increase glucose uptake, thus 65% of the drug will remain in the GIT to inhibit α -amylase and α -glucosidase. Acetyeugenol and myrcene had an oral bioavailability of 100%, which means most of the administered drug gets absorbed into the systemic circulation. Thus, little drug remains in the GIT, where inhibitory action is required.

The druggability of the compounds was compared using the #stars function. The QikProp function of Canvas includes 24 descriptors in the calculation of the #stars (Schrodinger-Press, 2012). The #stars of each compound indicates the number of descriptor values that fall outside of 95% of similar values for known drugs (Jain *et al.*, 2013). Therefore, a lower #stars indicates a better drug-like molecule (Rohini & Shanthi, 2018). All the compounds have a lower #stars than acarbose, which means the herbal compounds are more drug-like than acarbose. All the herbal compounds had no more than 5 stars (Table 15), indicating that all 24 pharmaceutically relevant descriptors lie within the recommended range of known drugs (Rohini & Shanthi, 2018).

6.4 Drug-Target networks through STITCH

STITCH is a database of known and predicted interactions between proteins, chemicals and small molecules. Knowledge regarding the interactions between proteins and small molecules is essential for the understanding of molecular and cellular function. The interactions include direct (physical) and indirect (functional) associations. Predictions of the associations stem from text mining, co-expression, databases, genomic context predictions and high-throughput laboratory experiments (Szklarczyk *et al.*, 2016).

There is an increasing trend to use network pharmacology to determine the cross-reactions, mechanisms of action and potential therapeutic effects of drugs. We included the evaluation on STITCH in our study, to determine whether the herbal compounds had any undesired or damaging cross-reactions with other proteins. Cross-reactivity can be defined as the reactivity of a drug which initiates reactions outside the primary expected reaction (Xie *et al.*, 2019). Here, the studied reactions included the inhibition of α -amylase and α -glucosidase and the effect of the herbal compounds on glucose uptake, thus associations with any proteins involved in those reactions were expected.

Acarbose had ten drug-protein interactions (Figure 16), mostly with different types of α -amylase and α -glucosidase enzymes (Table 17) found in the body. In the present study the *in vitro* results of acarbose on α -amylase and α -glucosidase, correlate well with the *in silico* findings on STITCH.

A few protein-target associations were generated for each herbal compound, however there were no associations generated between the herbal compounds and α -amylase and α -glucosidase. This does not correspond to the experimental results of this study. Even when the interaction score was set to low confidence (0.150), no interactions between the herbal compounds and the starch hydrolysing enzymes were generated on STITCH. The interaction sources on STITCH were set to include experimental results and literature. There are various studies on the inhibition α -amylase and α -glucosidase by these herbal compounds (Proença *et al.*, 2019; Rivera-Chavez *et al.*, 2013; Stoilova *et al.*, 2017; Zhang *et al.*, 2019), thus one would expect to see interactions between the herbal compounds and α -amylase and α -glucosidase on STITCH.

Eriodictyol had four drug-protein interactions (Table 18 and Figure 17). Heme oxygenase (HMOX₁) is a phase II detoxifying enzyme. According to Lee *et al.* (2015b), activation of HMOX₁ by eriodictyol protects endothelial cells from oxidative stress. STITCH showed the interaction of eriodictyol to TANK binding kinase (TBK₁), a protein kinase that plays a vital role in inflammatory responses. The *in silico* findings have been confirmed *in vitro* by Yu *et al.* (2012). Several studies reported that TBK₁ plays a pivotal role in diabetes, cancers, viral and bacterial infections, arthritis and hepatitis (Yu *et al.*, 2012). According to the STITCH database, eriodictyol inhibited glutathione S-transferase (GST), GSTs play an essential role in detoxification of xenobiotics. Inhibition of GSTs will affect the metabolism and biological effects of many drugs. Studies have confirmed that flavonoids such as eriodictyol inhibit GSTs (Bousova & Skalova, 2012), although only at very high concentrations (Bousova & Skalova, 2012).

Cinnamic acid (Table 20 and Figure 19) generated ten interactions according to STITCH, the most significant being the activation of adiponectin, a molecule involved in glucose and fat metabolism. *In vitro* studies have shown the activation of adiponectin by cinnamic acid in adipocytes, to improve insulin sensitivity via AMPK activation (Kopp *et al.*, 2014). Cinnamic acid showed activation of various UDP glucuronosyltransferase targets, which is responsible for the elimination of toxic compounds.

Table 19 and Figure 18, shows that apigenin forms associations with ten protein targets, the most significant being the inhibition of cytochrome P450 (CYP_{1B1}). Effects on the cytochrome (CYP) enzyme family can cause adverse reactions involving the metabolism and drug detoxification. If apigenin inhibits CYP_{1B1}, it may affect the CYP mediated metabolism of another drug, which can accumulate within the body to toxic levels. On the other hand, CYP_{1B1} is over-expressed in human cancer cells and metabolises both polycyclic aromatic hydrocarbons and oestradiol to potentially carcinogenic intermediates (Chaudhary & Willett, 2006). Various studies have shown the anti-carcinogenic effect of apigenin through the inhibition of CYP_{1B1} (Chaudhary & Willett, 2006). The drug-target network of apigenin also showed activation of tumour protein p53 and caspase 3, two proteins that play an important role in the regulation and progression of the cell cycle. Studies have proven the activation of these two proteins by apigenin *in vitro* and *in vivo* (Liu *et al.*, 2017) (Granato *et al.*, 2017). UDP glucuronosyl-transferase 1 (UGT_{1A1}) plays an essential role in the elimination of toxins and xenobiotics. Apigenin has been shown to activate UGT_{1A1} *in vitro* (Walle & Walle, 2002).

Piperine (Table 21 and Figure 20) had ten drug-protein interactions, the most notable being with cytochrome P450 (CYP_{7A1}), interleukin 6 (IL₆) and tumour necrosis factor (TNF). CYP_{7A1} plays a critical role in bile acid control and the maintenance of mammalian cholesterol homeostasis. STITCH did not indicate whether piperine activates or inhibits CYP_{7A1}, and no literature could be found on any association between piperine and CYP_{7A1}. TNF and IL₆ are two factors that play a vital role in the inflammatory process in humans. In an *in vivo* study Zhai *et al.* (2016) showed the inhibition of both proinflammatory factors by piperine, thereby having the ability to alleviate inflammation.

STITCH generated seven associations for rosmarinic acid (Table 22 and Figure 21), the most notable being inhibition of interleukin 2 (IL₂), a cytokine. Lembo *et al.* (2014) showed the natural anti-inflammatory properties of rosmarinic acid through the inhibition of IL₂. No literature was found on the association of rosmarinic acid with tyrosine kinase (TYR), chemokine receptor C (CCR₃) and inhibitor of kappa light polypeptide gene enhancer (IKBKB).

In general, the associations generated by STITCH corresponded well with literature. The herbal compounds showed no associations that could lead to harmful cross-reactions. The drug-target networks generated on STITCH highlighted the anti-carcinogenic and anti-inflammatory properties of the herbal compounds. According to Deans and Sattar (2006), there is growing evidence of the role of inflammation in type 2 diabetes and, thus drugs that have apparent anti-inflammatory properties may reduce the incidence and/or delay the onset of type 2 diabetes. Aside from the anti-inflammatory properties of the herbal compounds, the anti-carcinogenic properties are extremely valuable, since type 2 diabetes is associated with an increased risks of developing several cancers (Collins, 2014).

6.5 Inhibition of α -amylase and α -glucosidase

The *in vitro* inhibition effect of the herbal compounds on α -amylase and α -glucosidase, was compared with acarbose, an anti-diabetic drug currently on the market. Acarbose belongs to the α -glucosidase inhibitor class of the oral hypoglycaemics and inhibits both α -amylase and α -glucosidase. For this reason, acarbose was used as a positive control in both assays. To ensure that acarbose and the herbal compounds do inhibit α -amylase and α -glucosidase, their kinetic parameters were statistically compared with those of α -amylase and α -glucosidase when no inhibition occurred. It can be confirmed that there was a statistically significant difference in either the K_m and/or V_{max} (Table 23 and 24) of α -amylase and α -glucosidase when inhibited by each of the herbal compounds, except for myrcene. Thus, the null hypothesis H_{10} (see section 2) was rejected for all the herbal compounds except for myrcene, which does not reject H_{10} .

The Lineweaver-Burk graphs of each compound were used to establish the type of inhibition exerted by each compound. Acarbose was verified as a competitive inhibitor of α -amylase (Poovitha & Parani, 2016; Rahimzadeh *et al.*, 2014; Stoilova *et al.*, 2017) and a mixed inhibitor of α -glucosidase (Son & Lee, 2013; Stoilova *et al.*, 2017). Acetylugenol, apigenin, cinnamic acid, eriodictyol, piperine, and rosmarinic acid displayed dose-dependent inhibition of α -amylase and α -glucosidase, with acarbose as the positive control. As seen in Figure S7, cinnamic acid, eriodictyol, and rosmarinic acid inhibited α -amylase non-competitively (K_m value remained constant and V_{max} value decreased, Table 23). Non-competitive inhibition occurs when the binding of the inhibitor to the enzyme or enzyme-substrate (ES) complex changes the conformation of the enzyme, preventing the substrate from binding (Aldred E.M,

2009). Acetyleguonol and apigenin inhibited α -amylase in a mixed fashion, indicating that the inhibitor binds to the enzyme or the ES complex with a greater affinity for one state (Berg *et al.*, 2007). This can either increase or decrease the K_m , but both cases will cause a decrease in V_{max} . In this case, the K_m was increased, thus the affinity of the enzyme for the substrate is decreased. This is seen in cases where the inhibitor favours binding to the free enzyme and not the enzyme-substrate (ES) complex, which mimics competitive inhibition (Berg *et al.*, 2007). Piperine inhibited α -amylase competitively. Competitive inhibition occurs when the inhibitor binds in the active site of the enzyme, preventing the substrate from binding (Engelking, 2015). This leads to an increased K_m since the affinity of the enzyme for the substrate is decreased, while the V_{max} of the reaction stays the same.

As seen in Figure S8, apigenin, eriodictyol, and piperine were mixed inhibitors of α -glucosidase, while acetyleguonol and cinnamic acid were non-competitive inhibitors. Rosmarinic acid inhibited α -glucosidase uncompetitively, binding to the ES complex. Uncompetitive inhibition is characterised by a decrease in both K_m and V_{max} (Table 24) due to increased binding efficiency, interference with substrate binding and hampered catalysis (Dougall & Unitt, 2015). Myrcene presented no inhibitory activity against α -amylase and α -glucosidase.

K_i values can be a useful tool to compare the inhibitory activity of the herbal compounds, reflecting the functional strength of the inhibitor. It is an indication of the binding affinity of the inhibitor thus, a lower K_i value suggests a higher binding affinity. The K_i values of acarbose when inhibiting α -amylase (Bemiller & Whistler, 2009; Proença *et al.*, 2019; Yoon & Robyt, 2003) and α -glucosidase (Proença *et al.*, 2017; Robyt, 2005) correlate well with literature values. The K_i values of the tested compounds against α -amylase were: acarbose < rosmarinic acid < apigenin < cinnamic acid < eriodictyol < piperine < acetyeugenol < myrcene. There was no statistically significant difference (Table 25, $p > 0.05$) between the K_i values of acarbose and those of rosmarinic acid, apigenin and cinnamic acid, therefore the null hypothesis (H_{20}) was not rejected. The K_i values of acetyeugenol, eriodictyol, myrcene, and piperine was significantly ($p < 0.05$) larger than the K_i of acarbose, thus rejecting the null hypothesis (H_{20}). None of the herbal compounds had a K_i value lower than that of acarbose, which might be therapeutically preferred. Mild inhibition of α -amylase is preferred in many cases to avoid excessive bacterial fermentation, leading to gastrointestinal side effects (Etxeberria *et al.*, 2012; Proença *et al.*, 2019). Regarding α -glucosidase, the decreasing order of the K_i values were: eriodictyol < apigenin < acarbose < piperine < cinnamic acid < acetyeugenol < myrcene < rosmarinic acid. There was no statistically significant difference (Table 26, $p > 0.05$) between the inhibition effect of apigenin, eriodictyol, and piperine when compared to acarbose, based on K_i values therefore, the null hypothesis (H_{20}) is not rejected. Indicating that these herbal compounds inhibit α -glucosidase with the same functional strength as acarbose. The results revealed that the K_i values of acetyeugenol, cinnamic acid, myrcene and rosmarinic acid were significantly larger than the K_i value of acarbose, thus the null hypothesis (H_{20}) was rejected.

The K_i values of apigenin (Sahnoun *et al.*, 2018) and cinnamic acid (Sahnoun *et al.*, 2017), inhibiting α -amylase, correlate well with literature, while the K_i values of apigenin (Kaewnarin & Rakariyatham, 2017) and rosmarinic acid (Lin *et al.*, 2011), inhibiting α -glucosidase, correlate well with literature. To the best of our knowledge, this is the first study documenting the K_i values for the inhibition of α -amylase and α -glucosidase by acetyleugenol, eriodictyol, myrcene and piperine.

One aim of the study was to determine the relationship between the *in silico* docking results and *in vitro* inhibitory strength. Figures 22 and 23 show the relationship between the negative docking scores and K_i values. The slopes of both graphs were positive, indicating a positive relationship between the docking scores and the K_i values of the herbal compounds. A high negative docking score corresponds to a low K_i value, both indicating a more potent inhibitor. One of the main reasons for a possible inverse correlation between the docking scores and K_i values is, *in silico* Maestro (Maestro, 2020) only docks the ligand into a single site, the Glide grid. However, during the *in vitro* enzyme assays, the ligand can bind to more than one site, especially when looking at non-competitive inhibition and some cases of competitive inhibition.

The compounds with better docking scores than acarbose to both α -amylase and α -glucosidase were apigenin, eriodictyol, piperine and rosmarinic acid. With regards to α -amylase, it can be seen that the *in vitro* results of apigenin and rosmarinic acid correspond well to the *in silico* results. For both enzymes, the herbal compounds with weaker docking scores than acarbose showed a significantly weaker inhibition effect than acarbose *in vitro*, except for cinnamic acid when inhibiting α -amylase. Concerning α -glucosidase, the docking scores of apigenin, eriodictyol, and piperine correlate well with the *in vitro* results, indicating a good overall correlation between the *in-silico* docking results and *in vitro* inhibition results.

6.6 Cytotoxicity in C2C12 and HepG2 cell lines

To establish if the herbal compounds were cytotoxic the IC_{50} (Table 27) was determined with a SRB assay, in C2C12 (Figure S9) and HepG2 cells (Figure S10). The toxic effect of the herbal compounds differed between the two cell lines, which supports the importance of using more than one cell line for toxicological profiling. All the herbal compounds had a concentration-dependent cytotoxic effect. Cytotoxicity was only observed at concentrations larger than 50 μ M, this provides evidence of the preclinical safety of these compounds at theoretically viable concentrations. The HepG2 cells were overall more cytotoxic resistant than the C2C12 cells, likely due to the liver's detoxification capabilities. Rosmarinic acid, myrcene, piperine, acetyeugenol and cinnamic acid did not induce a 50% decrease in cell viability at the highest tested concentration (500 μ M) in HepG2 cells, confirming their low toxicity.

Only two compounds, apigenin and eriodictyol, had toxic effects on both cell lines. These compounds have significantly lower IC_{50} values than acarbose, rejecting H_3 . Apigenin and eriodictyol are both flavones and therefore have very similar structures. Various studies have proven the toxicity of flavonoids, including eriodictyol and apigenin, at high concentrations (Ahmed *et al.*, 2014). The toxic effect of flavones occurs as a result of their ability to generate intracellular ROS. Eriodictyol has a lower IC_{50} than apigenin, in both cell lines, since it contains an additional catechol group. Catechol groups have been identified as cytotoxic since they induce dose and time-dependent cytotoxicity through apoptosis (de Oliveira *et al.*, 2010). Studies have also shown that apigenin activates p53 and caspase 3 (Choi & Kim, 2009; Granato *et al.*, 2017), two critical molecules in the induction of apoptosis in cells, this finding is supported by our results generated on STITCH.

In C2C12 cells, the IC₅₀ values of acetyleugenol, cinnamic acid, myrcene, piperine, rosmarinic acid, and acarbose were similar ($p > 0.05$), not rejecting H₃₀, indicating that these compounds are not more toxic than acarbose, a widely prescribed drug. All of these compounds had higher IC₅₀ values than acarbose, implying that they are less toxic than acarbose at the same dose. Neiro and Machado-Santelli (2013) confirmed cinnamic acid's low cytotoxicity *in vitro* and *in vivo*. Şahin *et al.* (2017) reported no cytotoxic activity when five different cell lines were treated with rosmarinic acid. The cytotoxicity of myrcene (Orlando *et al.*, 2019) and piperine (Han *et al.*, 2008; Paarakh *et al.*, 2015) has been reported to be low in HepG2 and other cell lines. To the extent of our knowledge, our work is the first report of the cytotoxicity of acetyleugenol in these cell lines. Each herbal compound tested in the study is currently found in commercially available herbs and spices, which assumes its apparent safety however high concentrations may have toxic effects.

6.7 Insulin mimicking effects *in vitro*

Glycaemic control is essential in the prevention of T2DM. It can be achieved by using oral agents that either interfere with the absorption of glucose (e.g. α -glucosidase inhibitors) and/or facilitate glucose uptake in peripheral tissue (e.g. insulin-mimetic agents) (Girón *et al.*, 2009). Skeletal muscles play an essential role in body energy balance and are one of the primary tissues targeted by insulin for glucose uptake (Akbarzadeh *et al.*, 2007). The liver plays an important role in blood glucose control, storage and utilisation of glucose (Cherrington, 1999). In view of the central role of the liver in maintaining glucose homeostasis, substances which stimulate glucose uptake in the liver might play a vital role in the pathogenesis of T2DM. Therefore, C2C12 and HepG2 cells are appropriate target tissues to test insulin-mimetic T2DM drugs.

In the present study, the tested herbal compounds significantly increased glucose uptake in C2C12 (Figure 24) and HepG2 (Figure 25) cells in comparison with the control, rejecting H_{40} . There was no significant ($p > 0.05$) difference between the stimulatory effect of the herbal compounds and that of insulin, not rejecting H_{50} . The latter may implicate that the herbal compounds may be potent therapies in preventing and alleviating hyperglycaemia. The stimulatory effect of the herbal compounds was in the same order of that of insulin, although 25 nM insulin and 100 nM of the herbal compounds was tested. We saw an effect on glucose uptake at a herbal dose 4-fold higher than that of insulin, however this is still good especially considering the bioavailability of the compounds and insulin. The oral route remains the preferred choice for drug administration because of its non-invasive nature. However, insulin needs to be administered subcutaneously, because the drug will be digested in the stomach and gut before it can reach the bloodstream where it is needed (Rolla, 2015).

Treatment with acetylugenol caused an increase in glucose uptake in C2C12 and HepG2 cells, causing higher glucose uptake than insulin at 1 μ M and 10 μ M in C2C12 cells and 10 μ M in HepG2 cells. The hypoglycaemic effect of acetylugenol is not well researched, but Mohan *et al.* (2019) showed the hypoglycaemic effect of clove extracts on L6 myotubes and HepG2 cells. Apigenin has been reported to lower blood glucose levels in diabetic rats and induce glucose uptake in HepG2 cells (Al-Ishaq *et al.*, 2019). No studies were found on the effect of apigenin on C2C12 cells. In this study, apigenin caused an increase in glucose uptake in C2C12 and HepG2 cells, with higher glucose uptake stimulation than insulin at concentrations of 0.1, 1 and 10 μ M in C2C12 cells. The results were less marked in HepG2 cells and were only higher at 10 μ M. Rosmarinic acid has been studied extensively and is known to have a hypoglycaemic effect, both *in vitro* and *in vivo* (Abe *et al.*, 2016; Prasannarong *et al.*, 2019; Tu *et al.*, 2013). Here rosmarinic acid caused glucose uptake in HepG2 cells and had higher glucose uptake than insulin at all tested concentrations in C2C12 cells and at 1 μ M and 10 μ M in HepG2 cells. Eriodictyol was found to enhance glucose uptake *in vitro*, in C2C12 and HepG2 cells, findings that support the results of the present study (Al-Ishaq *et al.*, 2019). The glucose-lowering effects of eriodictyol have been shown *in vivo* as well (Al-Ishaq *et al.*, 2019; Hameed *et al.*, 2018). Cinnamic acid increased glucose uptake in C2C12 and HepG2 cells and caused higher glucose uptake than insulin at all tested concentrations in myotubes and at 10 μ M in the hepatocytes. Shen *et al.* (2014) and Huang and Shen (2012) showed the hypoglycaemic effects of cinnamic acid in C2C12 cells and hepatocytes. Piperine caused glucose uptake in C2C12 and HepG2 cells. Studies have confirmed that piperine promotes glucose uptake in both cell lines (Kim *et al.*, 2017; Wan *et al.*, 2017). Myrcene increased the amount of glucose absorbed into myotubes with higher glucose uptake stimulation than insulin at 10 μ M. Myrcene displayed a hormetic effect in HepG2 cells. As far as our knowledge extends, this is the first study that investigated the glucose uptake activity mediated by myrcene, thus no other literature could be found.

6.8 Possible mechanism(s) of action of the herbal compounds

Since DM is such a complex multi-factorial disease (Kaku, 2010), the need arises for multi-targeted compounds. In the present study, the herbal compounds displayed inhibitory activity against two key carbohydrate hydrolysing enzymes, α -amylase and α -glucosidase, and significantly ($p < 0.05$) increased glucose uptake in C2C12 and HepG2 cells. Based on the findings of the study, it can be hypothesised that the herbal compounds exert their hypoglycaemic effect via an extra-pancreatic mechanism, independent from insulin.

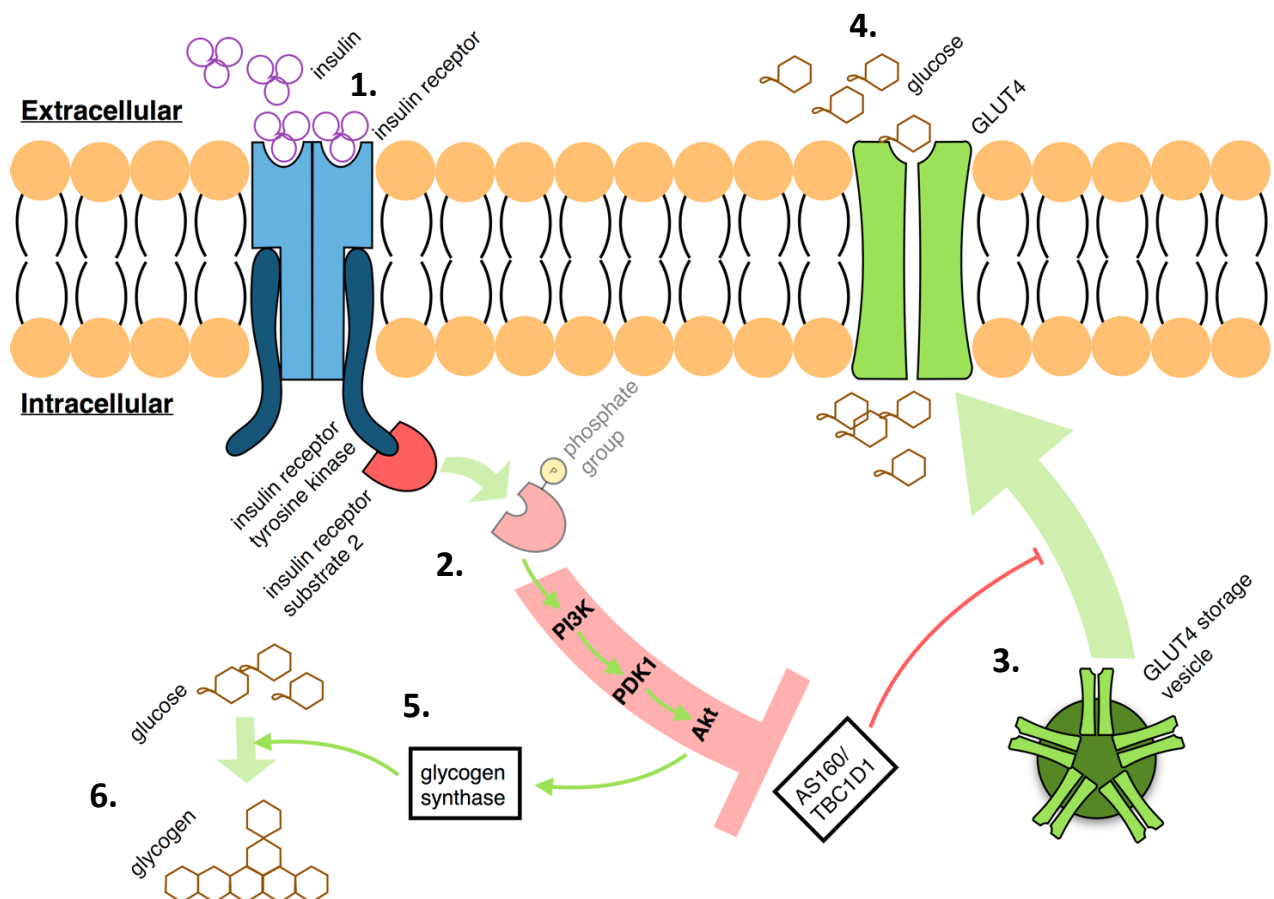


Figure 26: Insulin mediated glucose uptake and metabolism, via the translocation of GLUT-4 in muscle (C2C12) cells. (1) Insulin bind to the INSR receptor, (2) activation of protein cascades involving PI3K and AKT, (3) translocation of GLUT-4 transporters to the plasma membrane, (4) influx of glucose, (5) glycogen synthesis, (6) glycolysis and (7) fatty acid synthesis (Zhang *et al.*,

The first possible mechanism of action of insulin-mediated glucose uptake (Figure 26) in C2C12 cells involves the insulin receptor (PDB: INSR) PI3K/AKT pathway, responsible for GLUT-4 translocation. GLUT-4 is a glucose transporter responsible for insulin-regulated glucose uptake in fat and muscle cells (Cabane *et al.*, 2003). Muscle and fat cells contain vesicles in which GLUT-4 transporters are stored when insulin levels are low. A series of intracellular cascades involving phosphatidylinositol-3-kinase (PI3K) are activated once insulin binds to its cell surface receptor (TMB, 2020). Activated PI3K phosphorylates membrane phospholipids to form phosphatidylinositol-3,4,5-trisphosphate, (PIP₃), which activates the enzyme PIP₃-dependent kinase 1 (PDK1). PDK1, in turn, activates another kinase called AKT (also known as protein kinase B, PKB) (TMB, 2020). Additional enzymes activated by insulin receptor signalling include the small ribosomal subunit protein 6 kinase (p70S6K) and protein kinase C (PKC) (TMB, 2020). PKC phosphorylates proteins associated with the intracellular vesicles containing GLUT-4, resulting in the migration and fusion with the plasma membrane (TMB, 2020). Once the GLUT-4 transporters fuse with the plasma membrane it leads to an increase in glucose uptake in muscle cells. Based on the findings of the study it is suggested that a manner in which the herbal compounds exert their hypoglycaemic effects in muscle cells could be mediated via interactions with the insulin receptor, resulting in the translocation of GLUT-4 to the plasma membrane through activation of the PI3K/AKT pathway. Several studies highlighted the potential of herbal compounds to increase insulin sensitivity in C2C12 muscle cells via PI3K/AKT signalling pathways (Li *et al.*, 2019; Mohiti-Ardekani *et al.*, 2019).

Activation of the AMPK and mitogen-activated protein kinase (MAPK) pathways (Figure 27) can also lead to increased glucose uptake in skeletal muscle cells and gluconeogenesis in the liver. Various factors can lead to AMPK activation, including stimulation of the α -adrenergic and leptin receptors, and conditions like heat shock, hypoxia and ischaemia, which cause increased levels of intracellular cyclic adenosine monophosphate (cAMP) (CST, 2006). The hormone adiponectin, secreted by adipose tissue, muscle cells and the liver, is also known to activate this pathway (CST, 2006). Adiponectin improves insulin sensitivity and glucose tolerance (Stefan & Strumvoll, 2002). Once the hormone binds to the adiponectin receptor 1 (AdipoR1) an adaptor protein (APPL1), it is recruited to the intracellular NH₂ terminus of the AdipoR1 (Deepa & Dong, 2009). This results in the activation of the AMPK and MAPK pathways. C2C12 (Mao *et al.*, 2006) and HepG2 (Neumeier *et al.*, 2005) cells express AdipoR1, furthermore the activation of the AMPK and MAPK pathways via interactions with AdipoR1 by adiponectin has been shown in these cell lines (Mao *et al.*, 2006) (Neumeier *et al.*, 2005). Thus, the herbal compounds could possibly mediate their hypoglycaemic effects by activation of the AMPK and MAPK pathways. This would result in increased glucose uptake in skeletal muscle via GLUT-4 translocation, and inhibition of gluconeogenesis in the liver (Deepa & Dong, 2009; Kadowaki & Yamauchi, 2005).

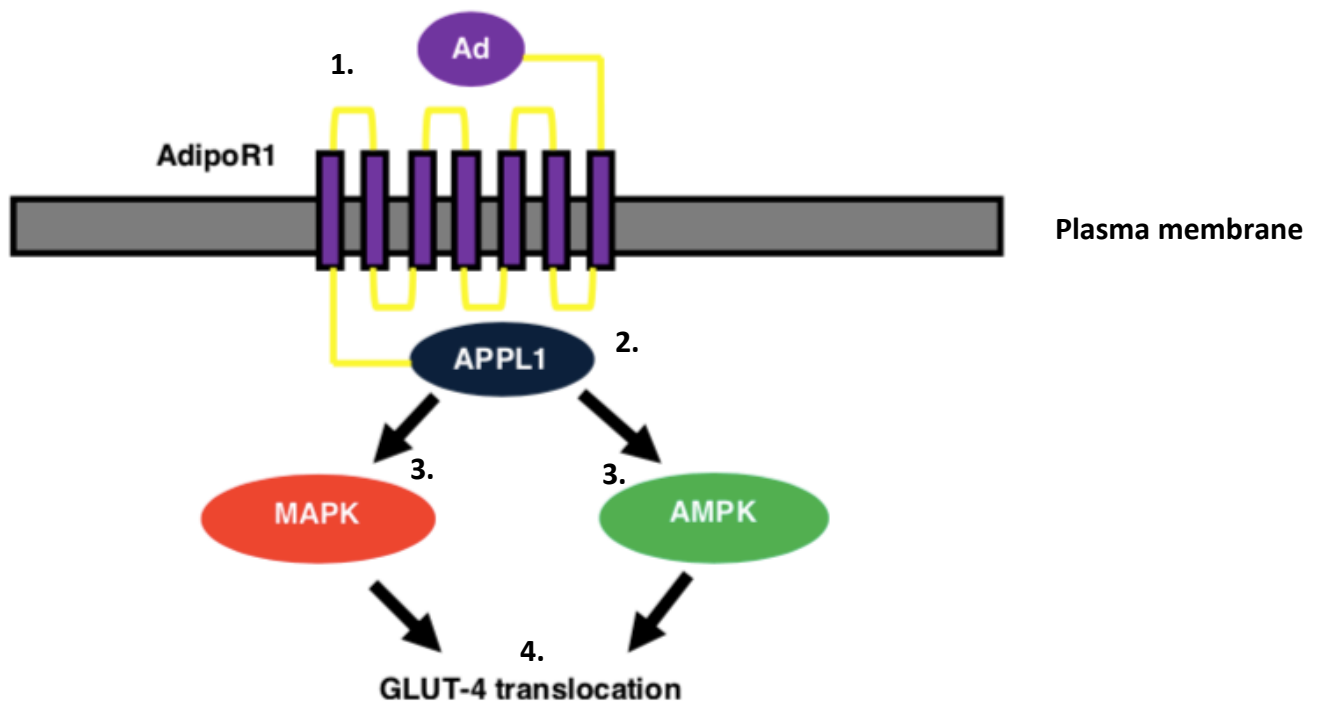


Figure 27: GLUT-4 translocation, mediated by the MAPK and AMPK pathways through the binding of adiponectin in C2C12. (1) Adiponectin (Ad) bind to adiponectin receptor (AdipoR1), (2) adaptor protein (APPL1) is recruited, (3) activation of mitogen activated protein kinase (MAPK) and 5' adenosine monophosphate activated protein kinase (AMPK) pathways, (4)

HepG2 cell lines are known to express GLUT-1 (Takanaga *et al.*, 2008), the insulin receptor (ATCC, 2020) and insulin-like growth factor II. GLUT-1 plays a major role in glucose influx in liver cells. The mammalian target of rapamycin (mTOR) is activated by PKB/Akt to coordinate with p70S6K for the synthesis of GLUT-1 (Figure 28). Glucose uptake can also be regulated by the AMPK pathways via GLUT-1. Glucose will be converted into glucose-6-phosphate (G6P), in the liver, which can then be converted into glycogen or enter glycolysis.

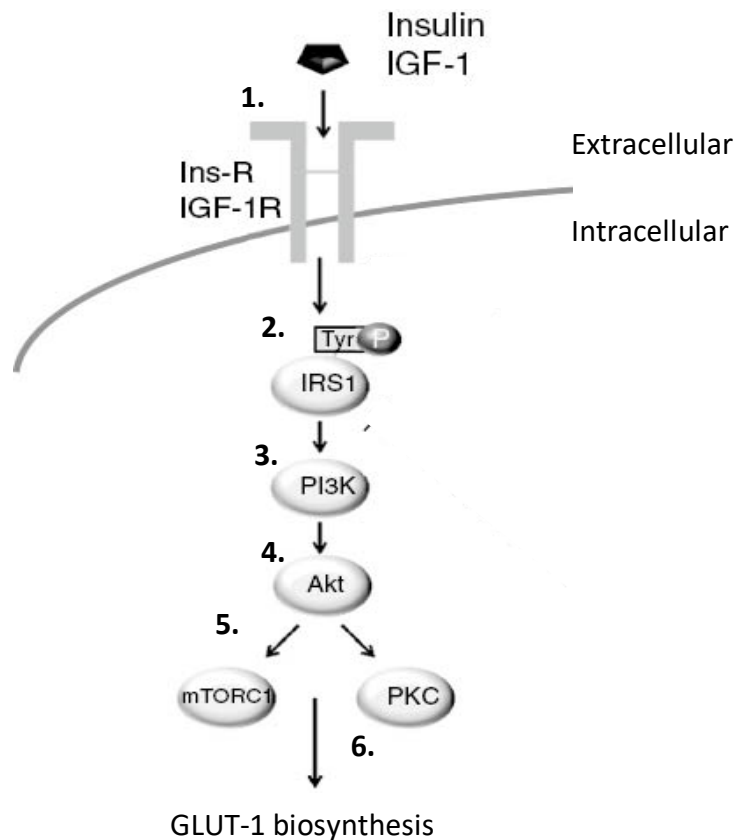


Figure 28: GLUT-1 biosynthesis in HepG2 cells. (1) Insulin binds and activates the insulin receptor (Ins-R), (2) phosphorylation of the insulin receptor substrate, (3) activation of the phosphatidylinositol-3-kinase/ protein kinase B (PI3K/AKT) insulin signalling cascade, (4) activation of mammalian target rapamycin (mTORC1) and protein kinase C (PKC), and (5) GLUT-1 biosynthesis (Lee *et al.*, 2011).

Another possible mechanism of action in which the herbal compounds exert hypoglycaemic effects can be via activation of PPAR- γ , a nuclear receptor found predominantly in adipose tissue cells but also in muscle cells and liver cells. It regulates the expression of genes involved in insulin signal transduction and glucose metabolism. The transcription of insulin sensitive genes is promoted when PPAR- γ associates with retinoid x receptor (RXR) to form PPAR- γ -RXR, a heterodimer, which binds to peroxisome proliferator response element (PPRE- γ) (Nazemzadeh, 2012; Verma *et al.*, 2004). Once again, glucose uptake occur via the upregulation of GLUT-4 translocation to the cell membrane. Both C2C12 and Hepg2 cell lines

express PPAR- γ , and hypoglycaemic effects in these cells via PPAR- γ have been shown (Nazemzadeh, 2012; Verma *et al.*, 2004). Some studies hypothesise that that PPAR- γ agonists mainly cause their hypoglycaemic effects in adipose tissue, with secondary effects in skeletal muscle and the liver (Berger & Wagner, 2004).

Protein tyrosine phosphatase 1B (PTP1B) is an intracellular phosphatase involved in the insulin signalling cascade (Liu *et al.*, 2015). PTP1B can dephosphorylate the insulin receptor and the insulin receptor substrate, which will inactivate the PI3K/AKT insulin signalling cascade (Liu *et al.*, 2015). PTP1B is expressed in HepG2 (Liu *et al.*, 2015) and C2C12 cells (Zhang *et al.*, 2019), thus the herbal compounds potentially inhibited PTP1B to enhance insulin receptor phosphorylation and stimulate glucose uptake in both cell lines. Various studies have shown the inhibition of PTP1B (Figure 29) in HepG2 (Ha do *et al.*, 2009) and C2C12 (Jiang *et al.*, 2012) cells by herbal compounds.

RBP4 is a protein secreted primarily by the liver and adipose tissue (Reinehr *et al.*, 2008). RBP4 disrupts insulin signalling, reduce glucose uptake in muscles and promote glucose production in the liver (Berry & Noy, 2012; Pereira *et al.*, 2019). Reinehr *et al.* (2008) showed that RBP4 increases hepatic glucose production through upregulation of phosphoenolpyruvate carboxykinase (PEPCK) expression and reduces insulin sensitivity through inhibition of both insulin receptor substrate 1 phosphorylation and PI3K activation. Inhibition of RBP4 might be a possible mechanism of action in which the herbal compounds exert their hypoglycaemic effect since both cell lines studied here express RBP4 (Yang *et al.*, 2005; Zhu *et al.*, 2015).

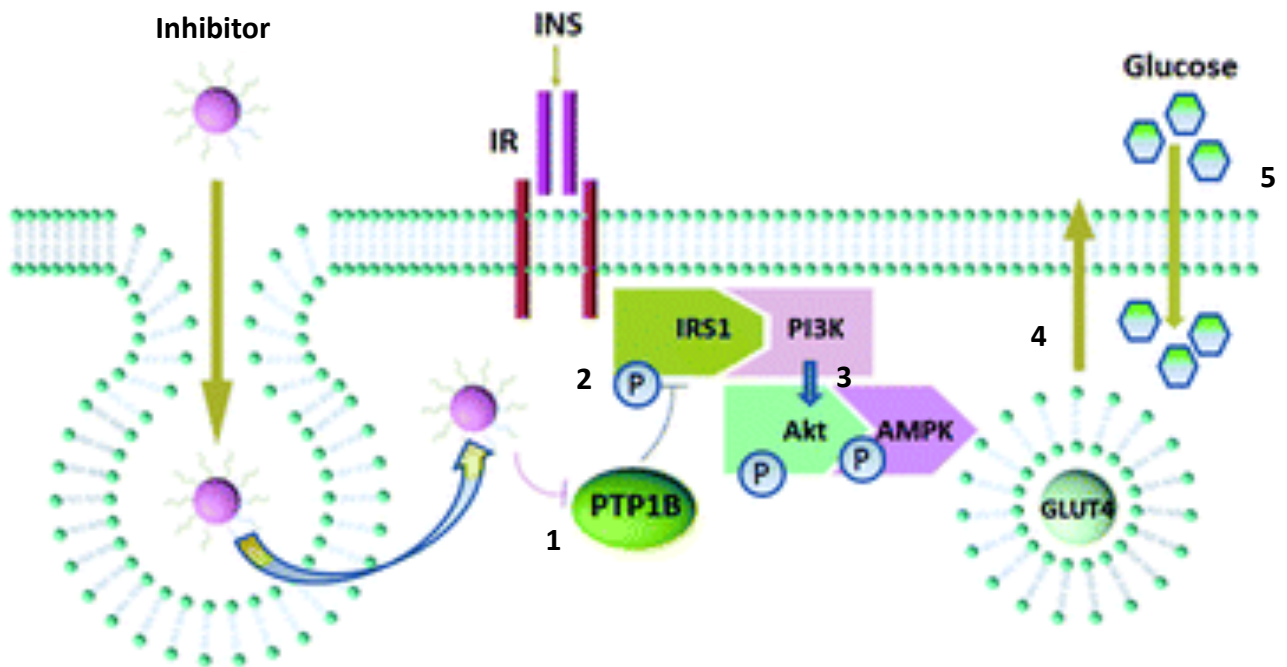


Figure 29: Inhibition of PTP1B to prevent dephosphorylation of the insulin receptor substrate, which activates the PI3K/AKT insulin signalling cascade. (1) Inhibition of PTP1B, (2) no dephosphorylation of the insulin receptor substrate (IRS1), (3) activation of the PI3K/AKT insulin signalling cascade, (4) translocation of GLUT-4 transporters to plasma membrane, and (5) influx of glucose (Yang *et al.*, 2018).

DPP4 is another insulin-regulating target expressed in both HepG2 (Miyazaki *et al.*, 2012) and C2C12 (Baek *et al.*, 2018) cells. DPP4 plays an important role in glucose metabolism, through degradation and inactivation of glucagon-like peptide-1. Research done by Giannocco *et al.* (2013) showed that the inhibition of DPP4 upregulates the translocation and expression of GLUT-4 in skeletal muscle (C2C12) cells. Circulating GLP-1 stimulates GLP-1 receptors on muscle cells which in turn activates the cAMP/protein kinase A (PKA) signal transduction pathway to leads to GLUT-4 translocation (Giannocco *et al.*, 2013). DPP4 is also known to cause impaired insulin sensitivity or insulin resistance in liver cells (HepG2) (Baumeier *et al.*, 2017). Insulin binds to the liver receptors, activating the insulin signalling pathways in the liver (Edgerton *et al.*, 2006). Insulin inhibits glucose production through the inhibition of gluconeogenesis and glycogenolysis and stimulates the liver to store glucose in the form of glycogen through glycogenesis (Bowen, 2019; Edgerton *et al.*, 2006).

The transmembrane receptor FFAR1 (free fatty acid receptor 1), also known as G-protein-coupled receptor 40, plays an important role in various physiological processes by coupling with the α -subunit of the G-protein in the Gq family. FFAR1 is expressed in the liver and regulates hepatic insulin sensitivity (Ou *et al.*, 2014). Activation of FFAR1 will reduce the blood glucose level, insulin resistance and improve glucose intolerance (Ou *et al.*, 2014). FFAR1 is expressed in HepG2 cells, furthermore various studies showed the agonistic effect of herbal compounds on FFAR1 in HepG2 cells (Suh *et al.*, 2008).

A few different mechanisms of action have been proposed as to how the herbal compounds in this study exert their hypoglycaemic effects. All of the compounds at a concentration of 100 nM stimulated glucose uptake in C2C12 and HepG2 cells, *in vitro*, with efficacy similar ($p > 0.05$) to 25 nM insulin. Although there are various different mechanisms of action in which drugs can cause glucose uptake, we can narrow down the selection by using the *in silico* results of the herbal compounds docked to six insulin-regulating targets. The *in silico* findings in the present study support three mechanisms of action, including binding to the INSR receptor and inhibition of RBP4 and DPP4 in C2C12 and HepG2 cells. The high docking scores (Table 14) of the herbal compounds to these targets shows a high binding ability to the receptor and possible inhibition of the three protein targets. However, as far as our knowledge extends, there is no literature to confirm these mechanisms of action *in vitro*.

Studies have shown that the hypoglycaemic effects of cinnamic acid, rosmarinic acid and piperine can be mediated via a mechanism similar to that of the anti-diabetic drug metformin, by activation of the AMPK pathway to stimulate GLUT-4 translocation in skeletal muscle cells (Abe *et al.*, 2016; Jayanthi *et al.*, 2017; Maeda *et al.*, 2018; Shen *et al.*, 2014; Tu *et al.*, 2013). This mechanism of action of cinnamic acid is supported by the results generated on STITCH, showing an association between cinnamic acid and adiponectin to activate the AMPK pathway. Lakshmi *et al.* (2009) showed that cinnamic acid could also stimulate GLUT-4 translocation via inhibition of PTP1B. Eriodictyol increase AKT phosphorylation by activating the PI3/AKT pathway in HepG2 cells and increase PPAR- γ expression in adipocytes (Zhang *et al.*, 2012a). Apigenin increased GLUT-4 translocation in cancer cell lines, however the molecular mechanism of action has not been established yet (Gonzalez-Menendez *et al.*, 2014). According to Mohan *et al.* (2019), treatment with acetyleugenol lead to inhibition of glycogen phosphorylase b in HepG2 cells. Inhibiting glycogen phosphorylase b will prevent glycogen from being broken down to glucose.

The findings of the present study support an extra-pancreatic mechanism of action for the hypoglycaemic effects of the herbal compounds, possibly acting as insulin mimicking compounds. The herbal compounds also exert other additive extra-pancreatic hypoglycaemic effects by inhibiting α -amylase and α -glucosidase. In addition to enzyme inhibition, the herbal compounds also displayed *in silico* anti-inflammatory and anti-carcinogenic properties.

6.9 Dosage

The results have shown that various herbal compounds are effective α -amylase and α -glucosidase inhibitors. We wanted to estimate the daily dose of each herbal plant that would be equivalent to the average daily dose of acarbose (150 mg). The daily dose of acarbose is 50 mg, three times a day for a body weight of 60 kg or less, and 100 mg three times per day for body weights greater than 60 kg (Mclver & Tripp, 2020).

Since the K_i of acarbose and those of eriodictyol, apigenin, piperine, cinnamic acid and rosmarinic acid was similar (Table 25 and 26, $p > 0.05$), it can be assumed that 150 mg of each compound will have the same effect than acarbose, without taking bioavailability into account. There are various simple ways to include herbs and spices in one's daily life. The most common way would be to add the herbs or spices to food. Another way would be to brew an herbal tea since. A tea bag usually consists of about 2.5 g dried leaves or herbs therefore, it would be an easy way to consume a large amount of herbs. The amount (Table 28) of acetyleugenol, apigenin, cinnamic acid, piperine, and rosmarinic acid that needs to be ingested, to relate to a daily dose of acarbose, can easily be consumed and are below the no observed adverse effect level (NOAEL) (Aquilina *et al.*, 2016) (Bampidis *et al.*, 2020) (World Health Organization, 2012) (Rychen *et al.*, 2017) (Rychen *et al.*, 2016) (EFSA, 2011) of these compounds. Cinnamon, oregano and pepper are insoluble in water and should thus be used as a spice to sprinkle over food. Cloves, mint, and parsley can be brewed in a tea (Mani *et al.*, 2012; Peđkal *et al.*, 2012; Pirički *et al.*, 2010).

7. STUDY OVERVIEW

Table 29: Overview of the most significant *in vitro* and *in silico* results of the study

	Compound	<i>In vitro</i> results				<i>In silico</i> results			
		K _i α-amylase (μM)	K _i α- glucosidase (μM)	Cytotoxicity in HepG2 cells (μM)	Cytotoxicity in C2C12 cells (μM)	Glucose uptake in C2C12 cells (RFU)*	Glucose uptake in HepG2 cells (RFU)*	Human oral absorption (%)	Dosage (to relate to acarbose dosage) (g)
Test Compounds	Acetylegenol	12.1	950	>500	96	219	220	100	7,2
	Apigenin	7.8	160	210	31	229	208	71	3,3
	Cinnamic acid	8	620	>500	87	239	200	45	3,2
	Eriodictyol	10.5	130	41	11	216	227	63	161
	Myrcene	49	1580	>500	84	211	203	100	123
	Piperine	10.9	280	>500	79	228	201	90	1,9
	Rosmarinic acid	4.5	2580	>500	83	229	223	35	2,2
Positive Controls	Acarbose	3.8	170	>500	60			0	
	Insulin					197	222		

Green = Significantly better or similar performance than the positive control (for more detail on statistical significance see Tables 25, 26 and 27 and Figures 24 and 25)

Red = Worse performance than positive control (for more detail on statistical significance see Tables 25, 26 and 27 and Figures 24 and 25)

*Average response

As seen in Table 29, acetylugenol stimulates glucose uptake in HepG2 and C2C12 cells and has a low cytotoxicity but does not inhibit α -amylase or α -glucosidase as effectively as acarbose. Apigenin was identified as a monotherapeutic agent with pleiotropic effects, inhibiting both α -amylase and α -glucosidase, and stimulating glucose uptake in C2C12 and HepG2 cells but, apigenin had cytotoxic effects in both C2C12 and HepG2 cells. Cinnamic acid inhibited α -amylase effectively and stimulate glucose uptake in both cell lines with no cytotoxicity. Cinnamic acid has an *in silico* human oral absorption of 45% which is ideal since 45% of the drug will be absorbed to increase glucose uptake in cells and 55% of the drug will remain in the colon to inhibit α -amylase and α -glucosidase. Only 3.2 g cinnamon is required to relate to the daily dose of acarbose. Eriodictyol is cytotoxic to both HepG2 and C2C12 cells. Myrcene does not inhibit the enzymes effectively and the dosage required to relate to the daily dose of acarbose is unrealistically high to consume daily. Piperine effectively inhibits α -glucosidase and stimulates glucose uptake in C2C12 and HepG2 cells with non-cytotoxic effects. The *in silico* human oral absorption of piperine is 90% and the dosage required to relate to acarbose is 1.9 g. Rosmarinic acid is a non-cytotoxic good α -amylase inhibitor, that cause glucose uptake in both HepG2 and C2C12 cells. Rosmarinic acid has a human oral absorption of 35% and the dosage rosmarinic acid required to relate to the daily dose of acarbose is 2.2 g, which can easily be managed.

The most promising compounds in this study was cinnamic acid, piperine and rosmarinic acid. These compounds were non cytotoxic, inhibited α -amylase and/or α -glucosidase and induced glucose uptake in HepG2 and C2C12 cells.

Taking the results into consideration, it will be best to combine two or more compounds for optimal effect. For example, the most advantageous result will be obtained if rosmarinic acid and piperine is ingested together, rosmarinic acid is a good α -amylase inhibitor and piperine a good α -glucosidase inhibitor, furthermore both compounds stimulate glucose uptake in C2C12 and HepG2 cells with a low cytotoxicity. Both compounds have a low dosage required to relate to the daily dose of acarbose, 1.9 g and 2.2 g for piperine and rosmarinic acid respectively. Piperine can also be combined with cinnamic acid, another good α -amylase inhibitor.

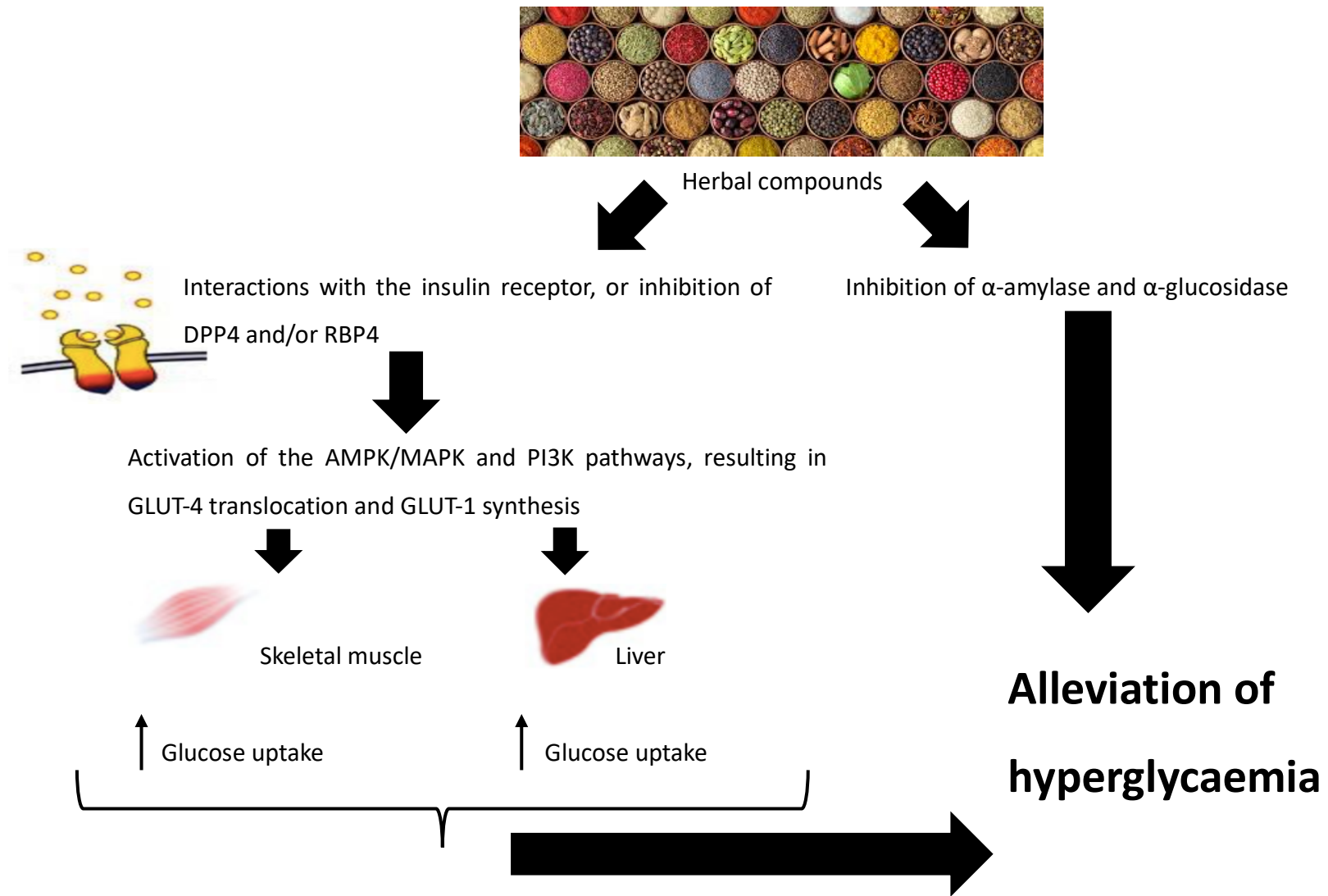


Figure 30: The proposed mechanisms of the anti-diabetic and hypoglycaemic effects of the herbal compounds.

8. CONCLUSION

Due to the increasing prevalence of T2DM, there has been an ongoing effort to find natural compounds that can prevent and possibly control hyperglycaemia. Diabetes has a complex disease process; thus, the need arises for multi-targeted compounds instead of a “single target-single drug” approach. This is why the herbal compounds presented here are attractive options for the control of diabetes, as multiple targets can be regulated with a single compound. Here we report that several herbal compounds possess potential anti-diabetic activities, due to their ability to inhibit both α -amylase and α -glucosidase and increase glucose uptake in two insulin target tissue cell lines without cytotoxic effects.

The nature of the enzyme inhibition was evaluated *in silico* using docking analysis and *in vitro* using enzymatic assays. The relationship between the *in silico* and *in vitro* results were well correlated, a more negative docking score translated to a higher *in vitro* inhibitory activity. The inhibitory mechanism of each herbal compounds was illustrated. Our results have shown that apigenin, cinnamic acid, and rosmarinic acid are effective α -amylase inhibitors, while apigenin, eriodictyol, and piperine inhibited α -glucosidase effectively. Here we provide *in vitro* evidence of the safety of each herbal compound tested at concentrations below 50 μ M in C2C12 and HepG2 cells. All of the herbal compounds caused a significant ($p < 0.05$) increase in glucose uptake in HepG2 and C2C12 cells, with effects in the same order of insulin. The mechanism is hypothesised to be an insulin-mimetic action, which initiates the translocation glucose transporters to the cell membrane, causing a glucose influx. The most promising compounds were identified as cinnamic acid, piperine and rosmarinic acid.

These herbal compounds can thus comprehensively treat numerous dysregulated and interconnected processes associated with diabetes. The herbal compounds are found in a wide variety of herbs and spices and can easily be incorporated into one's daily life. Using herbs and spices would have several advantages, including its widespread availability, affordability and health benefits. Generally, many of these herbs are part of our daily diet and based on this study consumption as part of a balanced diet can be promoted to help prevent the onset of T2DM. Here we used bioinformatics and enzyme assays to support traditional knowledge acquired over many centuries, to confirm that some herbs and spices do contain compounds that inhibit starch hydrolysing enzymes and increase glucose uptake in cells helping with the treatment of DM.

9. FUTURE WORK

- To determine the amount (mg) of herbal compound per dry weight of the herb or spice in different commercial sources through LC/MS. The different commercial sources might contain different amount of each compound.

For example, cinnamic acid is a good α -amylase inhibitor that induce glucose uptake in cells with low cytotoxicity and has a preferable bioavailability. Cinnamic acid is found in cinnamon, however cinnamon can be bought at several different commercial stores like a tuisnywerheid, health food stores and different supermarket chains. It will be interesting to determine if the different commercial sources of cinnamon contain comparable amounts of cinnamic acid, this will have an influence on the amount of cinnamon that needs to be ingested to get the desired anti-diabetic effects (Lee *et al.*, 2015a). The other compounds that can be evaluated include piperine and rosmarinic acid found in black pepper and origanum respectively.

- Elucidate the mechanism(s) of action of glucose uptake using a more targeted *in vitro* approach. According to previous literature one can perform a glucose uptake assay as described in this study and follow up with a western blot to determine whether insulin signalling molecules like AMPK, p-AMPK, AKT, p-AKT, p-IRS, GLUT-4, GLUT-1, PTP1B, DPP4 and RBP4 are upregulated or downregulated (Gonzalez-Menendez *et al.*, 2014; Kim *et al.*, 2013). From the results of the western blot one can determine whether the glucose uptake occurs via Interactions with the insulin receptor, or inhibition of DPP4 and/or RBP4 to activate the PI3K/AKT pathway or AMPK pathway.

- Determine the accurate dosage effect of insulin and the herbal compounds on glucose uptake. Preliminary data has shown that there is a beneficial effect however we would like to more accurately determine a dosage effect.
- Test combinations of herbal compounds for synergistic activity. Based on the results of this study it will be nice to choose one compound that is less bioavailable to target the enzymes in the colon, and one compound that is more bioavailable to target glucose uptake in cells. An example of such a combination is piperine and cinnamic acid.
- A limitation in the study is that although beneficial *in vitro* effects have been observed in this study, it will be beneficial to determine the *in vivo* inhibitory activity of the herbal compounds on diabetic mice/rats in future studies.

The most promising compounds in this *in vitro* study were cinnamic acid, piperine and rosmarinic acid. These compounds were non cytotoxic and inhibited α -amylase and/or α -glucosidase. The α -amylase and α -glucosidase inhibitory activity of these three herbal compounds should be evaluated in streptozotocin-induced diabetic rat model (Lee *et al.*, 2007; Ouassou *et al.*, 2018). In short, the diabetic induced rats should be fed a diet enriched with the herbal compounds and, blood samples should be collected from which the plasma glucose levels are measured to construct a response curve. The response curve is used to calculate the area under the response curve (AUC). If the herbal compounds are effective in lowering the blood glucose level the AUC will be lower in the treated group than in the control group.

10. REFERENCES

- Abbas, G., Al Harrasi, A., Hussain, H., Hamaed, A. & Supuran, C.T. 2019. The management of diabetes mellitus-imperative role of natural products against dipeptidyl peptidase-4, α -glucosidase and sodium-dependent glucose co-transporter 2 (SGLT2). *Bioorganic Chemistry*, 86(1):305-315.
- Abe, D., Saito, T. & Nogata, Y. 2016. Rosmarinic Acid Regulates Fatty Acid and Glucose Utilization by Activating the CaMKK/AMPK Pathway in C2C12 Myotubes. *Food Science and Technology Research*, 22(6):779-785.
- Ademiluyi, A.O. & Oboh, G. 2013. Soybean phenolic-rich extracts inhibit key-enzymes linked to type 2 diabetes (alpha-amylase and alpha-glucosidase) and hypertension (angiotensin I converting enzyme) in vitro. *Experimental and Toxicologic Pathology*, 65(3):305-309.
- Ahmed, N., Konduru, N.K., Ahmad, S. & Owais, M. 2014. Synthesis of flavonoids based novel tetrahydropyran conjugates (Prins products) and their antiproliferative activity against human cancer cell lines. *European Journal of Medicinal Chemistry*, 75:233-246.
- Akbarzadeh, A., Norouzian, D., Mehrabi, M.R., Jamshidi, S. & Farhangi, A. 2007. Introduction of Diabetes by Streptozotocin in Rats. *Indian Journal of Clinical Biochemistry*, 22(2):60-64.
- Al-Ishaq, R.K., Abotaleb, M., Kubatka, P., Kajo, K. & Busselberg, D. 2019. Flavonoids and Their Anti-Diabetic Effects: Cellular Mechanisms and Effects to Improve Blood Sugar Levels. *Biomolecules*, 9(9):1-35.
- al-Rubeaan, K. & Ryan, E.A. 1991. Phenytoin-induced insulin insensitivity. *Diabetes Medicine*, 8(10):968-970.
- Alberti, K.D., Gavin, J.R.G., Davidson, M.B., DeFonzo, R.A., Drash, A., Gabbe, S.G. & Genuth, S. 1998. Report of the Expert Committee on the Diagnosis and Classification of Diabetes Mellitus. *Diabetes care*, 21(S1):5-19.

Aldred E.M. 2009. Pharmacodynamics: How drugs elicit a physiological effect. *Pharmacology A Handbook for Complementary Healthcare Professionals*. Churchill Livingstone.

Altzuler, N., Moranu, E. & Hampshire, J. 1977. On the mechanism of diazoxide-induced hyperglycemia. *Diabetes* 26(10):931-935.

Amaro, R.E., Baudry, J., Chodera, J., Demir, Ö., McCammon, J.A., Miao, Y. & Smith, J.C. 2018. Ensemble Docking in Drug Discovery. *Biophysical Journal*, (114):1-8.

American Diabetes Association 2008. Diagnosis and Classification of Diabetes Mellitus. *Diabetes care*, 31(1):S62-S67.

Aquilina, G., Azimonti, G., Bampidis, V., Bastos, M.L., Bories, G., Cocconcelli, P.S., Flachowsky, G., Gropp, J., Kolar, B., Kouba, M., Lopez Puente, S., Lopez-Alonso, M., Mantovani, A., Mayo, B., Ramos, F., Saarela, M., Villa, R.E., Wallace, R.J., Wester, P. & Brantom, P. 2016. Safety and efficacy of eight compounds belonging to chemical group 31 (aliphatic and aromatic hydrocarbons) when used as flavourings for all animal species and categories. *European Food Safety Authority*, 14(1):4339-4356.

Aronoff, S.L., Berkowitz, K., Shreiner, B. & Want, L. 2005. Glucose Metabolism and Regulation-Beyond Insulin and Glucagon. *Diabetes Spectrum*, 17(3):183-190.

Aslantürk, Ö.S. 2018. In Vitro Cytotoxicity and Cell Viability Assays: Principles, Advantages, and Disadvantages. *Genotoxicity - A Predictable Risk to Our Actual World*

Asowata-Ayodele, A.M., Afolayan, A.J. & Otunola, G.A. 2016. Ethnobotanical survey of culinary herbs and spices used in the traditional medicinal system of Nkonkobe Municipality, Eastern Cape, South Africa. *South African Journal of Botany*, 104:69-75.

ATCC. 2020. *HepG2 [HepG2] (ATCC HB-8065)*. [Online] Available from: <https://www.atcc.org/products/all/HB-8065.aspx> [Accessed: 5 September 2020].

- Baek, H.J., Jeong, Y.J., Kwon, J.E., Ra, J.S., Lee, S.R. & Kang, S.C. 2018. Antihyperglycemic and Antilipidemic Effects of the Ethanol Extract Mixture of *Ligularia fischeri* and *Momordica charantia* in Type II Diabetes-Mimicking Mice. *Evidence-Based Complementary and Alternative Medicine*, 2018:1-15.
- Bailey, C.J. 2017. Metformin: historical overview. *Diabetologia*, 60(9):1566-1576.
- Bailey, C.J. & Day, C. 1989. Traditional Plant Medicines as Treatments for Diabetes. *Diabetes care*, 12(8):553-564.
- Bailey, C.J. & Turner, R.C. 1996. Metformin. *The New England Journal of Medicine*, 334(-):574-579.
- Balachandran, P., Parthasarathy, V. & Kumar, A.T.V. 2016. Isolation of Compounds from *Sargassum wightii* by GCMS and the Molecular Docking against Anti-Inflammatory Marker COX2. *International Letters of Chemistry, Physics and Astronomy*, 63(-):1-12.
- Bampidis, V., Azimonti, G., Bastos, M.L., Christensen, H. & Kouba, M. 2020. Safety and efficacy of a dried aqueous ethanol extract of *Melissa officinalis* L. leaves when used as a sensory additive for all animal species. *European Food Safety Authority Journal*, 18(2):e06016.
- Banerjee, K., Gupta, U., Gupta, S., Wadhwa, G., Gabrani, R., Sharma, S.K. & Jain, C.K. 2011. Molecular docking of glucosamine-6-phosphate synthase in *Rhizopus oryzae*. *Biomedical informatics*, 7(6):285-290.
- Bansal, V. 2006. Diabetic neuropathy. *Postgraduate Medical Journal*, 82(964):95-100.
- Barua, H., Bhagat, N. & Toraskar, M.P. 2016. Study of Binding Interactions of Human Carbonic Anhydrase Xii. *International Journal of Current Pharmaceutical Research*, 9(1):118-125.
- Bastaki, S. 2005. Diabetes mellitus and its treatment. *International Journal of Diabetes & Metabolism*, 13:111-134.

Baumeier, C., Schluter, L., Saussenthaler, S., Laeger, T., Rodiger, M., Alaze, S.A., Fritsche, L., Haring, H.U., Stefan, N., Fritsche, A., Schwenk, R.W. & Schurmann, A. 2017. Elevated hepatic DPP4 activity promotes insulin resistance and non-alcoholic fatty liver disease. *Molecular Metabolism*, 6(10):1254-1263.

Bemiller, J.N. & Whistler, R.L. 2009. Inhibitors of amylase action. *Starch: Chemistry and Technology*. 3rd ed.: Academic Press.

Berg, J.M., Tymoczko, J.L. & Stryer, L. 2007. *Biochemistry*. 6th ed. New York: W.H Freeman and Company.

Berger, J. & Wagner, J.A. 2004. Physiological and Therapeutic Roles of Peroxisome Proliferator-Activated Receptors. *Diabetes Technology & Therapeutics*, 4(2).

Berman, H.M., Westbrook, J., Feng, Z., Gilliland, G., Bhat, T.N., Weissig, H., Shindyalov, I.N. & Bourne, P.E. 2000. The Protein Data Bank. *Nucleic Acids Research*, 28(1):235-242.

Bernfeld, P. 1955. Amylase α and β . *Methods in Enzymology*, 1:149-158.

Berry, D.C. & Noy, N. 2012. Signaling by vitamin A and retinol-binding protein in regulation of insulin responses and lipid homeostasis. *Biochimica et Biophysica Acta (BBA) - Molecular and Cell Biology of Lipids*, 1821(1):168-176.

Bohme, T., Engel, C.K. & Ritter, K. 2013. 1,1-Dioxo-5,6-dihydro-[4,1,2]oxathiazines, a novel class of 11-HSD1 inhibitors for the treatment of diabetes. *Bioorg Med Chem Lett*, 23(2):4685-4691.

Bousova, I. & Skalova, L. 2012. Inhibition and induction of glutathione S-transferases by flavonoids: possible pharmacological and toxicological consequences. *Drug Metab Rev*, 44(4):267-286.

Bowen, R. 2019. *Physiologic Effects of Insulin*. [Online] Available from: http://www.vivo.colostate.edu/hbooks/pathphys/endocrine/pancreas/insulin_phys.html [Accessed: 3 September].

Brayer, G.D., Sidhu, G., Maurus, R., Rydberg, E.H., Braun, C., Wang, Y., Nguyen, N.T., Overall, C.M. & Withers, S.G. 2000. Subsite Mapping of the Human Pancreatic R-Amylase Active Site through Structural, Kinetic, and Mutagenesis Techniques. *Biochemistry* 39(16):4778-4791.

Cabane, C., Englaro, W., Yeow, K. & Derijard, B. 2003. Regulation of C2C12 myogenic terminal differentiation by MKK3/p38 α -pathway. *American Journal of Physiology-Cell Physiology*, 284(3):C658-666.

Castonguay, R., Lherbet, C. & Keillor, J.W. 2002. Mapping of the active site of rat kidney γ -glutamyl transpeptidase using activated esters and their amide derivatives. *Bioorganic & Medicinal Chemistry*, 10(12):4185-4191.

Cersosimo, E., Triplitt, C., Solis-Herrera, C., Mandarino, L.J. & DeFronzo, A.R. 2018. Pathogenesis of Type 2 Diabetes Mellitus. *Endotext*

Chamberlain, S.D., Redman, A.M., Wilson, J.W., Moorthy, G. & Patnaik, S. 2009. Optimization of 4,6-bis-anilino-1H-pyrrolo[2,3-d]pyrimidine IGF-1R tyrosine kinase inhibitors towards JNK selectivity. *Bioorg Med Chem Lett* 19(1):360-364.

Chaudhary, A. & Willett, K.L. 2006. Inhibition of human cytochrome CYP 1 enzymes by flavonoids of St. John's wort. *Toxicology*, 217(2-3):194-205.

ChemDraw. 2020. *PerkinElmer Informatics*. [Online] Available from: <https://informatics.perkinelmer.com>.

Cherrington, A.D. 1999. Banting Lecture 1997. Control of glucose uptake and release by the liver in vivo. *Diabetes*, 48(5):1198-1214.

Cho, N.H., Shaw, J.E., Karuranga, S., Huang, Y., da Rocha Fernandes, J.D., Ohlrogge, A.W. & Malanda, B. 2018. IDF Diabetes Atlas: Global estimates of diabetes prevalence for 2017 and projections for 2045. *Diabetes Research and Clinical Practice*, 138:271-281.

Choi, E.J. & Kim, G. 2009. Apigenin Induces Apoptosis through a Mitochondria:Caspase-Pathway in Human Breast Cancer MDA-MB-453 Cells. *Journal of Clinical Biochemistry and Nutrition* 44(-):260-265.

Collins, K.K. 2014. The Diabetes-Cancer Link. *Diabetes Spectrum*, 27(4):276-280.

Collins, R.A., Ng, T.B., Fong, W.P., Wan, C.C. & Yeung, H.W. 1997. Inhibition of glycohydrolase enzymes by aqueous extracts of chinese medicinal herbs in microplate format. *Biochemistry and Molecular Biology International*, 42(6):1163-1169.

de Oliveira, D.M., Pitanga, B.P., Grangeiro, M.S., Lima, R.M., Costa, M.F., Costa, S.L., Clarencio, J. & El-Bacha, R.S. 2010. Catechol cytotoxicity in vitro: induction of glioblastoma cell death by apoptosis. *Human & Experimental Toxicology*, 29(3):199-212.

Deans, K.A. & Sattar, N. 2006. Anti-Inflammatory Drugs and Their Effects on Type 2 Diabetes. *Diabetes Technology & Therapeutics*, 8(1):18-27.

Deepa, S.S. & Dong, L.Q. 2009. APPL1: role in adiponectin signaling and beyond. *Endocrinology and Metabolism* 269(1):E22-E36.

Dham, S., Shan, V., Hirsch, S. & Banjeri, M.A. 2006. The role of complementary and alternative medicine in diabetes. *Current Diabetes Reports*, 6(-):251-258.

Dizdaroglu, Y., Albay, C., Arslan, T., Ece, A., Turkoglu, E.A., Efe, A., Senturk, M., Supuran, C.T. & Ekinci, D. 2019. Design, synthesis and molecular modelling studies of some pyrazole derivatives as carbonic anhydrase inhibitors. *Journal of Enzyme Inhibition and Medicinal Chemistry*, 35(1):289-297.

Dougall, I.G. & Unitt, J. 2015. *The Practice of Medicinal Chemistry* 4th ed. United Kingdom: Academic Press.

Dowshen, S. 2018. Diabetes Control: Why It's Important. *Kids Health* [Online] Available from: <https://www.brennerchildrens.org/KidsHealth/Kids/Diabetes-Center/Medication-and-Monitoring/Diabetes-Control-Why-Its-Important.htm> [Accessed: 21 October 2019].

Dresner, L.S., Andersen, D.K., Kahng, K.U., Munshi, I.A. & Wait, R.B. 1989. Effects of cyclosporine on glucose metabolism. *Surgery*, 106(2):163-169.

Duh, E.J., Sun, J.K. & Stitt, A.W. 2017. Diabetic retinopathy: current understanding, mechanisms, and treatment strategies. *JCI Insight*, 2(14):1-13.

Duke, J.A. 1992. *Handbook of phytochemical constituents of GRAS herbs and other economic plants*. Florida, USA: CRC Press. [Accessed: 2 October 2020].

Edgerton, D.S., Lautz, M., Scott, M., Everett, C.A., Stettler, K.M., Neal, D.W., Chu, C.A. & Cherrington, A.D. 2006. Insulin's direct effects on the liver dominate the control of hepatic glucose production. *Journal of Clinical Investigations*, 116(2):521-527.

EFSA 2011. Scientific Opinion on the safety and efficacy of allylhydroxybenzenes (chemical group 18) when used as flavourings for all animal species. *European Food Safety Authority Journal*, 9(12):2440-2453.

Ekins, S., Mestres, J. & Testa, B. 2007. In silico pharmacology for drug discovery: applications to targets and beyond. *British Journal of Pharmacology*, 152(1):21-37.

Eleazu, C., Charles, A., Eleazu, K. & Achi, N. 2018. Free fatty acid receptor 1 as a novel therapeutic target for type 2 diabetes mellitus-current status. *Chemico-Biological Interactions*, 289:32-39.

Engelking, L.R. 2015. *Textbook of Veterinary Physiological Chemistry*. 3rd ed.: Academic Press. [Accessed: 14 April 2020].

Essop, M.F., Arcaro, C.A., Gutierrez, V.O., Assis, R.P., Moreira, T.F., Costa, P.I., Baviera, A.M. & Brunetti, I.L. 2014. Piperine, a Natural Bioenhancer, Nullifies the Antidiabetic and Antioxidant Activities of Curcumin in Streptozotocin-Diabetic Rats. *PLoS ONE*, 9(12):1-21.

Etxeberria, U., de la Garza, A.L., Campión, J., Martínez, J.A. & Milagro, F.I. 2012. Antidiabetic effects of natural plant extracts via inhibition of carbohydrate hydrolysis enzymes with emphasis on pancreatic alpha amylase. *Expert Opinion on Therapeutic Targets*, 16(3):269-297.

Feher, J. 2017. Digestion and Absorption of the Macronutrients. *Quantitative Human Physiology* (2).

Friesner, R.A., Banks, J.L. & Murphy, R.B. 2004. Glide: A New Approach for Rapid, Accurate Docking and Scoring. 1. Method and Assessment of Docking Accuracy. *Journal of Medicinal Chemistry*, 47(7):1739-1749.

Fu, Z., Gilbert, E.R. & Lui, D. 2013. Regulation of Insulin Synthesis and Secretion and Pancreatic Beta-Cell Dysfunction in Diabetes. *Current Diabetes Revisions*, 9(1):25-53.

Giannocco, G., Oliveira, K.C., Crajoinas, R.O., Venturini, G., Salles, T.A., Fonseca-Alaniz, M.H., Maciel, R.M.B. & Girardi, A.C.C. 2013. Dipeptidyl peptidase IV inhibition upregulates GLUT4 translocation and expression in heart and skeletal muscle of spontaneously hypertensive rats. *European Journal of Pharmacology*, 698(1-3):74-86.

Girón, M.D., Sevillano, N., Salto, R., Haidour, A., Jiménez, M.L., Rueda, R. & López-Pedrosa, J.M. 2009. Salacia oblonga extract increases glucose transporter 4-mediated glucose uptake in L6 rat myotubes: role of mangiferin. *Clinical Nutrition*, 28(5):565-574.

Gittoes, N.J.L., Ayuk, J. & Ferner, R.E. 2010. Drug - Induced Diabetes. *Textbook of Diabetes*. United Kingdom: Wiley-Blackwell.

Goldenberg, R. & Punthakee, Z. 2013. Definition, classification and diagnosis of diabetes, prediabetes and metabolic syndrome. *Canadian Journal of Diabetes*, 37 Suppl 1:S8-11.

Gonzalez-Menendez, P., Hevia, D., Rodriguez-Garcia, A., Mayo, J.C. & Sainz, R.M. 2014. Regulation of GLUT transporters by flavonoids in androgen-sensitive and -insensitive prostate cancer cells. *Endocrinology*, 155(9):3238-3250.

Granato, M., Gilardini Montani, M.S., Santarelli, R., D'Orazi, G., Faggioni, A. & Cirone, M. 2017. Apigenin, by activating p53 and inhibiting STAT3, modulates the balance between pro-apoptotic and pro-survival pathways to induce PEL cell death. *Journal of Experimental & Clinical Cancer Research*, 36(1):1-9.

Ha do, T., Tuan, D.T., Thu, N.B., Nhiem, N.X., Ngoc, T.M., Yim, N. & Bae, K. 2009. Palbinone and triterpenes from Moutan Cortex (*Paeonia suffruticosa*, Paeoniaceae) stimulate glucose uptake and glycogen synthesis via activation of AMPK in insulin-resistant human HepG2 Cells. *Bioorganic & Medicinal Chemistry Letters*, 19(1):5556-5559.

Hafizur, R.M., Hameed, A., Shukrana, M., Raza, S.A., Chishti, S., Kabir, N. & Siddiqui, R.A. 2015. Cinnamic acid exerts anti-diabetic activity by improving glucose tolerance in vivo and by stimulating insulin secretion in vitro. *Phytomedicine*, 22(2):297-300.

Hajirahimkhan, A., Dietz, B.M. & Bolton, J.L. 2013. Botanical modulation of menopausal symptoms: mechanisms of action. *Planta Medica*, 79(7):538-553.

Hameed, A., Hafizur, R.M., Hussain, N., Raza, S.A., Rehman, M., Ashraf, S., Ul-Haq, Z., Khan, F., Abbas, G. & Choudhary, M.I. 2018. Eriodictyol stimulates insulin secretion through cAMP/PKA signaling pathway in mice islets. *European Journal of Pharmacology*, 820:245-255.

Han, Y., Chin Tan, T.M. & Lim, L.Y. 2008. In vitro and in vivo evaluation of the effects of piperine on P-gp function and expression. *Toxicology and Applied Pharmacology*, 230(3):283-289.

Hanley, N.A. 2010. Endocrine Disorders that Cause Diabetes. *Textbook of Diabetes*. United Kingdom: Wiley-Blackwell.

Haytowitz, D.B., Wu, X. & Bhagwat, S. 2018. *USDA Database for the Flavonoid Content of Selected Foods*. Maryland, USA: Agriculture, U.S.D.O. [Online] Available from: <http://www.ars.usda.gov/nutrientdata>.

HealthJADE. 2019. *Insulin*. [Online] Available from: <https://healthjade.net/insulin/>.

Huang, D.-W. & Shen, S.-C. 2012. Caffeic acid and cinnamic acid ameliorate glucose metabolism via modulating glycogenesis and gluconeogenesis in insulin-resistant mouse hepatocytes. *Journal of Functional Foods*, 4(1):358-366.

IDF. 2019. *IDF Diabetes Atlas*. [Online] Available from: www.diabetesatlas.org.

Ighodaro, O.M. 2018. Molecular pathways associated with oxidative stress in diabetes mellitus. *Biomedicine & Pharmacotherapy*, 108:656-662.

Israili, Z.H. 2011. Advances in the Treatment of Type 2 Diabetes Mellitus. *American Journal of Therapeutics*, 18(2):117-152.

Jain, P.P., Degani, M.S., Raju, A., Ray, M. & Rajan, M.G.R. 2013. Rational drug design based synthesis of novel arylquinolines as anti-tuberculosis agents. *Bioorganic & Medicinal Chemistry Letters*, 23(-):6097-6105.

Jayanthy, G., Roshana Devi, V., Ilango, K. & Subramanian, S.P. 2017. Rosmarinic Acid Mediates Mitochondrial Biogenesis in Insulin Resistant Skeletal Muscle Through Activation of AMPK. *Journal of Cellular Biochemistry*, 118(7):1839-1848.

Jiang, C.S., Liang, L.F. & Guo, Y.W. 2012. Natural products possessing protein tyrosine phosphatase 1B (PTP1B) inhibitory activity found in the last decades. *Acta Pharmaceutica Sinica B*, 33(10):1217-1245.

Jones, A. & Hattersley, A.T. 2010. Monogenic Causes of Diabetes. *Textbook of Diabetes*. United Kingdom: Wiley-Blackwell.

Kadowaki, T. & Yamauchi, T. 2005. Adiponectin and adiponectin receptors. *Endocrine Reviews*, 26(3):439-451.

Kaewnarin, K. & Rakariyatham, N. 2017. Inhibitory Effects of Phenolic Compounds in *Ocimum sanctum* Extract on the α -Glucosidase Activity and the Formation of Advanced Glycation End-products. *Chiang Mai J. Sci*, 44(1):203-214.

Kaku, K. 2010. Pathophysiology of Type 2 Diabetes and Its Treatment Policy. *Journal of the Japan Medical Association*, 53(1):41-46.

Kampmann, U., Madsen, L.R., Skajaa, G.O., Iversen, D.S., Moeller, N. & Ovesen, P. 2015. Gestational diabetes: A clinical update. *World Journal of Diabetes*, 6(8):1065-1072.

Karam, A. 2017. *What are the disadvantages of radioactivity?* [Online] Available from: <https://www.quora.com/What-are-the-disadvantages-of-radioactivity> [Accessed: 1 September].

Kashyap, D., Sharma, A., Tuli, H.S., Sak, K., Garg, V.K., Buttar, H.S., Setzer, W.N. & Sethi, G. 2018. Apigenin: A natural bioactive flavone-type molecule with promising therapeutic function. *Journal of Functional Foods*, 48:457-471.

Kim, N., Nam, M., Kang, M.S., Lee, J.O., Lee, Y.W., Hwang, G.S. & Kim, H.S. 2017. Piperine regulates UCP1 through the AMPK pathway by generating intracellular lactate production in muscle cells. *Scientific Reports*, 7(-):1-13.

Kim, S.H., Hwang, J.T., Park, H.S., Kwon, D.Y. & Kim, M.S. 2013. Capsaicin stimulates glucose uptake in C2C12 muscle cells via the reactive oxygen species (ROS)/AMPK/p38 MAPK pathway. *Biochemical and Biophysical Research Communications*, 439(1):66-70.

King, H., Aubert, R.E. & Herman, W.H. 1998. Global Burden of Diabetes, 1995–2025: Prevalence, numerical estimates, and projections. *Diabetes Care* 21(9):1414-1431.

Kopp, C., Singh, S.P., Regenhard, P., Muller, U., Sauerwein, H. & Mielenz, M. 2014. Trans-cinnamic acid increases adiponectin and the phosphorylation of AMP-activated protein kinase through G-protein-coupled receptor signaling in 3T3-L1 adipocytes. *International Journal of Molecular Sciences*, 15(2):2906-2915.

Kuchi, V.S., Ilahy, R. & Siddiqui, M.W. 2018. Commercial Disinfectants in Skirmishing Postharvest Diseases. *Postharvest Disinfection of Fruits and Vegetables*: Academic Press.

Kumar, P. 2016. *Molecular Docking*. [Online] Available from: <https://www.slideshare.net/prateekkumar100/docking-69323428>.

Kwon, Y.I., Vatter, D.A. & Shetty, K. 2006. Evaluation of clonal herbs of Lamiaceae species for management of diabetes and hypertension. *Asia Pacific Journal of Clinical Nutrition*, 15(1):107-118.

Lakshmi, B.S., Sujatha, S., Anand, S., Sangeetha, K.N., Narayanan, R.B., Katiyar, C., Kanaujia, A., Duggar, R., Singh, Y., Srinivas, K., Bansal, V., Sarin, S., Tandon, R., Sharma, S. & Singh, S. 2009. Cinnamic acid, from the bark of *Cinnamomum cassia*, regulates glucose transport via activation of GLUT4 on L6 myotubes in a phosphatidylinositol 3-kinase-independent manner. *Journal of Diabetes*, 1(2):99-106.

Lee, J., Lee, D.G., Park, J.Y., Chae, S. & Lee, S. 2015a. Analysis of the trans-Cinnamic Acid Content in *Cinnamomum* spp and Commercial Cinnamon Powder Using HPLC. *Journal of Agricultural Chemistry and Environment*, 04(04):102-108.

Lee, S.E., Yang, H., Son, G.W., Park, H.R., Park, C.S., Jin, Y.H. & Park, Y.S. 2015b. Eriodictyol Protects Endothelial Cells against Oxidative Stress-Induced Cell Death through Modulating ERK/Nrf2/ARE-Dependent Heme Oxygenase-1 Expression. *International Journal of Molecular Sciences*, 16(7):14526-14539.

Lee, S.K., Hwang, J.Y., Song, J.H., Jo, J.R. & Kim, M.J. 2007. Inhibitory activity of *Euonymus alatus* against alpha-glucosidase in vitro and in vivo. *Nutrition Research and Practice*, 1(3):184-188.

Lee, Y.K., Kim, J.E., Nam, S.H., Goo, J.S., Choi, S.I., Choi, Y.H., Bae, C.J., Woo, J.M., Cho, J.S. & Hwang, D.Y. 2011. Differential regulation of the biosynthesis of glucose transporters by the PI3-K and MAPK pathways of insulin signaling by treatment with novel compounds from *Liriope platyphylla*. *International Journal of Molecular Medicine*, 27(3):319-327.

Lembo, S., Balato, A., Di Caprio, R., Cirillo, T., Giannini, V., Gasparri, F. & Monfrecola, G. 2014. The modulatory effect of ellagic acid and rosmarinic acid on ultraviolet-B-induced cytokine/chemokine gene expression in skin keratinocyte (HaCaT) cells. *BioMed Research International*, 2014:1-8.

Li, J., Bai, L., Wei, F., Zhao, J., Wang, D., Xiao, Y., Yan, W. & Wei, J. 2019. Therapeutic Mechanisms of Herbal Medicines Against Insulin Resistance: A Review. *Frontiers in Pharmacology*, 10:661- 686.

Lin, L., Dong, Y., Zhao, H., Wen, L., Yang, B. & Zhao, M. 2011. Comparative evaluation of rosmarinic acid, methyl rosmarinate and pedalitin isolated from *Rabdosia serra* (MAXIM.) HARA as inhibitors of tyrosinase and alpha-glucosidase. *Food Chemistry*, 129(3):884-889.

Liu, R., Ji, P., Liu, B., Qiao, H., Wang, X., Zhou, L., Deng, T. & Ba, Y. 2017. Apigenin enhances the cisplatin cytotoxic effect through p53-modulated apoptosis. *Oncology Letters*, 13(2):1024-1030.

Liu, Z.Q., Liu, T., Chen, C., Li, M.Y., Wang, Z.Y., Chen, R.S., Wei, G.X., Wang, X.Y. & Luo, D.Q. 2015. Fumosorinone, a novel PTP1B inhibitor, activates insulin signaling in insulin-resistance HepG2 cells and shows anti-diabetic effect in diabetic KKAy mice. *Toxicology and Applied Pharmacology*, 285(1):61-70.

Lloyd, P.G., Hardin, C.D. & Sturek, M. 1999. Examining glucose transport in single vascular smooth muscle cells with a fluorescent glucose analog. *Physiological Research*, 48(6):401-410.

Luyen, N.T., Binh, P.T., Tham, P.T., Hung, T.M., Dang, N.H., Dat, N.T. & Thao, N.P. 2019. Wedtrilosides A and B, two new diterpenoid glycosides from the leaves of *Wedelia trilobata* (L.) Hitchc. with α -amylase and α -glucosidase inhibitory activities. *Bioorganic Chemistry*, 85(-):319-324.

Machius, M., Vertesy, L., Huber, R. & Wiegand, G. 1996. Carbohydrate and protein-based inhibitors of porcine pancreatic alpha-amylase- structure analysis and comparison of their binding characteristics. *J. Mol. Biol.*, 260(1):409-421.

Maeda, A., Shirao, T., Shirasaya, D., Yoshioka, Y., Yamashita, Y., Akagawa, M. & Ashida, H. 2018. Piperine Promotes Glucose Uptake through ROS-Dependent Activation of the CAMKK/AMPK Signaling Pathway in Skeletal Muscle. *Molecular Nutrition & Food Research*, 62(11):1-11.

Mani, F., Braga, C.P., Novelli, E.L.B. & Sforcin, J.M. 2012. Influence of Clove Tea (*Syzygium Aromaticum*) on Body Weight and Biochemical Parameters of Rats Subjected to Ethanol Consumption and Abstinence. *Medicinal chemistry*, 2(4):81-85.

Mao, X., Kikani, C.K., Roijas, R.A., Langlais, P. & Wang, L. 2006. PPL1 binds to adiponectin receptors and mediates adiponectin signalling and function. *Nature Cell Biology*, 8(5):516-523.

Marin-Penalver, J.J., Martin-Timon, I., Sevillano-Collantes, C. & Del Canizo-Gomez, F.J. 2016. Update on the treatment of type 2 diabetes mellitus. *World Journal of Diabetes*, 7(17):354-395.

McKee, L.S. 2017. *Methods in Molecular Biology*. New York: Humana Press.

Mclver LA, Tripp J. Acarbose [StatPearls Publishing] 2020. <https://www.ncbi.nlm.nih.gov/books/NBK493214/>. [Accessed: 27 April 2020].

Merriam-Webster. 2020. *Herbal medicine*. [Online] Available from: <https://www.merriam-webster.com/dictionary/herbal%20medicine> [Accessed: 14 April].

Meyer, B.J., van Papendorp, D.H., Meij, H.S. & Viljoen, M. 2008. *Human Physiology*. 3rd ed ed. South Africa: Lansdowne.

Miyazaki, M., Kato, M., Tanaka, K. & Tanaka, M. 2012. Increased hepatic expression of dipeptidyl peptidase-4 in non-alcoholic fatty liver disease and its association with insulin resistance and glucose metabolism. *Molecular Medicine Report*, 5(3):729-733.

Mohan, R., Jose, S., Mulakkal, J., Karpinsky-Semper, D., Swick, A.G. & Krishnakumar, I.M. 2019. Water-soluble polyphenol-rich clove extract lowers pre- and post-prandial blood glucose levels in healthy and prediabetic volunteers: an open label pilot study. *BMC Complementary and Alternative Medicine*, 19(1):2-9.

Mohiti-Ardekani, J., Asadi, S., Ardakani, A.M., Rahimifard, M., Baeeri, M., Momtaz, S. & Yildiz, F. 2019. Curcumin increases insulin sensitivity in C2C12 muscle cells via AKT and AMPK signaling pathways. *Cogent Food & Agriculture*, 5(1):1-14.

Motani, A., Wang, Z., Conn, M., Siegler, K., Lui, Q., Shan, B. & Coward, P. 2009. Identification and Characterization of a Non-retinoid Ligand for Retinol-binding Protein 4 Which Lowers Serum Retinol-binding Protein 4 Levels in Vivo*. *J Biol Chem*, 284(12):7673-7680.

Mousinho, N.M.H., Steenkamp, V. & Van Tonder, J.J. 2013. In vitro assessment of the anti-diabetic activity of *Sclerocarya birrea* and *Ziziphus mucronata*. *Natural product communications* 8(9):1-5.

National Institute of Diabetes and Digestive and Kidney Diseases. 2016. *Type 2 Diabetes*. [Online] Available from: <https://www.niddk.nih.gov/health-information/diabetes/overview/preventing-type-2-diabetes> [Accessed: 18 January].

Nazemzadeh. 2012. *Regulation of PPAR- γ target genes by GW501516 in HepG2 cells*. USA: California State University.

Neiro, E.L. & Machado-Santelli, M. 2013. Cinnamic acid induces apoptotic cell death and cytoskeleton disruption in human melanoma cells. *Journal of Experimental & Clinical Cancer Research*, 32(31):1-14.

Neumeier, M., Weigert, J., Weiss, T. & Kirchner, S. 2005. Regulation of adiponectin receptor 1 in human hepatocytes by agonists of nuclear receptors. *Biochemical and Biophysical Research Communications*, 334:924-929.

Nickerson, H.D. & Dutta, S. 2012. Diabetic Complications: Current Challenges and Opportunities. *Journal of Cardiovascular Translational Research*, 5(4):375-379.

Nolte, M. 2009. *Pancreatic hormones and antidiabetic drugs in Basic and Clinical Pharmacology*. 11th ed ed.: McGraw-Hill Education.

Orlando, J.B., Silva, B.O., Pires-Cunha, C.L., Hiruma-Lima, C.A., Gaivao, I.O.M. & Maistro, E.L. 2019. Genotoxic effects induced by beta-myrcene following metabolism by liver HepG2/C3A human cells. *Journal of Toxicology and Environmental Health A*, 82(3):176-185.

Ou, H.Y., Wu, H.T., Lu, F.H., Su, Y.C., Hung, H.C., Wu, J.S., Yang, Y.C., Wu, C.L. & Chang, C.J. 2014. Activation of free fatty acid receptor 1 improves hepatic steatosis through a p38-dependent pathway. *Journal of Molecular Endocrinology*, 53(2):165-174.

Ouassou, H., Zahidi, T., Bouknana, S., Bouhrim, M., Mekhfi, H., Ziyat, A., Legssyer, A., Aziz, M. & Bnouham, M. 2018. Inhibition of alpha-Glucosidase, Intestinal Glucose Absorption, and Antidiabetic Properties by *Caralluma europaea*. *Evidence Based Complementary and Alternative Medicine*, 2018:1-8.

Paarakh, P.M., Sreeram, D.C., D, S.S. & Ganapathy, S.P. 2015. In vitro cytotoxic and in silico activity of piperine isolated from *Piper nigrum* fruits Linn. *In Silico Pharmacology*, 3(1):1-9.

Panda, S. & Kar, A. 2007. Apigenin (4',5,7-trihydroxyflavone) regulates hyperglycaemia, thyroid dysfunction and lipid peroxidation in alloxan-induced diabetic mice. *Journal of Pharmacy and Pharmacology*, 59(11):1543-1548.

Papatheodorou, K., Banach, M., Bekiari, E., Rizzo, M. & Edmonds, M. 2018. Complications of Diabetes *Journal of Diabetes Research*, 2018:1-4.

Patolia, S.K. & Mahmood, E. 2018. *What is glucose*. [Online] Available from: <https://emedicine.medscape.com/article/2087913-overview#a4> [Accessed: 30 April].

Pękal, A., Drózd, P., Biesaga, M. & Pyrzynska, K. 2012. Screening of the antioxidant properties and polyphenol composition of aromatised green tea infusions. *Journal of Science of Food and Agriculture*, 92(11).

Pendsey, S.A. 2010. Understanding diabetic foot. *International Journal of Diabetes in Developing Countries*, 30(2):75-79.

Pereira, A.S.P., Banegas-Luna, A.J., Peña-García, J., Pérez-Sánchez, H. & Apostolides, Z. 2019. Evaluation of the Anti-Diabetic Activity of Some Common Herbs and Spices: Providing New Insights with Inverse Virtual Screening. *Molecules*, 24(22):1-42.

Peter, K.V. 2012. *Handbook of herbs and spices*. 2 ed. Cambridge, United Kingdom: Woodhead Publishing.

Petersen, M., Abdullah, Y., Benner, J., Eberle, D., Gehlen, K., Hucherig, S., Janiak, V., Kim, K.H., Sander, M., Weitzel, C. & Wolters, S. 2009. Evolution of rosmarinic acid biosynthesis. *Phytochemistry*, 70(15-16):1663-1679.

Petersen, M. & Simmonds, S.J.M. 2003. Rosmarinic acid. *Phytochemistry*, 62(2):121-125.

Pirički, A.P., Moslavac, T. & Vugrinec, M. 2010. Acceptability of parsley tea by adolescents. *Glasnik Zastite Bilja*, 33(1):46-53.

Poovitha, S. & Parani, M. 2016. In vitro and in vivo α -amylase and α -glucosidase inhibiting activities of the protein extracts from two varieties of bitter melon (*Momordica charantia* L.). *BMC Complementary and Alternative Medicine*, 16(S1):1-15.

Powers AC, Niswender KD, Evans-Molina C. Diabetes Mellitus: Diagnosis, Classification, and Pathophysiology. In: Jameson J, Fauci AS, Kasper DL, Hauser SL, Longo DL and Loscalzo J editors. Diabetes Mellitus: Diagnosis, Classification, and Pathophysiology. Harrison's Principles of Internal Medicine; [Online]: McGraw-Hill Medical 2003. <https://accesspharmacy.mhmedical.com/content.aspx?bookid=2129§ionid=192288322>. [Accessed:17 April 2020].

Prasannarong, M., Saengsirisuwan, V., Surapongchai, J., Buniam, J., Chukijrunroat, N. & Rattanavichit, Y. 2019. Rosmarinic acid improves hypertension and skeletal muscle glucose transport in angiotensin II-treated rats. *BMC Complementary and Alternative Medicine*, 19(1):1-8.

Priscilla, D.H., Roy, D., Suresh, A., Kumar, V. & Thirumurugan, K. 2014. Naringenin inhibits alpha-glucosidase activity: a promising strategy for the regulation of postprandial hyperglycemia in high fat diet fed streptozotocin induced diabetic rats. *Chemico-Biological Interactions*, 210(-):77-85.

Proenca, C., Freitas, M., Ribeiro, D., Oliveira, E.F.T., Sousa, J.L.C., Tome, S.M., Ramos, M.J., Silva, A.M.S., Fernandes, P.A. & Fernandes, E. 2017. alpha-Glucosidase inhibition by flavonoids: an in vitro and in silico structure-activity relationship study. *Journal of Enzyme Inhibition and Medicinal Chemistry*, 32(1):1216-1228.

Proença, C., Freitas, M., Ribeiro, D., Tomé, S.M., Oliveira, E.F.T., Viegas, M.F., Araújo, A.N., Ramos, M.J., Silva, A.M.S., Fernandes, P.A. & Fernandes, E. 2019. Evaluation of a flavonoids library for inhibition of pancreatic α -amylase towards a structure–activity relationship. *Journal of Enzyme Inhibition and Medicinal Chemistry*, 34(1):577-588.

Qiung, G., Xue, S., Yang, J.J., Pang, X., Li, X., Goswami, D., Griffin, P.R., Chan, C.B. & Ye, K. 2014. Identification of a Small Molecular Insulin Receptor Agonist With Potent Antidiabetes Activity. *Diabetes*, 63(4):1394-1409.

Rahimzadeh, M., Jahanshahi, S., Moein, S. & Moein, M.R. 2014. Evaluation of alpha- amylase inhibition by *Urtica dioica* and *Juglans regia* extracts. *Iran Journal of Basic Medical Science*, 17(-):465-469.

Rehman, A., Setter, S.M. & Mays, H.V. 2011. Drug-Induced Glucose Alterations Part 2: Drug-Induced Hyperglycemia. *Diabetes Spectrum* 24(4):234-238.

Reinehr, T., Stoffel-Wagner, B. & Roth, C.L. 2008. Retinol-Binding Protein 4 and Its Relation to Insulin Resistance in Obese Children before and after Weight Loss. *The Journal of Clinical Endocrinology and Metabolism*, 93(6):2287-2293.

Riss, T.L. & Moravec, R.A. 2004. Use of Multiple Assay Endpoints to Investigate the Effects of Incubation Time, Dose of Toxin, and Plating Density in Cell-Based Cytotoxicity Assays. *Assay and Drug Development Technologies*, 2(1):51-62.

Rivera-Chavez, J., Gonzalez-Andrade, M., Gonzalez Mdel, C., Glenn, A.E. & Mata, R. 2013. Thielavins A, J and K: alpha-Glucosidase inhibitors from MEXU 27095, an endophytic fungus from *Hintonia latiflora*. *Phytochemistry*, 94(-):198-205.

Robertson, R.P., Harmon, J., Tran, P.O., Tanaka, Y. & Takahashi, H. 2003. Glucose Toxicity in β -Cells: Type 2 Diabetes, Good Radicals Gone Bad, and the Glutathione Connection. *Diabetes*, 52(3):581-587.

Roby, J.F. 2005. Inhibition, activation, and stabilization of α -amylase family enzymes. *Biologica*, 60(16):17-26.

Rohini, K. & Shanthi, V. 2018. Discovery of Potent Neuraminidase Inhibitors Using a Combination of Pharmacophore-Based Virtual Screening and Molecular Simulation Approach. *Biotechnology and Applied Biochemistry*, 184(-):1421-1440.

Rolla, A. 2015. *About Insulin*. [Online] Available from: <https://www.nfb.org/sites/www.nfb.org/files/images/nfb/publications/vodold/vow982.htm> [Accessed: 18 January].

Rotshteyn, Y. & Zito, S.W. 2004. Application of modified in vitro screening procedure for identifying herbals possessing sulfonylurea-like activity. *Journal of Ethnopharmacology*, 93(2-3):337-344.

Runtuwene, J., Cheng, K.C., Asakawa, A., Amitani, H., Amitani, M., Morinaga, A., Takimoto, Y., Kairupan, B.H. & Inui, A. 2016. Rosmarinic acid ameliorates hyperglycemia and insulin sensitivity in diabetic rats, potentially by modulating the expression of PEPCK and GLUT4. *Drug Design, Development and Therapy*, 10:2193-2202.

Rychen, G., Aquilina, G., Azimonti, G., Bampidis, V., Bastos, M.L., Bories, G., Cocconcelli, P.S., Flachowsky, G., Gropp, J., Kolar, B., Kouba, M., Lopez Puente, S., Lopez-Alonso, M., Mantovani, A., Mayo, B., Ramos, F., Saarela, M., Villa, R.E., Wallace, R.J., Wester, P., Brantom, P., Dusemund, B., Hogstrand, C., Van Beelen, P., Westendorf, J., Gregoretto, L., Manini, P. & Chesson, A. 2016. Safety and efficacy of pyridine and pyrrole derivatives belonging to chemical group 28 when used as flavourings for all animal species. *EFSA Journal*, 14(2):1-19.

Rychen, G., Aquilina, G., Azimonti, G., Bampidis, V., Bastos, M.L., Bories, G., Cocconcelli, P.S., Flachowsky, G., Gropp, J., Kolar, B., Kouba, M., Lopez Puente, S., Lopez-Alonso, M., Mantovani, A., Mayo, B., Ramos, F., Saarela, M., Villa, R.E., Wallace, R.J., Wester, P., Brantom, P., Dusemund, B., Hogstrand, C., Van Beelen, P., Westendorf, J., Gregoretto, L., Manini, P. & Chesson, A. 2017. Safety and efficacy of aryl-substituted primary alcohol, aldehyde, acid, ester and acetal derivatives belonging to chemical group 22 when used as flavourings for all animal species. *EFSA J*, 15(2):1-21.

Rychilik, I., Miltenberger-Miltenyi, G. & Ritz, E. 1998. The drama of the continuous increase in end-stage renal failure in patients with type II diabetes mellitus. *Nephrology Dialysis Transplantation*, 13(8):6-10.

Saeidnia, S., Manayi, A. & Abdollahi, M. 2013. The Pros and Cons of the In-silico Pharmacotoxicology in Drug Discovery and Development. *Journal of Pharmacology*, 9(-):176-181.

Şahin, S., Tezcan, G., Demir, C., Tunca, B., Çeçener, G. & Egeli, Ü. 2017. Cytotoxicity activity of rosmarinic acid isolated from *Prunella vulgaris* L. AND *Prunella grandiflora* L. in different tumor cells. *Trakya University Journal of Natural Sciences*, 18(1):9-13.

Sahnoun, M., Saibi, W., Brini, F. & Bejar, S. 2018. Apigenin isolated from *A. americana* encodes Human and *Aspergillus oryzae* S2 alpha-amylase inhibitions: credible approach for antifungal and antidiabetic therapies. *Journal of Food Science and Technology*, 55(4):1489-1498.

Sahnoun, M., Trabelsi, S. & Bejar, S. 2017. Citrus flavonoids collectively dominate the α -amylase and α -glucosidase inhibitions. *Biologia*, 72(7).

Sánchez-Pérez, A., Andrés, M., Peña-García, J., den-Haan, H., Bekas, N., Katsikoudi, A., Tzakos, A.G. & Sánchez-Pérez, H. 2015. DIA-DB: A Web-Accessible Database for the Prediction of Diabetes Drugs. *Bioinformatics and Biomedical Engineering*, 9(44):655-663.

Schrodinger. 2017. *Docking and Scoring*. [Online] Available from: <https://www.schrodinger.com/science-articles/docking-and-scoring> [Accessed: 19 April].

Schrodinger-Press. 2012. *QikProp 3. 5 User Manual*. Schrodinger Press. [Online] Available from: <https://www.schrodinger.com>.

Sela, F., Karapandzova, M., Stefkov, G. & Kulevanova, S. 2015. Chemical composition and antimicrobial activity of essential oils of *Juniperus excelsa* Bieb. (Cupressaceae) grown in R. Macedonia. *Pharmacognosy Research*, 7(1):74-80.

Shan, B., Cai, Y.Z., Sun, M. & Corke, H. 2005. Antioxidant capacity of 26 spice extracts and characterization of their phenolic constituents. *Journal of Agricultural and Food Chemistry* 53(-):7749-7759.

Shen, Y., Honma, N., Kobayashi, K., Jia, L.N., Hosono, T., Shindo, K., Ariga, T. & Seki, T. 2014. Cinnamon extract enhances glucose uptake in 3T3-L1 adipocytes and C2C12 myocytes by inducing LKB1-AMP-activated protein kinase signaling. *PLoS ONE*, 9(2):1-9.

Shityakov, S., Bigdelian, E., Hussein, A.A., Hussain, M.B., Tripathi, Y.C., Khan, M.U. & Shariati, M.A. 2019. Phytochemical and pharmacological attributes of piperine: A bioactive ingredient of black pepper. *European Journal of Medicinal Chemistry*, 176(-):149-161.

Silverthorn, D.U. & Johnson, B.R. 2010. *Human physiology: an integrated approach*. 5th edition ed. San Francisco: Pearson Education Inc.

Sim, L., Jakakanthan, K., Mohan, S., Nasi, R., Johnston, B.D., Pinto, B.M. & Rose, D.R. 2010. New glucosidase inhibitors from an ayurvedic herbal treatment for type 2 diabetes: structures and inhibition of human intestinal maltase-glucoamylase with compounds from *Salacia reticulata*. *Biochem*, 49(1):443-451.

Sim, L., Quezada-Calvillo, R., Sterchi, E.E., Nichols, B.L. & Rose, D.R. 2008. Human intestinal maltase-glucoamylase: crystal structure of the N-terminal catalytic subunit and basis of inhibition and substrate specificity. *Journal of Molecular Biology*, 375(3):782-792.

Singh, B. & Sharma, R.A. 2015. Anti-Inflammatory and Antimicrobial Properties of Flavonoids from *Heliotropium subulatum* Exudate. *Inflammation & Allergy Drug Targets*, 14(2):125-132.

Son, H.U. & Lee, S.H. 2013. Comparison of alpha-glucosidase inhibition by *Cudrania tricuspidata* according to harvesting time. *Biomedical Reports*, 1(4):624-628.

Srivastava, A., Yano, J., Hirozane, Y., Jennings, A. & Okada, K. 2014. High-resolution structure of the human GPR40 receptor bound to allosteric agonist TAK-875. *Nature*, 513(1):124-127.

Stats SA. 2017. *Mortality and causes of death in South Africa: Findings from death notification*. Pretoria.

Stefan, N. & Strumvoll, M. 2002. Adiponectin--its role in metabolism and beyond. *Hormone and Metabolic Research*, 34(9):469-474.

Stoilova, I., Trifonova, D., Marchev, A., Stanchev, V., Angelova, G. & Krastanov, A. 2017. Phytochemical Constituents and In Vitro Anti-Diabetic Properties of Ziziphus jujuba (Rhamnaceae) Fruits. *International Journal of Pharmacognosy and Phytochemical Research*, 9(2):150-158.

Subramaniyan, V., Palani, M., Srinivasan, P. & Kumar Singh, S. 2017. Novel ligand-based docking; molecular dynamic simulations; and absorption, distribution, metabolism, and excretion approach to analyzing potential acetylcholinesterase inhibitors for Alzheimer's disease. *Journal of Pharmaceutical Analysis*, 8(6):413-420.

Suh, H.N., Huong, H.T., Song, C.H., Lee, J.H. & Han, H.J. 2008. Linoleic acid stimulates gluconeogenesis via Ca²⁺/PLC, cPLA₂, and PPAR pathways through GPR40 in primary cultured chicken hepatocytes. *American Journal of Physiology-Cell Physiology*, 295(6):1518-1527.

Suh, S. & Park, M.K. 2017. Glucocorticoid-Induced Diabetes Mellitus: An Important but Overlooked Problem. *Endocrinology and Metabolism (Seoul)*, 32(2):180-189.

Sulaiman, M.K. 2019. Diabetic nephropathy: recent advances in pathophysiology and challenges in dietary management. *Diabetology & Metabolic Syndrome*, 11(-):1-7.

Sutton, J.M., Clark, D.E., Dunsdon, S.J. & Baeschlin, D.K. 2012. Novel Heterocyclic Dpp-4 Inhibitors for the Treatment of Type 2 Diabetes. *Bioorganic, Medicine and Chemistry Letters*, 22(1):1464-1465.

Szklarczyk, D., Santos, A., Von Mering, C., Jensen, L.J., Bork, P. & Kuhn, M. 2016. STITCH 5: augmenting protein-chemical interaction networks with tissue and affinity data. *Nucleic Acids Research*, 44(4):380-384.

Takanaga, H., Chaudhuri, B. & Frommer, W.B. 2008. GLUT1 and GLUT9 as major contributors to glucose influx in HepG2 cells identified by a high sensitivity intramolecular FRET glucose sensor. *Biochimica et Biophysica Acta* 1778(4):1091-1099.

Thomas, I. & Gregg, B. 2017. Metformin; a review of its history and future: from lilac to longevity. *Pediatric Diabetes*, 18(1):10-16.

Thongprajukaew, K., Choodum, A., Sa, E.B. & Hayee, U. 2014. Smart phone: a popular device supports amylase activity assay in fisheries research. *Food Chemistry*, 163:87-91.

TMB. 2020. *Insulin Function, Insulin Resistance, and Food Intake Control of Secretion*. [Online] Available from: <http://themedicalbiochemistrypage.org/insulin-function-insulin-resistance-and-food-intake-control-of-secretion/> [Accessed: 5 September].

Trott, O. & Olson, A.J. 2009. AutoDock Vina: Improving the speed and accuracy of docking with a new scoring function, efficient optimization, and multithreading. *Journal of Computational Chemistry*, 31(2):455-461.

Tu, Z., Moss-Pierce, T., Ford, P. & Jiang, T.A. 2013. Rosemary (*Rosmarinus officinalis* L.) extract regulates glucose and lipid metabolism by activating AMPK and PPAR pathways in HepG2 cells. *Journal of Agricultural and Food Chemistry*, 61(11):2803-2810.

Turner, J.V. & Agatonovic-Kustrin, S. 2007. In Silico Prediction of Oral Bioavailability. *Comprehensive Medicinal Chemistry II*, 5(-):699-724.

UNAIDS. 2019. *Global HIV & AIDS statistics — 2020 fact sheet*. [Online] Available from: <https://www.unaids.org/en/resources/fact-sheet> [Accessed: 31 August].

Unnikrishnan, R. & Mohan, V. 2010. Pancreatic Diseases and Diabetes. *Textbook of Diabetes*. United Kingdom: Wiley-Blackwell.

Valentina, P., Ilango, K., Chander, S. & Murugesan, S. 2017. Design, synthesis and alpha-amylase inhibitory activity of novel chromone derivatives. *Bioorganic Chemistry*, 74:158-165.

Van Tonder, J.J. 2011. *Development of an in vitro mechanistic toxicity screening model using cultured hepatocytes*. Pretoria: University of Pretoria.

Verma, N.K., Singh, J. & Dey, C.S. 2004. PPAR-gamma expression modulates insulin sensitivity in C2C12 skeletal muscle cells. *British Journal of Pharmacology*, 143(8):1006-1013.

Vichai, V. & Kirtikara, K. 2006. Sulforhodamine B colorimetric assay for cytotoxicity screening. *Nature Protocols*, 1(3):1112-1116.

Walle, U.K. & Walle, T. 2002. Introduction of human ADP-Glucuronosyltransferase UGT1A1 by flavonoids. *Drug Metabolism and Dispositions*, 30(5):565-569.

Wan, C.P., Wei, Y.G., Li, X.X., Zhang, L.J. & Bao, Z.R. 2017. Piperine regulates glucose metabolism disorder in HepG2 cells of insulin resistance models via targeting upstream target of AMPK signaling pathway. *China Journal of Chinese Materia Medica*, 42(3):542-547.

WHO. 2013. *Traditional Medicine*. [Online] Available from: https://apps.who.int/gb/ebwha/pdf_files/EB134/B134_24-en.pdf [Accessed: 31 August 2020].

WHO. 2020a. *Malaria*. [Online] Available from: <https://www.who.int/news-room/fact-sheets/detail/malaria> [Accessed: 31 August].

WHO. 2020b. *Tuberculosis*. [Online] Available from: <https://www.who.int/news-room/fact-sheets/detail/tuberculosis> [Accessed: 31 August].

Wilcox, G. 2005. Insulin and Insulin Resistance. *Clinical Biochemistry Revision*, 26(-):19-39.

Williams, L.K., Li, C., Withers, S.G. & Brayer, G.D. 2012. Order and Disorder: The Differential Structural Impacts of Myricetin and Ethyl Caffeteate on Human Amylase, an Anti-Diabetic Target. *J. Med. Chem*, 55(1):10177-10186.

Williams, R., Colagiuri, S., Almutairi, R., Montoya, P.A., Basit, A., Beran, D., Bommer, C. & Borgnakke, W. 2019. *IDF Diabetes Atlas*. 9th ed.: International Diabetes Federation. [Online] Available from: www.diabetesatlas.org [Accessed: 24 April 2020].

World Health Organization. 2012. *Safety evaluation of certain food additives*. Geneva: Seventy-Sixth Meeting of the Joint Fao/Who Expert Committee on Food Additives (Jecfa).

- Xie, Y., Liang, D., Wu, Q., Chen, X., Buabeid, M.A. & Wang, Y. 2019. A System-Level Investigation into the Mechanisms of Apigenin Against Inflammation. *Natural product communications*, 14(9):1-11.
- Yang, Q., Graham, T.E., Mody, N., Preitner, F. & Peroni, O.D. 2005. Serum retinol binding protein 4 contributes to insulin resistance in obesity and type 2 diabetes. *Nature* 436(-):356-362.
- Yang, Z., Wu, F., He, Y. & Zhang, Q. 2018. A novel PTP1B inhibitor extracted from *Ganoderma lucidum* ameliorates insulin resistance by regulating IRS1-GLUT4 cascades in the insulin signaling pathway. *Food & Function*, 9(1):397-406.
- Yoon, M., Campbell, J.L., Andersen, M.E. & Clewell, H.J. 2012. Quantitative in vitro to in vivo extrapolation of cell-based toxicity assay results. *Critical Reviews in Toxicology*, 42(8):633-652.
- Yoon, S., Lee, H.J., Kwon, S.J., Kang, H.J. & Chung, S.J. 2018. Ginkgolic acid as a dual-targeting inhibitor for protein tyrosine phosphatases relevant to insulin resistance. *Bioorganic Chemistry*, 81:264-269.
- Yoon, S. & Robyt, J.F. 2003. Study of the inhibition of four alpha amylases by acarbose and its 4IV- α -maltohexaosyl and 4IV- α -maltododecaosyl analogues. *Carbohydrate Research*, 338(19):1969-1980.
- Yu, T., Yi, Y.S., Yang, Y., Oh, J., Jeong, D. & Cho, J.Y. 2012. The pivotal role of TBK1 in inflammatory responses mediated by macrophages. *Mediators of Inflammation*, 2012:1-8.
- Zhai, W., Zhang, Z., Xu, N., Guo, Y. & Qiu, C. 2016. Piperine Plays an Anti-Inflammatory Role in *Staphylococcus aureus* Endometritis by Inhibiting Activation of NF-. *Evidence-Based Complementary and Alternative Medicine*, 2016(-):1-10.
- Zhang, M., Li, X., Liang, H., Cai, H., Hu, X., Bian, Y., Dong, L., Ding, L., Wang, L., Yu, B., Zhang, Y. & Zhang, Y. 2018. Semen Cassiae Extract Improves Glucose Metabolism by Promoting GLUT4 Translocation in the Skeletal Muscle of Diabetic Rats. *Frontiers in Pharmacology*, 9:235-246.

Zhang, Q., Kong, X., Yuan, H., Guan, H., Li, Y. & Niu, Y. 2019. Mangiferin Improved Palmitate-Induced-Insulin Resistance by Promoting Free Fatty Acid Metabolism in HepG2 and C2C12 Cells via PPARalpha: Mangiferin Improved Insulin Resistance. *Journal of Diabetes Research*, 2019:1-13.

Zhang, W., Lee, J.-J., Kim, Y., Kim, I.-S., Han, J.-H., Lee, S.-G., Ahn, M.-J., Jung, S.-H. & Myung, C.-S. 2012a. Effect of Eriodictyol on Glucose Uptake and Insulin Resistance in Vitro. *Journal of Agricultural and Food Chemistry*, 60(31):7652-7658.

Zhang, Z.Y., Lui, S. & Zhang, S. 2012b. A Highly Selective and Potent PTP-MEG2 Inhibitor with Therapeutic Potential for Type 2 Diabetes. *Journal of American Chemistry Society* 134(1):18116-18124.

Zhu, C., Xiao, Y., Liu, X., Han, J., Zhang, J., Wei, L. & Jia, W. 2015. Pioglitazone lowers serum retinol binding protein 4 by suppressing its expression in adipose tissue of obese rats. *Cellular Physiology and Biochemistry*, 35(2):778-788.

Zhu, Q., Ge, F., Dong, Y., Sun, W., Wang, Z., Shan, Y., Chen, R., Sun, J. & Ge, R.S. 2018. Comparison of flavonoids and isoflavonoids to inhibit rat and human 11beta-hydroxysteroid dehydrogenase 1 and 2. *Steroids*, 132:25-32.

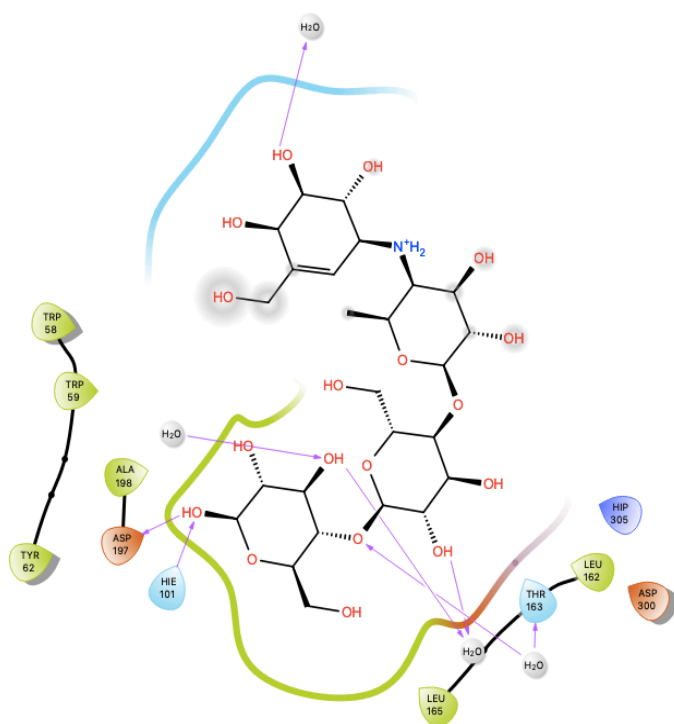
Zink, D., Chuah, J.K.C. & Ying, J.Y. 2020. Assessing Toxicity with Human Cell-Based In Vitro Methods. *Trends in Molecular Medicine*:1-13.

Zou, C., Wang, Y. & Shen, Z. 2005. 2-NBDG as a fluorescent indicator for direct glucose uptake measurement. *Journal of Biochemical and Biophysical Methods*, 64(3):207-215.

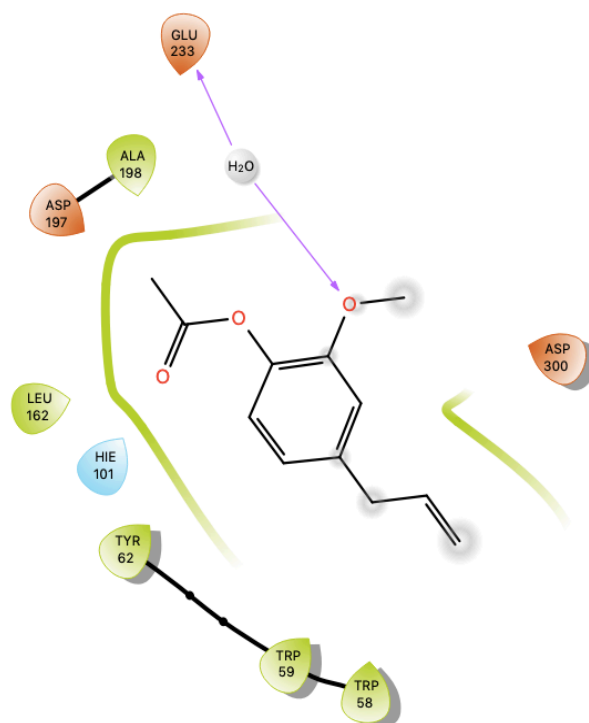
11. APPENDIX I: ADDITIONAL RESULTS

11.1 *In silico* results

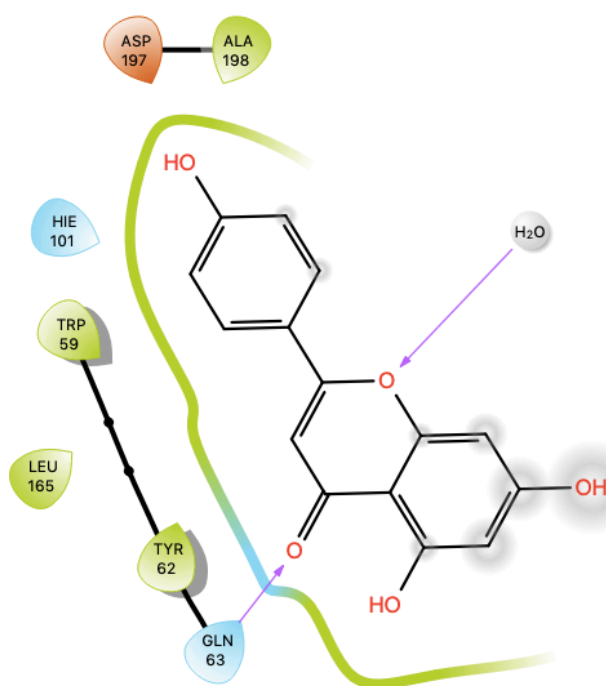
Acarbose



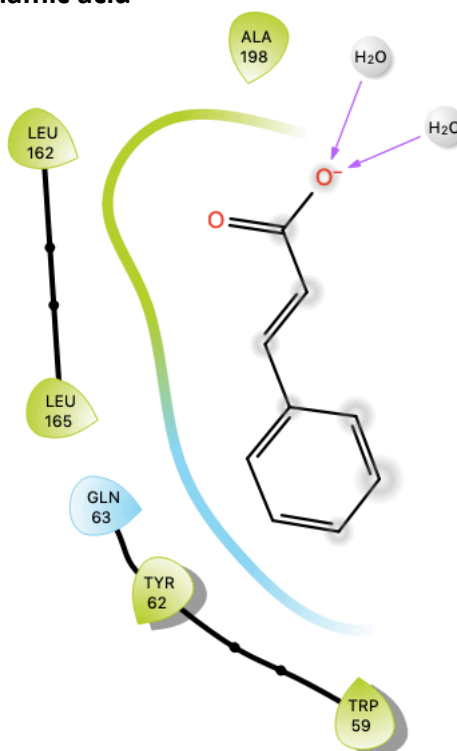
Acetylugenol



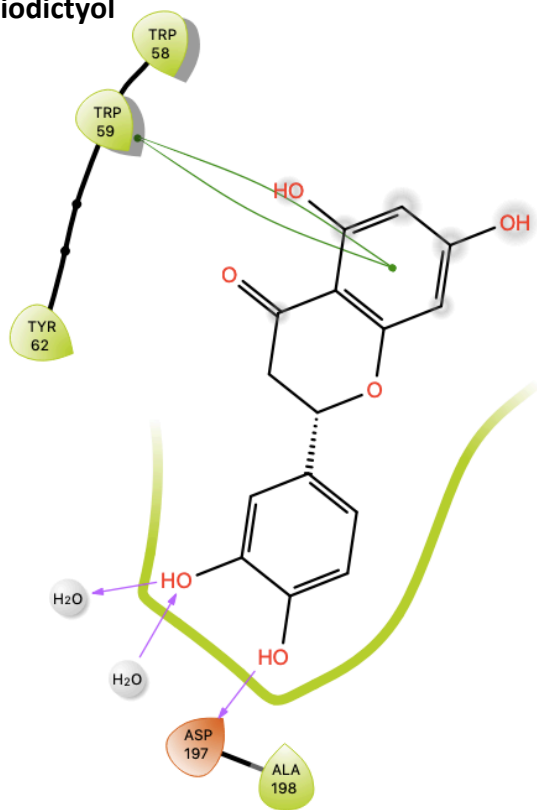
Apigenin



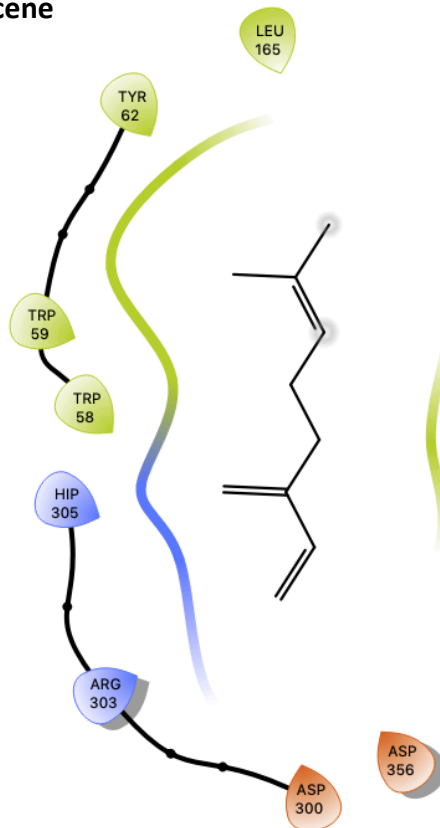
Cinnamic acid



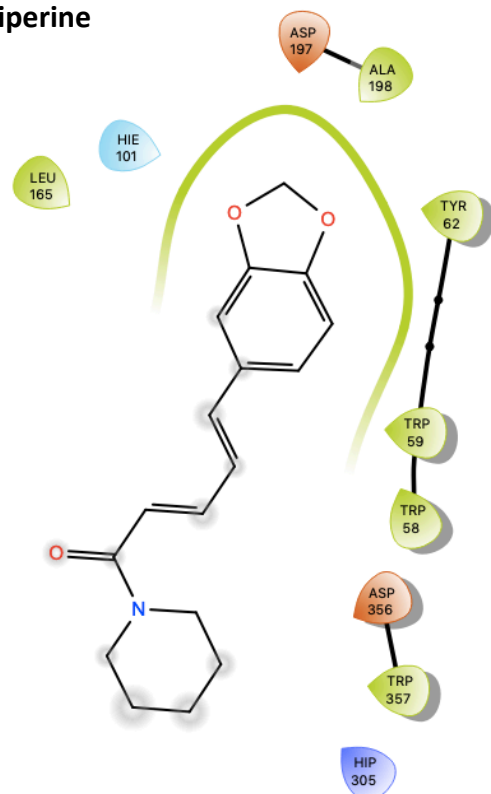
Eriodictyol



Myrcene



Piperine



Rosmarinic acid

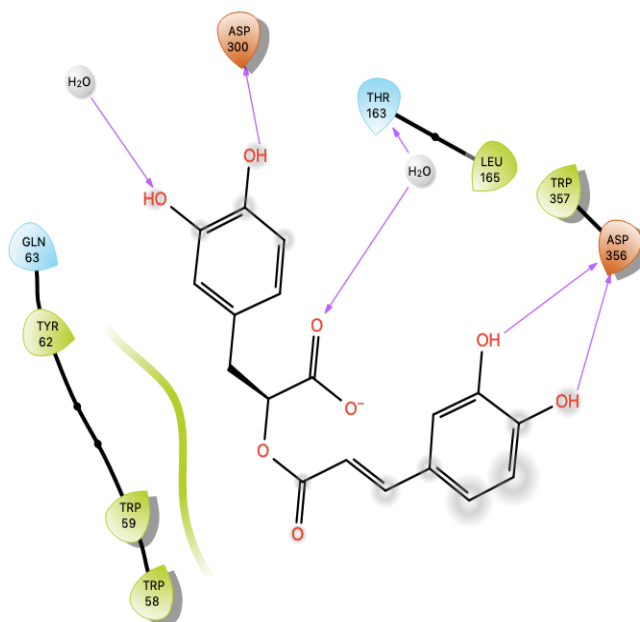
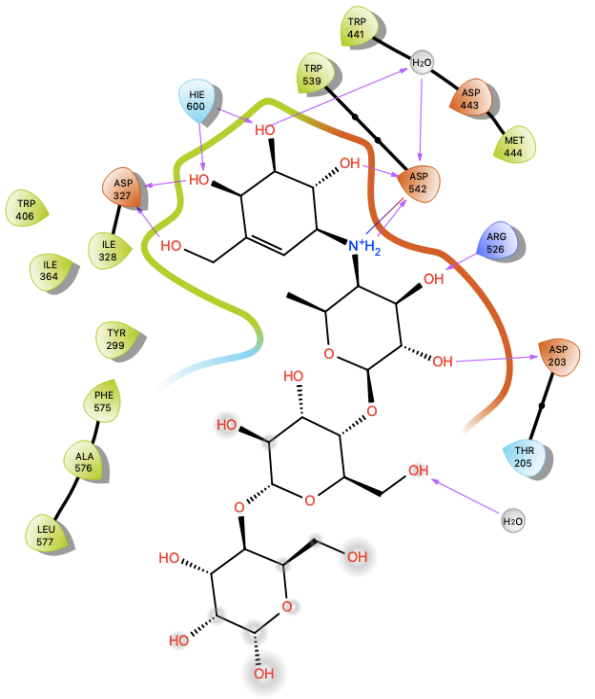
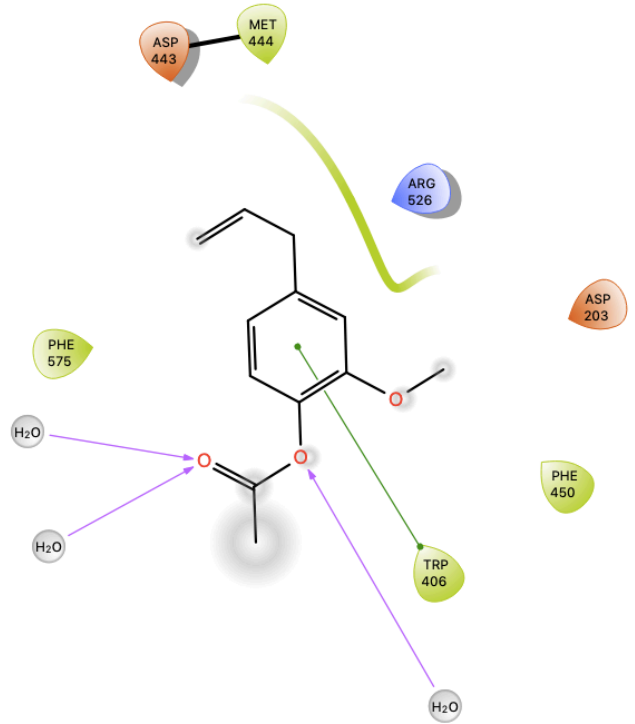


Figure S1: Ligand interaction diagrams showing the amino acids interacting acarbose and the herbal compounds in the active site of the enzyme, α -amylase (4GQR) (Williams *et al.*, 2012).

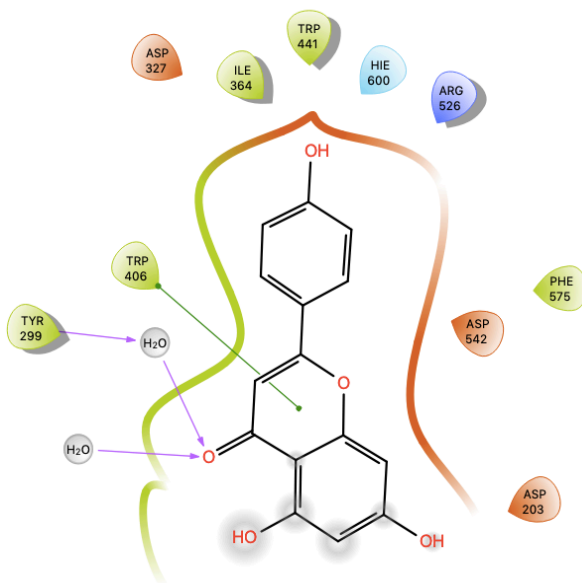
Acarbose



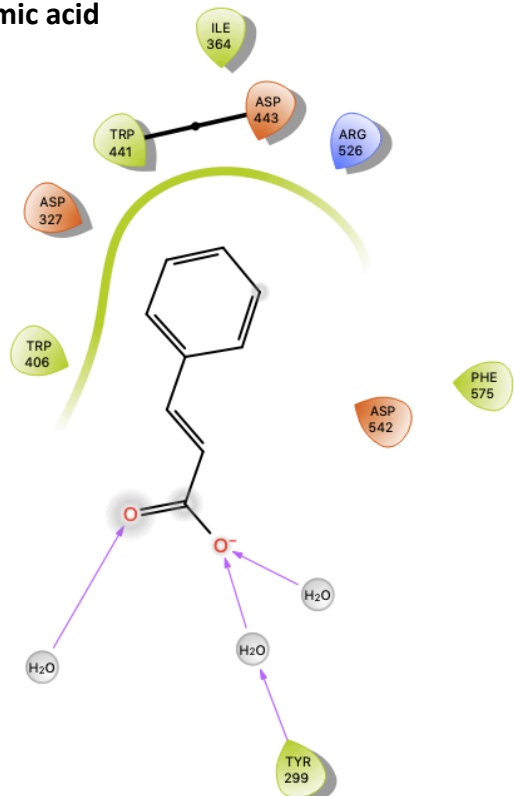
Acetylugenol



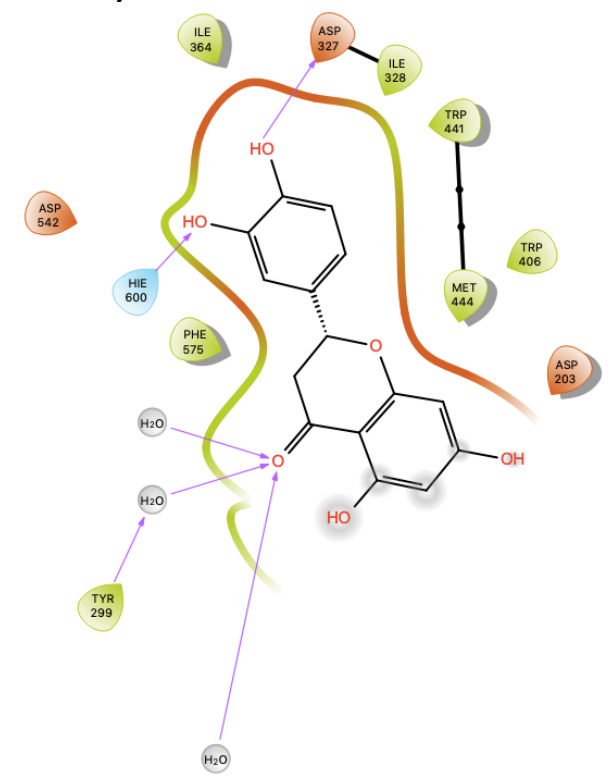
Apigenin



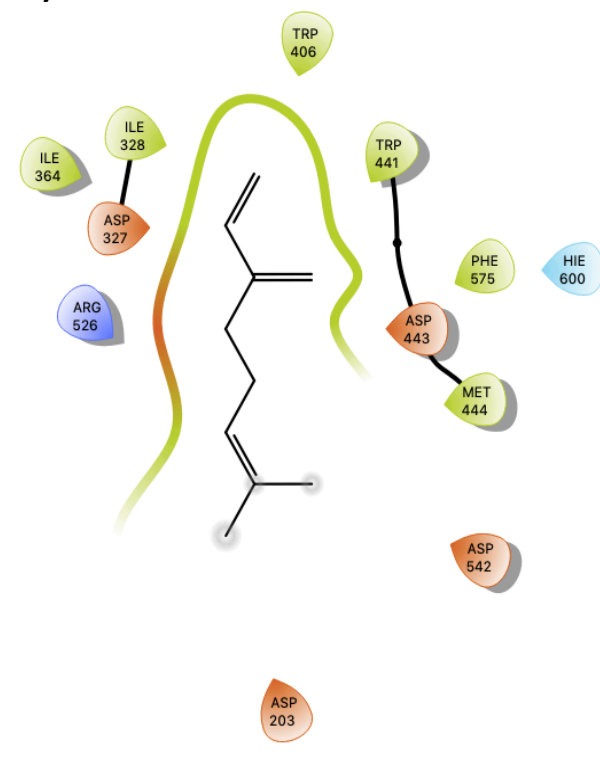
Cinnamic acid



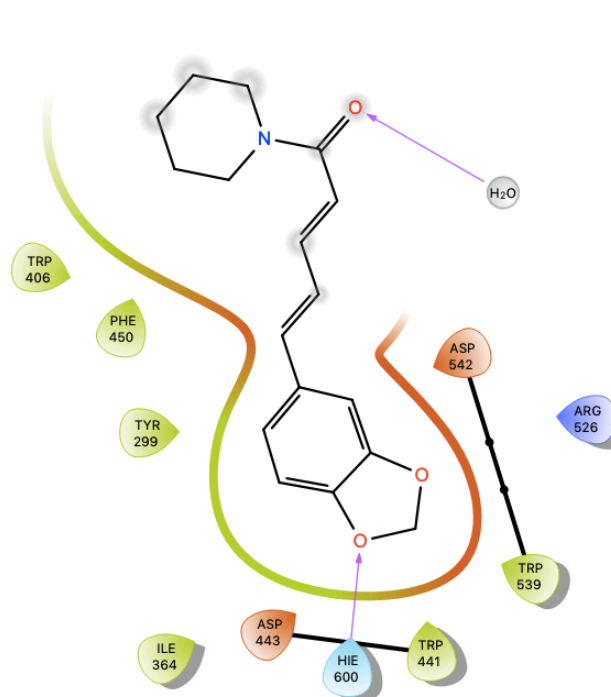
Eriodictyol



Myrcene



Piperine



Rosmarinic acid

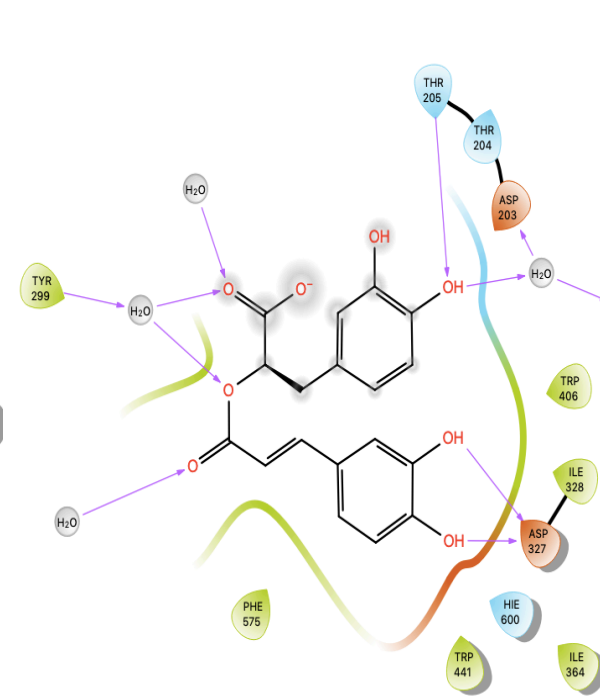


Figure S2: Ligand interaction diagrams showing the amino acids interacting with acarbose and the herbal compounds in the active site of the enzyme, α -glucosidase (3L4Y) (Sim *et al.*,

11.2 *In vitro* results

To calculate kinetic parameters of α -amylase a maltose standard curve (Figure S1) was constructed, and from the line equation the molar extinction coefficient of maltose was calculated to be $1319.22 \text{ M}^{-1}\cdot\text{cm}^{-1}$. Likewise, for α -glucosidase a *p*-nitrophenol standard curve (Figure S2) was constructed and the molar extinction coefficient of *p*-nitrophenol was calculated to be $14857.14 \text{ M}^{-1}\cdot\text{cm}^{-1}$.

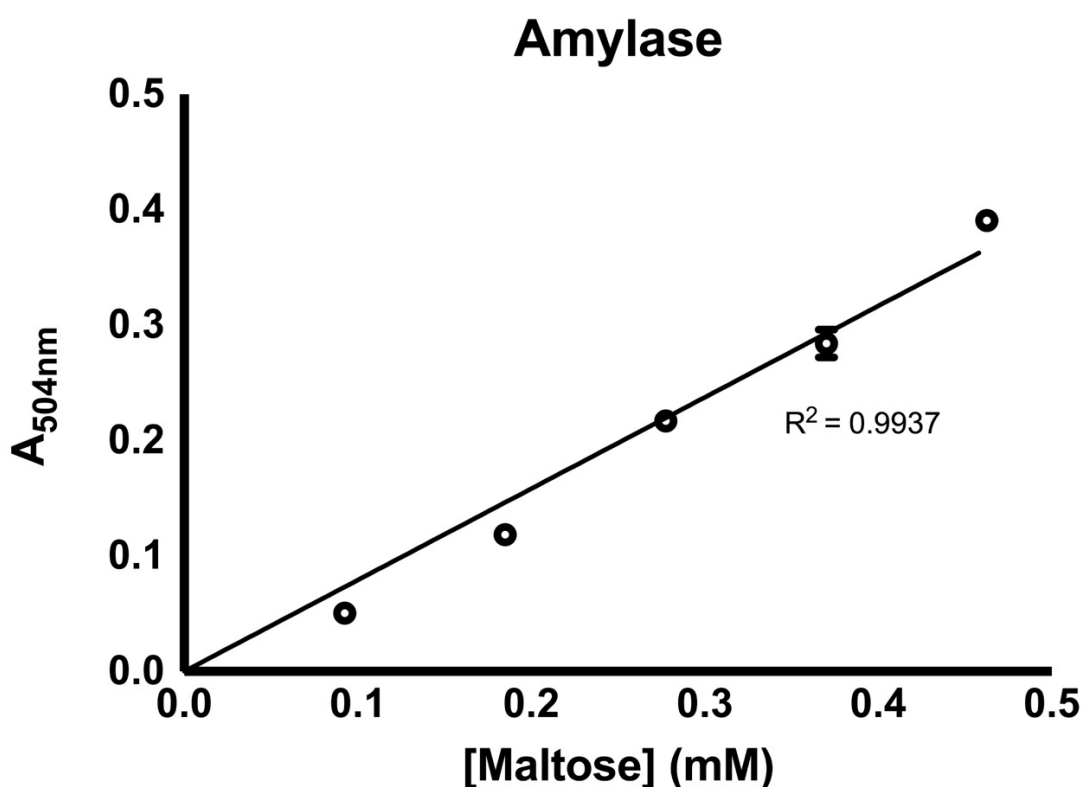


Figure S3: The linear increase in absorbance with increasing concentrations of maltose (0 – 0.46 mM). From this standard curve the slope is used to calculate the molar extinction coefficient of maltose. The data is expressed as means derived from three independent experiments with SD error bars.

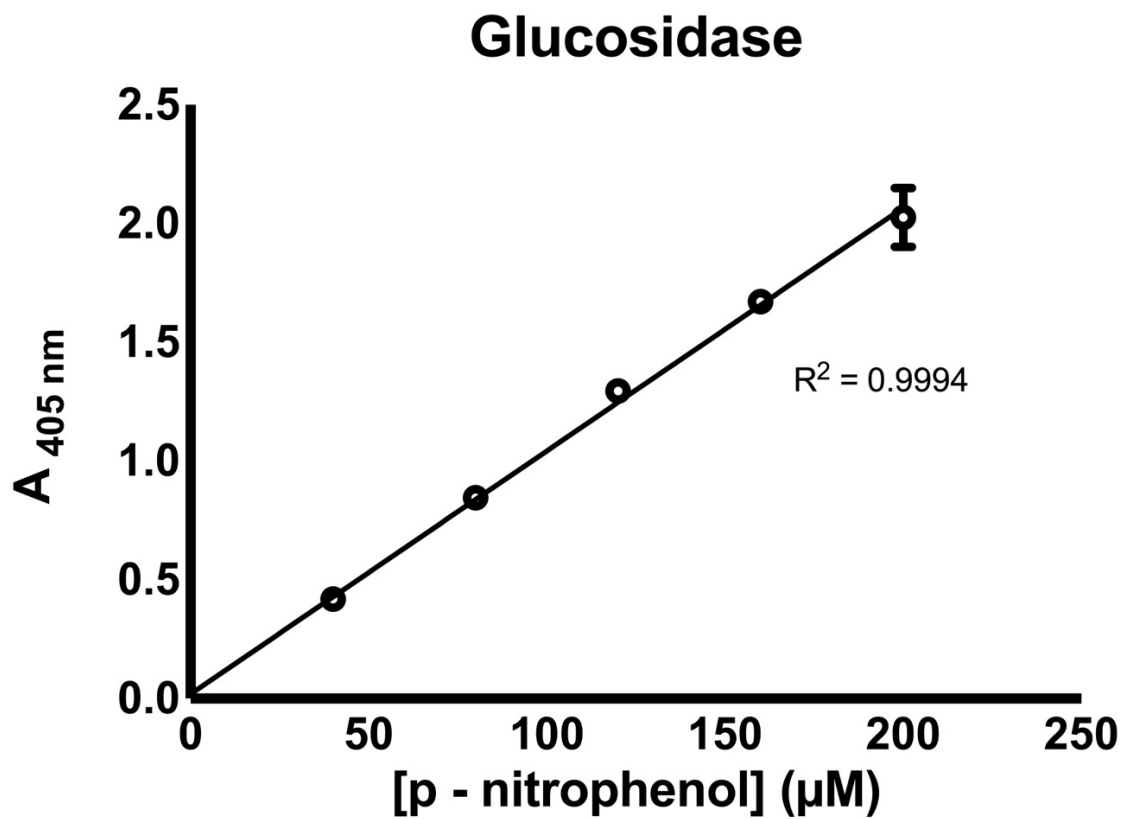


Figure S4: The linear increase in absorbance with increasing concentrations of p-nitrophenol (0 – 200 μM). From this standard curve the slope is used to calculate the molar extinction coefficient of p-nitrophenol. The data is expressed as means derived from three independent experiments with SD error bars.

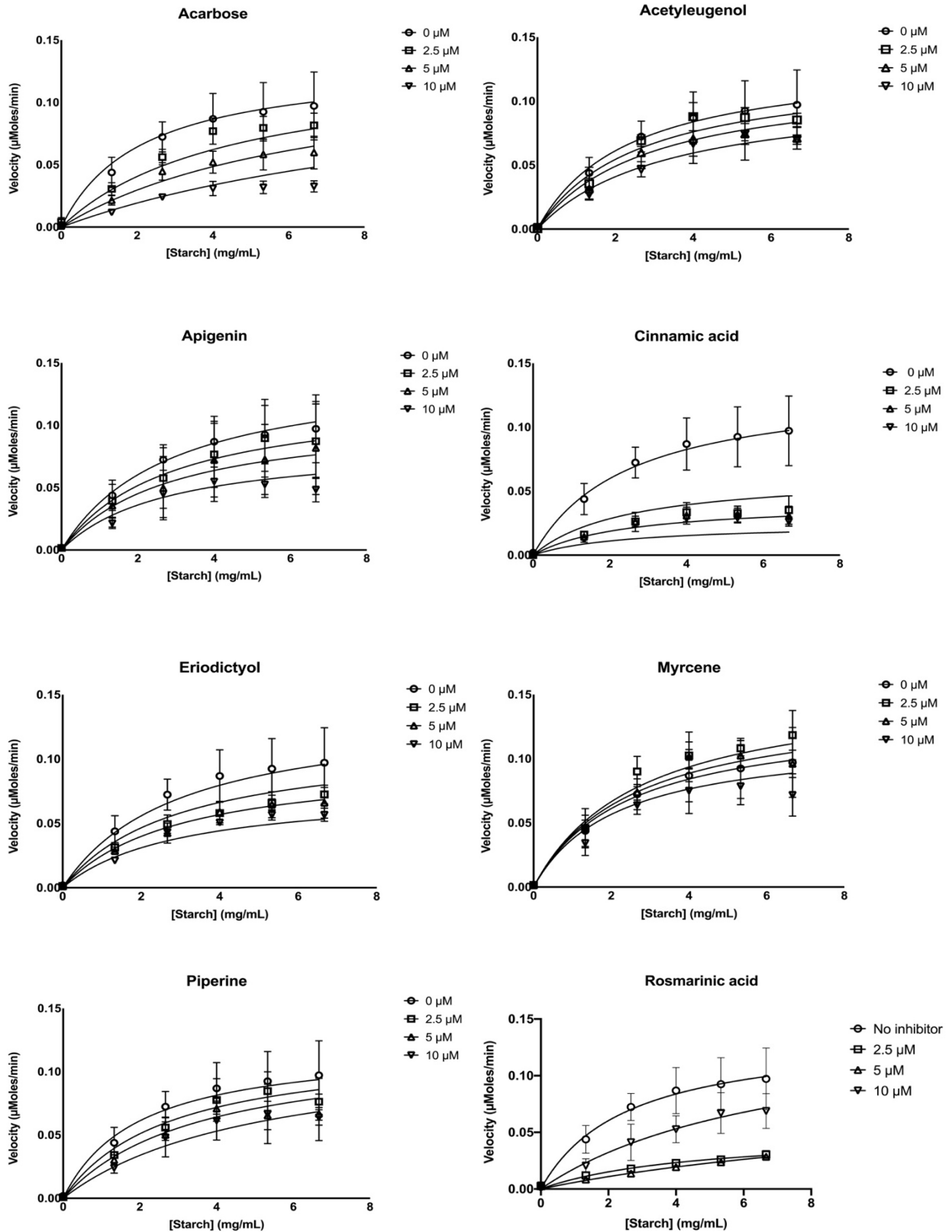


Figure S5: Michaelis-Menten graphs of the inhibition of α -amylase by acarbose (control) and herbal compounds. The mean is an average of three independent experiments ($n=3$) with, SD error bars.

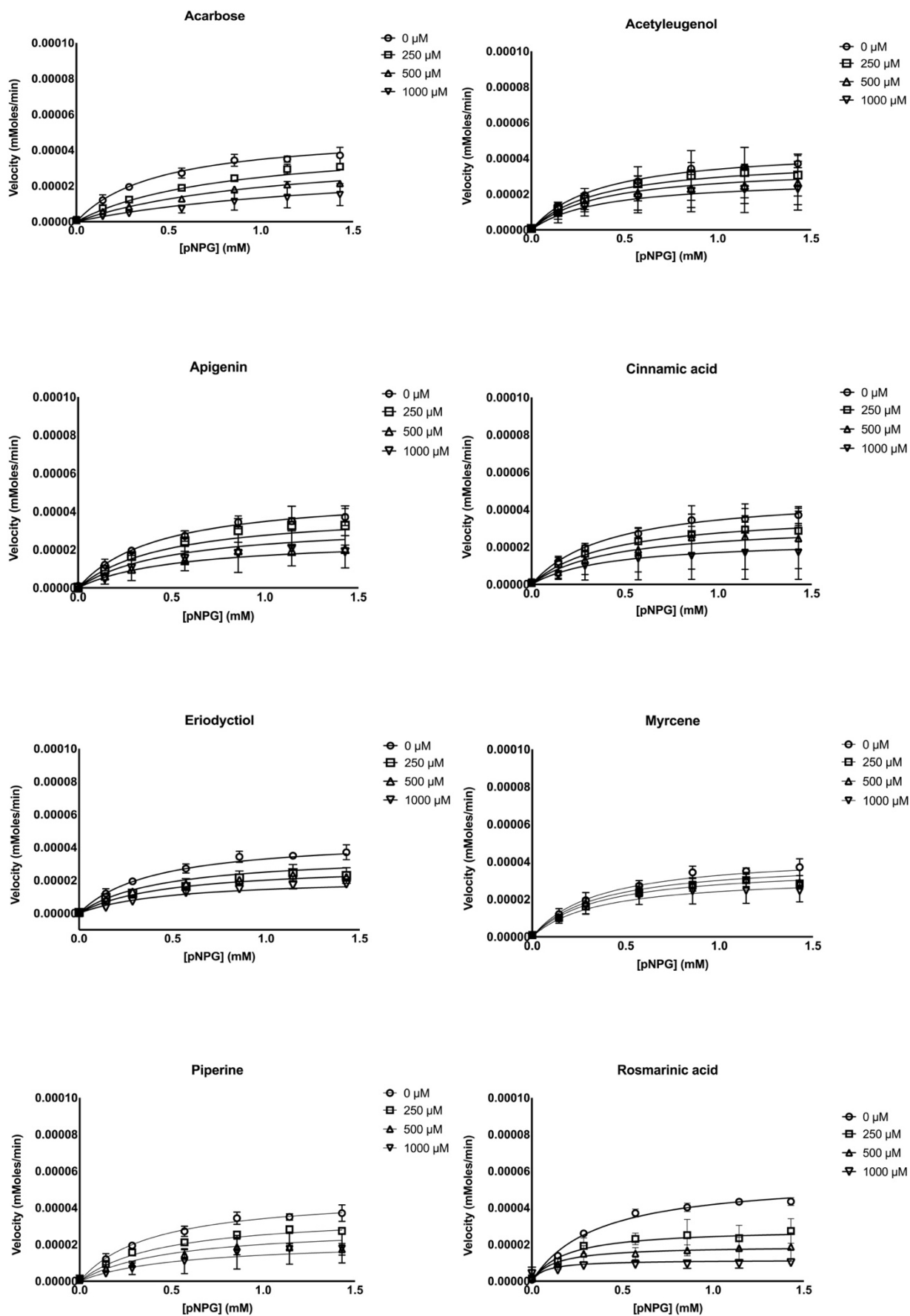


Figure S6: Michaelis-Menten graphs of the inhibition of α -glucosidase by acarbose (control) and herbal compounds. The mean is n=3, with SD error bars.

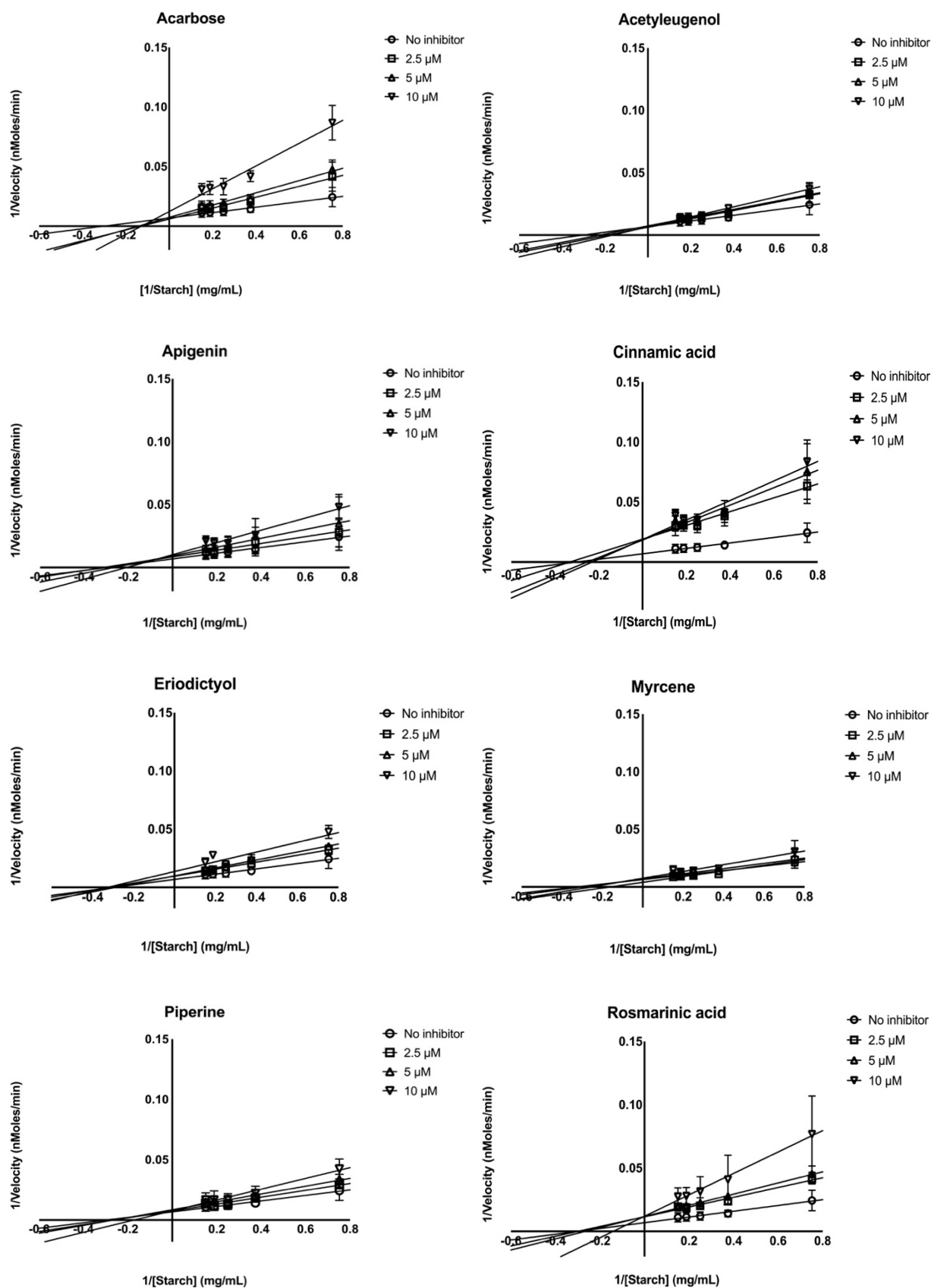


Figure S7: Lineweaver-Burk graphs of the inhibition of α -amylase by acarbose (control) and herbal compounds. The mean is n=3, with SD error bars.

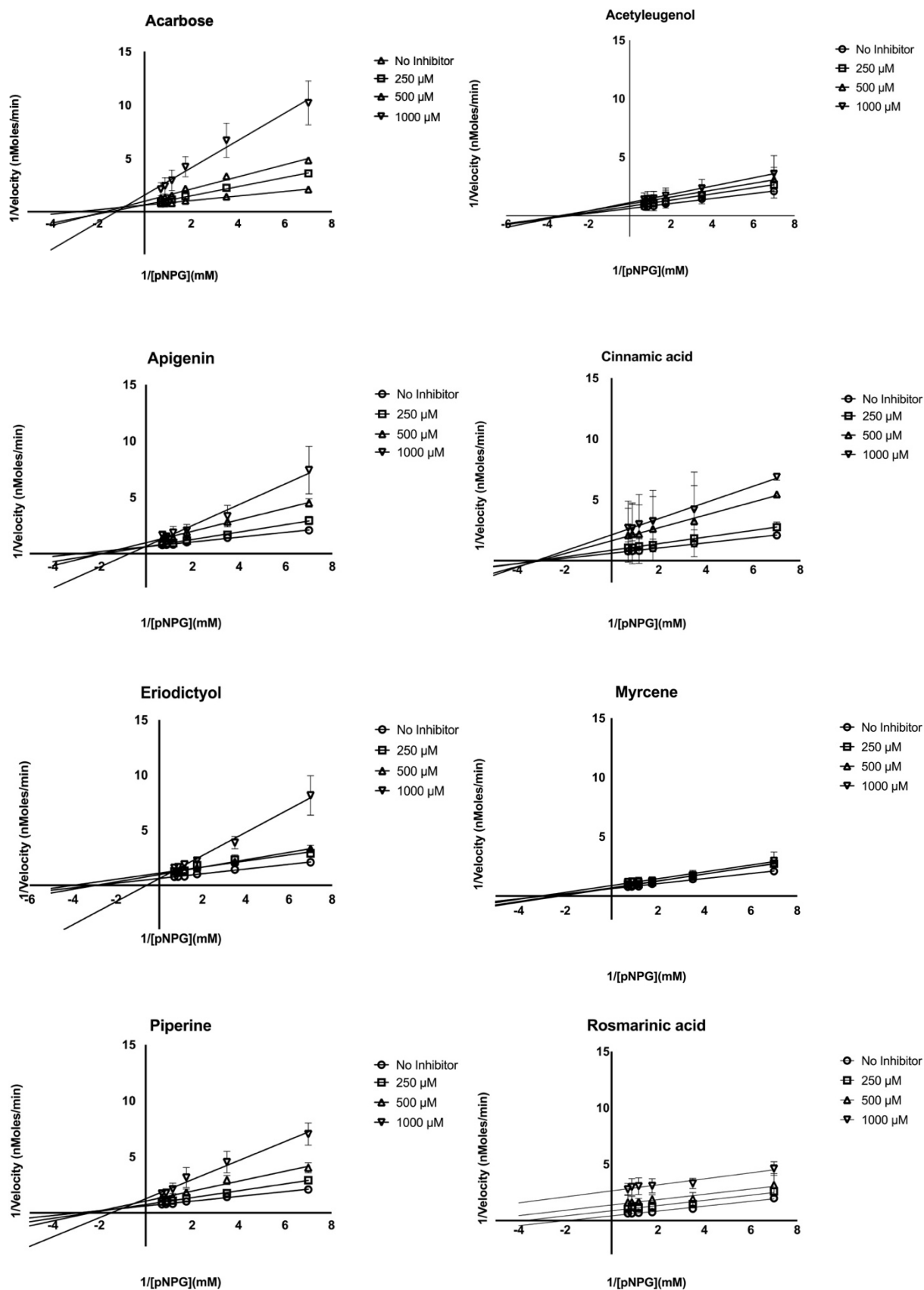


Figure S8: Lineweaver-Burk graphs of the inhibition of α -glucosidase by acarbose (control) and herbal compounds. The mean is $n=3$, with SD error bars.

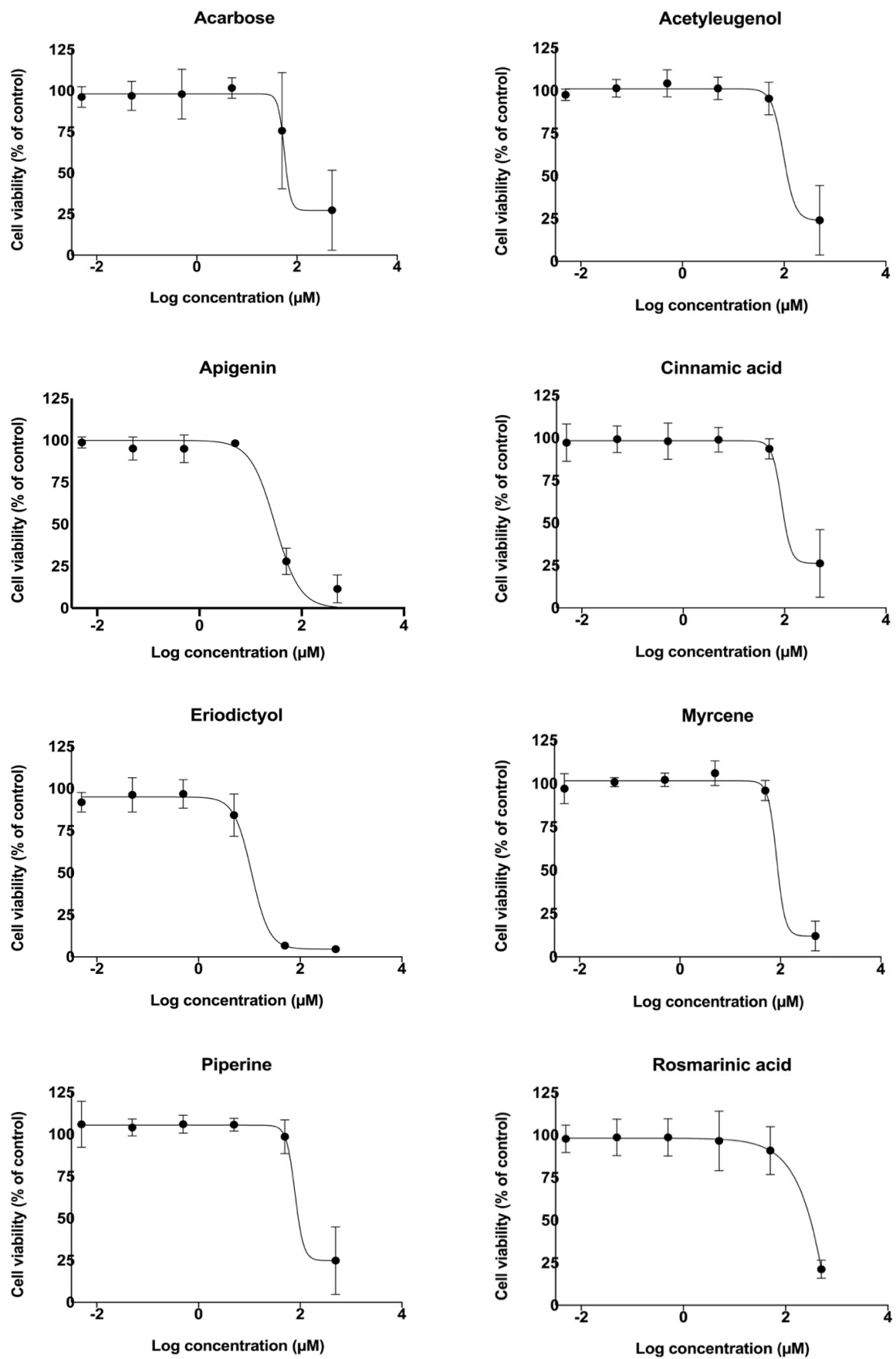


Figure S9: Viability of C2C12 cells after 72 h exposure to acarbose (control) and herbal compounds. The mean is n=3, with SD error bars.

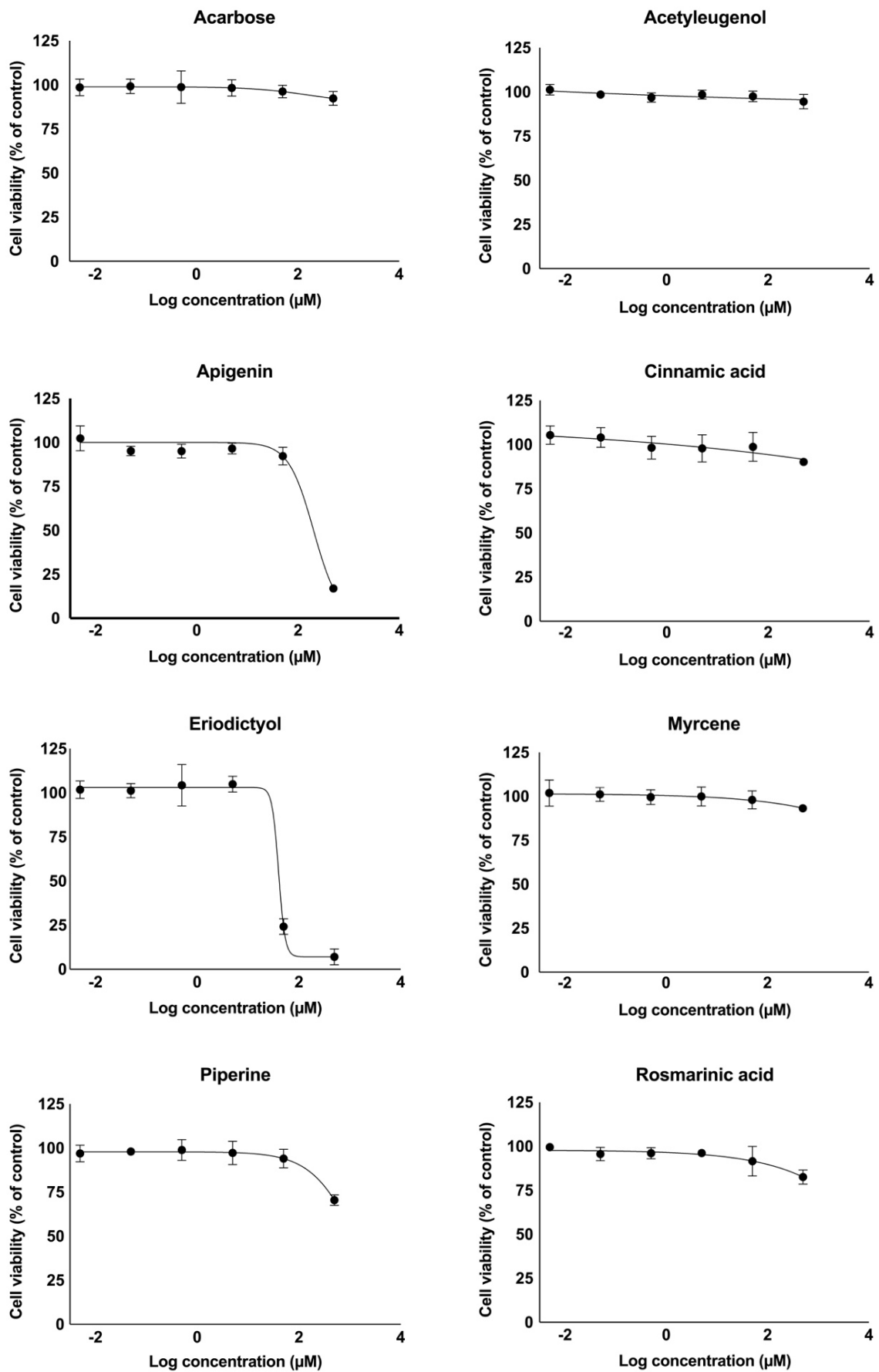


Figure S10: Viability of HepG2 cells after 72 h exposure to acarbose (control) and herbal compounds. The mean is n=3, with SD error bars.

12. APPENDIX II: ETHICAL APPROVAL



UNIVERSITEIT VAN PRETORIA
UNIVERSITY OF PRETORIA
YUNIBESITHI YA PRETORIA

Faculty of Natural and Agricultural Sciences
Ethics Committee

E-mail: ethics.nas@up.ac.za

30 July 2020

ETHICS SUBMISSION: LETTER OF APPROVAL

Ms M Tolmie
Department of Biochemistry, Genetics and Microbiology
Faculty of Natural and Agricultural Science
University of Pretoria

Reference number: NAS015/2020
Project title: An in vitro and in silico relationship study of the inhibition of α -glucosidase and α -amylase by herbal compounds

Dear Ms M Tolmie,

We are pleased to inform you that your submission conforms to the requirements of the Faculty of Natural and Agricultural Sciences Research Ethics committee.

Please note the following about your ethics approval:

- Please use your reference number (NAS015/2020) on any documents or correspondence with the Research Ethics Committee regarding your research.
- Please note that the Research Ethics Committee may ask further questions, seek additional information, require further modification, monitor the conduct of your research, or suspend or withdraw ethics approval.
- Please note that ethical approval is granted for the duration of the research (e.g. Honours studies: 1 year, Masters studies: two years, and PhD studies: three years) and should be extended when the approval period lapses.
- The digital archiving of data is a requirement of the University of Pretoria. The data should be accessible in the event of an enquiry or further analysis of the data.

Ethics approval is subject to the following:

- The ethics approval is conditional on the research being conducted as stipulated by the details of all documents submitted to the Committee. In the event that a further need arises to change who the investigators are, the methods or any other aspect, such changes must be submitted as an Amendment for approval by the Committee.
- **Applications using Animals:** NAS ethics recommendation does not imply that AEC approval is granted. The application has been pre-screened and recommended for review by the AEC. Research may not proceed until AEC approval is granted.

Post approval submissions including application for ethics extension and amendments to the approved application should be submitted online via the Ethics work centre.

We wish you the best with your research.

Yours sincerely,

Chairperson: NAS Ethics Committee



Faculty of Health Sciences

Institution: The Research Ethics Committee, Faculty Health Sciences, University of Pretoria complies with ICH-GCP guidelines and has US Federal wide Assurance.

- FWA 00002567, Approved dd 22 May 2002 and Expires 03/20/2022.
- IORG #: IORG0001762 OMB No. 0990-0279 Approved for use through February 28, 2022 and Expires: 03/04/2023.

23 October 2020

Endorsement Notice

Ethics Reference No: NAS015/2020

Title: An in vitro and in silico relationship study of the inhibition of α -glucosidase and α -amylase by herbal compounds

Dear Ms M Tolmie

The **New Application** as described in your documents specified in your cover letter dated 2020-09-23 received on 2020-10-23 was approved by the Faculty of Health Sciences Research Ethics Committee on 2020-10-21 as resolved by its quorate meeting.

Please note the following about your ethics approval:

- Please remember to use your protocol number NAS015/2020 on any documents or correspondence with the Research Ethics Committee regarding your research.
- Please note that the Research Ethics Committee may ask further questions, seek additional information, require further modification, monitor the conduct of your research, or suspend or withdraw ethics approval.

Ethics approval is subject to the following:

- The ethics approval is conditional on the research being conducted as stipulated by the details of all documents submitted to the Committee. In the event that a further need arises to change who the investigators are, the methods or any other aspect, such changes must be submitted as an Amendment for approval by the Committee.

We wish you the best with your research.

Yours sincerely

Dr R Sommers; MBChB; MMed (Int); MPharMed, PhD

Deputy Chairperson of the Faculty of Health Sciences Research Ethics Committee, University of Pretoria

The Faculty of Health Sciences Research Ethics Committee complies with the SA National Act 61 of 2003 as it pertains to health research and the United States Code of Federal Regulations Title 45 and 46. This committee abides by the ethical norms and principles for research, established by the Declaration of Helsinki, the South African Medical Research Council Guidelines as well as the Guidelines for Ethical Research: Principles Structures and Processes, Second Edition 2015 (Department of Health).

Research Ethics Committee
Room 4-60, Level 4, Tswelopele Building
University of Pretoria, Private Bag x323
Gezina 0031, South Africa
Tel +27 (0)12 358 3084
Email: deepika.behari@up.ac.za
www.up.ac.za

Fakulteit Gesondheidswetenskappe
Lefapha la Disaense tsa Maphelo